

# **In-line/on-line measuring techniques in the solution crystallization processes**

Dissertation

zur Erlangung des  
Doktorgrades der Ingenieurwissenschaften (Dr. –Ing.)

des

Zentrums für Ingenieurwissenschaften

der Martin-Luther-Universität  
Halle-Wittenberg

Vorgelegt

von Frau M. Sc. Maryam Mostafavi  
geb. am 26.01.1979 in Tehran, Iran

Gutachter:

- 1) Prof. Dr.-Ing. habil. Dr. h. c. Joachim Ulrich
- 2) Prof. Dr. -Ing. Sigrid Schuldei

Halle (Saale), den 30.04.2015

## **Acknowledgement**

The research work presented in this dissertation was carried out during my stay at the chair of Thermal Process Technology, Center of Engineering Science at Martin-Luther University Halle-Wittenberg as a PhD student from April 2012 to March 2015.

I would like to express my sincere thanks to Prof. Dr.-Ing. Dr. h.c. Joachim Ulrich for the supervision of my PhD thesis and giving me the great opportunity to work on the subject of crystallization. His scientific suggestions lead my work goes ahead. All of his endless helps in doing my PhD work are unforgettable.

I would like to appreciate deeply from my parents as well as my brother for their strong supports and their never ending encouragement during my PhD work.

Moreover, I would like to thank all of my TVT colleagues and friends, **Lydi, Sandra, Isabell, Steffi, Xiaoxi, Miaomiao, Dan, Anke, Kati, Phuong, Kristin, Franzi, Claudia, Ronny, Patrick, Anne, Julia, Haihao, Mohammad, Ahmed, Hamid** for helping in my lab work and making my work place such as a desirable place. I wish them all the best.

Finally, I appreciate from German Academic Exchange Service (DAAD) for providing financial support to make my stay in Germany comfortable and memorable.

<b><u>1. INTRODUCTION</u></b> .....	<b>1</b>
<b><u>2. STATE OF THE ART</u></b> .....	<b>3</b>
<b><u>2.1 Principles of solution crystallization</u></b> .....	<b>3</b>
<u>2.1.1 Solubility and the metastable zone width (MZW)</u> .....	3
<u>2.1.2 Supersaturation</u> .....	5
<u>2.1.3 Nucleation</u> .....	5
<u>2.1.4 Crystal growth</u> .....	6
<u>2.1.5 Crystallization product properties</u> .....	7
<u>2.1.5.1 Crystal shape (habit)</u> .....	7
<u>2.1.5.2 Crystal size</u> .....	8
<u>2.1.5.3 Crystalline form</u> .....	8
<b><u>2.2 Characterization techniques in the solution crystallization</u></b> .....	<b>10</b>
<u>2.2.1 The liquid phase monitoring</u> .....	12
<u>2.2.1.1 The spectroscopic methods</u> .....	12
<u>2.2.1.1.1 Attenuated total reflectance-fourier transform infrared (ATR-FTIR) spectroscopy</u> .....	13
<u>2.2.1.1.1.1 Solubility measurement</u> .....	14
<u>2.2.1.1.1.2 Determination of the crystal growth rate</u> .....	14
<u>2.2.1.1.1.3 Polymorphic phase transition</u> .....	14
<u>2.2.1.1.2 ATR UV/Vis spectroscopy</u> .....	14
<u>2.2.1.1.3 Raman spectroscopy</u> .....	15
<u>2.2.1.2 Densitometry and electrical conductivity</u> .....	15
<u>2.2.1.3 Ultrasound technique (single frequency)</u> .....	15
<u>2.2.1.3.1 Determination the metastable zone width and the concentration of solute</u> .....	16
<u>2.2.1.3.2 Measuring crystal growth rate</u> .....	18
<u>2.2.2 The solid phase monitoring</u> .....	18
<u>2.2.2.1 Image analysis</u> .....	19
<u>2.2.2.2 Ultrasound technique (multi frequency)</u> .....	19
<u>2.2.2.3 Turbidimetry</u> .....	20
<u>2.2.2.4 Ultrasound technique (single- frequency)</u> .....	20
<u>2.2.2.5 Three dimensional optical reflectance measurement (3D ORM (advanced particle analyzing system (APAS) with multi capture signal technology (MCST))</u> .....	21
<u>2.2.2.6 FBRM (focused beam reflectance measurement)</u> .....	25
<u>2.2.2.6.1 Determination of the solubility and metastable zone width by the FBRM technique</u> .....	28
<u>2.2.2.6.2 Polymorphic or solvate phase transformation</u> .....	28
<u>2.2.2.6.3 Advantages and limitations in the FBRM technique</u> .....	28
<u>2.2.3 The polymorphic or solvate forms monitoring</u> .....	30

2.2.3.1 Microscopy .....	30
2.2.3.1.1 Optical microscopy .....	30
2.2.3.1.2 Scanning electron microscopy (SEM) .....	30
2.2.3.2 Spectroscopic analysis .....	30
2.2.3.2.1 Fourier transform infrared (FTIR) spectroscopy .....	30
2.2.3.2.2 Raman spectroscopy .....	30
2.2.3.3 Ultrasound technique (single-frequency) .....	31
2.2.3.4 FBRM techniques .....	31
2.2.3.5 3D ORM (APAS with MCST) technique .....	31
<b>3. AIM OF THE PRESENT WORK.....</b>	<b>33</b>
<b>4. MATERIALS, METHODS AND PROCEDURES .....</b>	<b>35</b>
<b>4.1 Materials .....</b>	<b>35</b>
<b>4.2 Methods and procedures .....</b>	<b>37</b>
4.2.1 Study of the sucrose crystallization using ultrasound technique .....	37
4.2.2 The influence of air bubbles on the measurement of different crystal sizes and suspension densities by the 3D ORM measurement technique .....	38
4.2.3 Effect of particle shape on inline particle size measurement technique .....	39
4.2.3.1 Ultrasound probe .....	39
4.2.3.2 Laser backscattering probes .....	39
4.2.4 The phase transition of crystals in-line .....	39
4.2.4.1 Magnesium sulfate .....	40
4.2.4.2 Di-sodium tetraborate pentahydrate .....	41
4.2.4.3 Sulfathiazole .....	42
<b>5. EXPERIMENTAL SETUP.....</b>	<b>45</b>
<b>6. RESULTS .....</b>	<b>47</b>
<b>6.1 The ultrasound technique: here the example of sucrose crystallization.....</b>	<b>47</b>
6.1.1 Determination of the metastable zone width using the single frequency ultrasound technique (case study: sucrose) .....	47
6.1.2 Measurement of the ultrasound velocity versus concentration and temperature using the single frequency ultrasound technique (case study: sucrose) .....	48
6.1.3 Desupersaturation curve determination by means of the single frequency ultrasound technique (case study: sucrose) .....	50
<b>6.2 The influence of air bubbles on the measurement of different crystal sizes and suspension densities by the 3D ORM (523 PsyA CSD Particle Analyzer) .....</b>	<b>51</b>

<b><u>6.3 Effect of particle shape on inline particle size measurement technique</u></b> .....	<b>52</b>
<u>6.3.1 Ultrasound device: Measurement of the ultrasound velocity in L-threonine and sugar suspensions</u> .....	53
<u>6.3.2 3D ORM (APAS) device: Measurement of the particle size (average length) in L-threonine and ammonium chloride suspensions</u> .....	54
<u>6.3.3 3D ORM (APAS) device: Measurement of the counts (number of particles) in L-threonine and ammonium chloride suspensions</u> .....	55
<u>6.3.4 FBRM device: Measurement of the mean chord length in L-threonine and ammonium chloride suspensions</u> .....	56
<u>6.3.5 FBRM device: Measurement of the counts (number of particles) in L-threonine and ammonium chloride suspensions</u> .....	57
<b><u>6.4 The phase transition of crystals in-line</u></b> .....	<b>58</b>
<u>6.4.1 Solvent mediated phase transition of magnesium sulfate hexahydrate to magnesium sulfate heptahydrate</u> .....	58
<u>6.4.2 Solvent mediated phase transition of di-sodium tetraborate pentahydrate to di-sodium tetraborate decahydrate</u> .....	61
<u>6.4.3 Solvent mediated phase transition of sulfathiazole polymorphic forms</u> .....	62
<b><u>7. DISCUSSION</u></b> .....	<b>64</b>
<b><u>7.1 The influence of air bubbles on the measurement of different crystal sizes and suspension densities by the 3D ORM technique</u></b> .....	<b>64</b>
<u>7.1.1 Effect of the viscosity during in-line measurement by the means of the 3D ORM technique</u> .....	64
<u>7.1.2 Investigation of the behavior of the 3D ORM measurement technique with three volume suspension densities and different particle size ranges</u> .....	65
<u>7.1.3 Influence of the volume suspension density on the mean chord length measured by mean of the 3D ORM (523 PsyA CSD Particle Analyzer) (with surfactant)</u> .....	67
<b><u>7.2 Effect of particle shape on inline particle size measurement technique</u></b> .....	<b>68</b>
<u>7.2.1 Ultrasound device: Measurement of the ultrasound velocity in L-threonine and sugar suspensions</u> .....	68
<u>7.2.2 3D ORM (APAS) device: Measurement of the particle size (average length) in L-threonine and ammonium chloride suspensions</u> .....	69
<u>7.2.3 3D ORM (APAS) device: Measurement of the counts (number of particles) in L-threonine and ammonium chloride suspensions</u> .....	72
<u>7.2.4 FBRM device: Measurement of the mean chord length in L-threonine and ammonium chloride suspensions</u> .....	74
<u>7.2.5 FBRM device: Measurement of the counts (number of particles) in L-threonine and ammonium chloride suspensions</u> .....	76

<b><u>8. CONCLUSION</u></b> .....	79
<b><u>9. SUMMARY</u></b> .....	82
<b><u>10. ZUSAMMENFASUNG</u></b> .....	85
<b><u>11. ABBREVIATION</u></b> .....	88
<b><u>12. REFERENCE</u></b> .....	89
<b><u>13. APPENDIX</u></b> .....	103
<b><u>13.1 Ultrasound device</u></b> .....	103
<b><u>13.2 Optical reflectance measurement</u></b> .....	104
<b><u>13.3 Focused beam reflectance measurement (FBRM)</u></b> .....	105
<b><u>14. STATEMENT OF AUTHORSHIP</u></b> .....	106
<b><u>15. CURRICULUM VITAE (CV)</u></b> .....	107

## 1. Introduction

Crystallization as an important unit operation applied in a variety of industries. Besides regularly used household products such as sugar, fats and salts, chemicals and pharmaceutical compounds are presented in the market as crystals. Crystallization is a thermal separation process that result a solid product from a melt, a solution or a vapor. Crystallization from the solution is an important process applied in several industries such as pharmaceutical, food and chemical industries as a technique for separating solid materials in the high purified forms **[Abu10]**. The significance of the crystallization in the pharmaceutical industries is because of a large number of active pharmaceutical ingredients (APIs) are utilized in the solid form. For instance, it is determined that more than 80% of APIs include at least one crystallization step in their production process **[Reu06]**.

The crystallization operation is often crucial since it determines the product properties such as crystal size distribution (CSD), morphology and polymorphic or solvate form. These properties affect some of the product specifications such as dissolution rate and bioavailability **[Abu10]**. For example, the bioavailability of an active pharmaceutical ingredient (API) is intensely affected by the dissolution rate of the crystals, which depends on the crystal size, the crystal size distribution (CSD) and the shape of crystals (the surface area of a crystal) **[Ste13]**.

In addition to mentioned product properties, the driving force, supersaturation, is of interest in a crystallization process. In order to evaluate the supersaturation, it is necessary to identify the concentration in the liquid state **[Per11]**.

To obtain efficient quality of the product, the conditions in the liquid state (supersaturation, concentration of solute) as well as the solid state (suspension density, crystal size) have to be controlled. For this purpose, the analyzing techniques are applied in the crystallization process.

The process analytical technology (PAT) tools including on- and in-line analyzing tools are considered as key tools for process understanding, risk management and product quality assurance **[Sim14b]**. For the crystallization process PATs have been extensively used in the last decade. In particular, the focused beam reflectance measurement (FBRM), ultrasound technique, 3D optical reflectance measurement (ORM), nuclear magnetic resonance (NMR), attenuated total reflectance (ATR)-UV/vis, attenuated total reflection (ATR)-fourier transform infrared (FTIR) and Raman spectroscopy are examples of the PAT tools in the crystallization processes **[Hel13a, Per11, Sim14b, Ste13]**. The application of these PAT tools to monitor liquid phase and solid phase as well as polymorphic phase transition is described in detail in chapter 2.

Many parameters can influence the outcome of these analyzing techniques. For instance, Helmdach et al. **[Hel12a]** evaluated that the role of air bubble on the result of some sizing techniques such as ultrasound, 3D ORM and FBRM techniques is not neglectable. Helmdach et al. **[Hel15]** also showed the sensitivity of the ultrasound technique to detect different concentrations is higher in the case of laboratory experiments. From the pilot plant results, it was observed that measured ultrasound velocity has higher fluctuation and less amount than the lab scale. The air bubbles

produced by pumping of the feed can be an explanation for the systematically lower measured ultrasound velocity in the pilot plant. According to Povey [**Pov97**], even very small amounts of undissolved air/gas can have a dramatic influence on the velocity of sound. As described in chapter 3, investigation of the air bubble on the outcome of analyzing technique such as 3D ORM is evaluated in this research work. The shape of the crystal is as other parameter can influence the recorded signals of some measuring techniques and needs more studies. The investigation of the particle shape on in-line sizing techniques such as ultrasound, 3D ORM and FBRM techniques is also scheduled in this research.

The impact of solvates and polymorphs on products like foods, especially, however, on chemical and pharmaceutical products is of increasing importance. In industries, especially, in the pharmaceutical industry, it is essential to obtain an understanding concerning conditions of the formation of different solvates or polymorphic forms as well as their specifications by using characterization techniques. In the polymorphic phase transition processes, the operating conditions have to be fixed under which the process can produce the desired product in a stable and reproducible way [**Str04**].

Several off-line analyzing tools including microscopy (optical and scanning electron microscopy (SEM)), thermal analysis (differential scanning calorimetry (DSC)), thermogravimetry (TG)), solid state nuclear magnetic resonance (ssNMR) and X-ray diffractometry (XRD)) can be used for the characterization of different polymorphic forms [**Abu10**]. These analytic techniques also require sample preparation which can lead to a time delay in the recognizing of the polymorphic forms. Furthermore, the polymorphic phase transition can occur during the sample transfer.

Moreover, extensive studies [**Abu10, Hel13a, How09, Sat10, Sim14**] have been performed that illustrate the importance of PAT tools such as Raman spectroscopy, FBRM, PVM, FTIR, 3D ORM or ultrasound sound single frequency techniques to monitor and control of the polymorphic phase transition. The applications of these tools allow obtaining instant measurements avoiding the time delay typical in off-line analysis techniques [**Sim14**].

The sensitivities, strengths and weakness of these different measurement techniques have to be considered to facilitate the selection of appropriate PAT tools for process design and scale up. The motivation for this work is to carry out further basic research in the field of phase transformations using new PAT tools including the ultrasound technique (single frequency) and the 3D ORM technique. Furthermore, the phase transition experiments were performed using organic and inorganic substances. It should be clarified whether the new techniques show potentials for a better control of the crystallization process!



## 2. State of the art

The knowledge of essential factors influencing the outcome of a crystallization process and the control of the process is required to achieve crystalline products with high quality [Str04]. This chapter provides an overview on the principles of solution crystallization including solubility, crystallization kinetics and crystalline material properties including polymorphic phase transition. A brief review on Process Analytical Technology (PAT) and its application in crystallization processes is described as well.

### 2.1 Principles of solution crystallization

Crystallization from solution is a unit operation applied in various industries as a process to separate solid materials out of liquids in purified form. Since a large number of active pharmaceutical ingredients (APIs) are in solid form, crystallization processes have an importance in pharmaceutical industries [Abu10]. It is reported that more than 80% of APIs include at least one crystallization step during the process of their manufacturing [Reu06].

#### 2.1.1 Solubility and the metastable zone width (MZW)

Concerning the aspect of solubility, substances can be categorized in very soluble (100-1000 g substance in 100 g solvent) to practically insoluble (0-0.01 g substance in 100 g solvent) [Jou10]. The solubility of most of the pharmaceutical compounds is low in water. This might result in a low bioavailability and a low pharmaceutical effect [Ton07].

Accurate solubility data are a crucial part in design and development of crystallization processes. Generally, the solubility data can hardly be obtained from literature and must therefore be measured in each case! The measurement includes the definition of a maximum amount of solute that can be dissolved in a specified solvent at a constant controlled temperature (isothermal) with agitation for a time period 24 - 48 hours. Subsequently the analysis of the solute can be accomplished either gravimetrically or spectroscopy [Sch02a].

For a two component system, the solubility of one component in the other one relies on temperature and pressure. For three or more component systems, the solubility of one component is also dependent on the temperature, pressure and the amount of other component in the system. For the liquid phase, the pressure dependence is ignorable in most cases [Ulr06].

The dependence of the solubility on temperature can be presented as a solubility curve. In the some cases, the solubility of the substances increases with temperature. Polymorphic forms, solvates and hydrates of the same compound have different physical properties that mean also different solubilities.

Additionally to the solubility curve, the phase diagram as a thermodynamic factor is constructed by a nucleation curve (the upper limit of the metastable zone width), a non-thermodynamic factor. The nucleation process is important in crystallization and

it has characteristic kinetics. The kinetics defines the time-scale and therefore the size of the equipment required, while the thermodynamics defines the limits of what can be achieved [Ulr06]. Since nucleation can be induced by different mechanisms, the metastable zone width is an unpredictable quantity and depends on process conditions such as the time, purity of the solution, cooling or evaporation rate, agitation etc. [Ulr06].

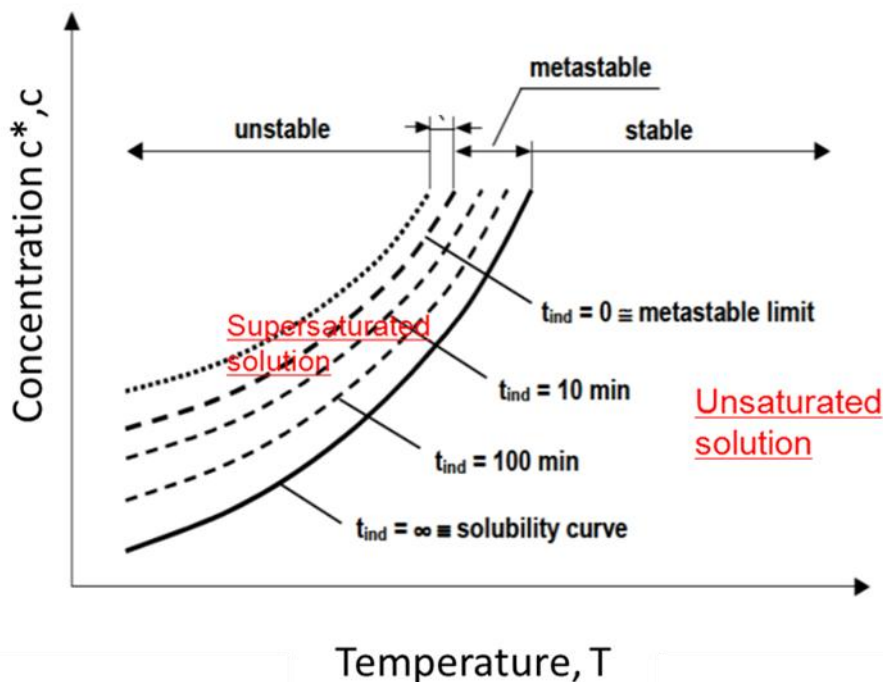


**Fig. 2-1:** Stages of stability in solution crystallization [Str04]. All points with finite induction time lie within the metastable zone. The induction time for nucleation at the nucleation curve disappears.

Considering the metastable zone width, the various stages of stability exist in solution crystallization (see Fig. 2-1). Below the solubility curve, all solutions are unsaturated. Due to no chances with respect to crystallization in unsaturated solution, this is region is called stable. The solubility curve represents an equilibrium state where growth and dissolution processes occur at the same magnitude, thus the induction time at solubility curve for nucleation is infinite.

During the build up of supersaturation, at a specified temperature the induction time becomes zero and instantaneous crystallization starts. This point is defined by the temperature and concentration is called the metastable limit (it is one point of the nucleation curve). The zone between the saturation curve and nucleation curve is called metastable zone. Crystal growth by addition of seed crystals is only possible in this region (above the solubility curve and below the nucleation curve). The metastable zone defines the operating window of the process [Cro11]. Operating

close to the saturation curve by addition of seed crystals result in slow growth rates. The optimum supersaturation level for a crystallization process is approximately half of the metastable zone width (MZW) which defines the operating zone of industrial crystallizer [Tit03]. The system will never reach the zone beyond the metastable zone (unstable zone) due to the immediately occurring of nucleation! [Str04].

### **2.1.2 Supersaturation**

Nucleation and crystal growth require a driving force. A crystallization process can only take place when the amount of solute is more than the solubility limit. A supersaturated solution has non-equilibrium conditions and tends to approach equilibrium state. Consequently it creates solids in form of nuclei [Abu10, Uir06]. The supersaturation is defined as difference in the chemical potentials between the equilibrium composition and the actual composition but in industrial applications usually the concentrations are used since the concentration can be measured using analytical techniques. Methods to generate supersaturation involve evaporation (removing of solvent from the solution), cooling (decreasing temperature of the saturated solution if the solubility increases with the temperature), anti-solvent addition (decrease in the solubility of the solute by addition of the second solvent), chemical reaction (generate the supersaturation with respect to the new compound produced from the chemical reaction) or freezing out the solvent (increase in the concentration of solute and subsequently removing of the frozen solvent) [Abu10].

### **2.1.3 Nucleation**

Generally, nucleation is divided into either primary (homogeneous or heterogeneous) or secondary nucleation.

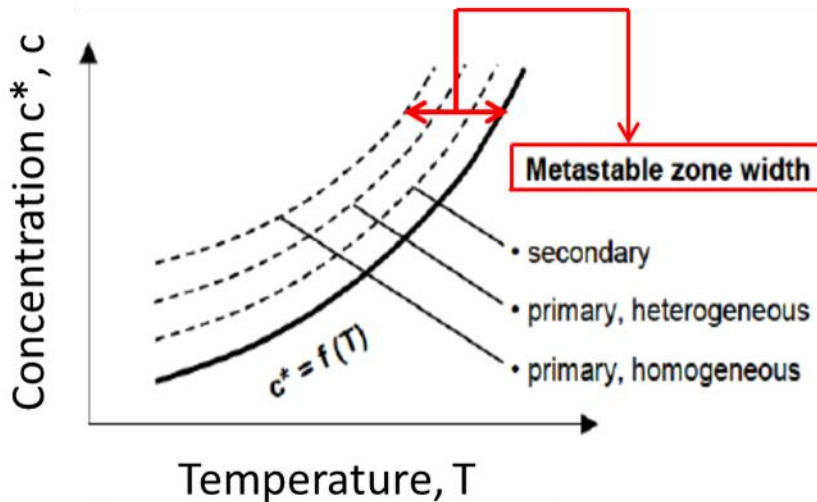


**Fig. 2-2:** Metastable zone width for different mechanisms of nucleation [Mer01].

The primary homogenous (spontaneous) nucleation occurs only when the system is free from impurities and is not disturbed in respect to mechanical effects. The primary heterogeneous nucleation occurs where impurities or rough vessel walls induce the nucleation. What is usually -in real life- the case. It needs less supersaturation than the primary homogenous nucleation. The most extensively observed nucleation is the secondary nucleation. The secondary nucleation occurs only in the presence of crystals of the substance that should be crystallized. Secondary nucleation occurs at much lower supersaturations than primary nucleation (see Fig. 2-2). The different known mechanisms for secondary nucleation are initial breeding (result from dust of the seed crystals added into the supersaturated solution), collision breeding (result from the breakage of existed crystals due to crystal – crystal, crystal – wall or crystal – impeller collisions) and fluid shear (result from shear forces outcomes from the liquid motion). Among these mechanisms, the collision breeding is most frequently observed in crystallization processes [Mul01, Uir06].

### 2.1.4 Crystal growth

The nucleated crystals in supersaturated solution start to grow to reach a specified size.

The three main steps for a crystal growth process include [Uir06]:

- (a) Mass transfer of solute molecules from the bulk solution to the proximity of the crystal surface (diffusion).
- (b) Transmission of the adsorbed solute molecules at the crystal surface into the crystal lattice (surface integration).
- (c) Release of the heat of the crystallization process at the point of growth.

Although these three steps always take place, one of them might be the determining step. For instance, diffusion or surface integration controlled is the growth rate usually in solution crystallization [Uir06].

## 2.1.5 Crystallization product properties

### 2.1.5.1 Crystal shape (habit)

According to literature (e.g. [Mul01]), crystals can be classified according to seven general systems. These systems are nominated as cubic, octahedral, tetragonal (pyramidal, quadratic), orthorhombic (rhombic), monoclinic (prismatic, isoclinic, trimetric, monosymmetric, clinorhombic, oblique), triclinic (anorthic, asymmetric), trigonal (rhombohedral) and hexagonal.

Although crystals can be categorized into seven general systems, the relative sizes of faces of a crystal can vary significantly. This change is called a modification of habit. As an example, three different habits of a crystal belonging to the hexagonal system are shown in Fig. 2-3. A stunted growth in the vertical direction results a tabular crystals, while an elongated growth in the vertical direction yields needle or acicular crystal. A number of factors effect on the face growth of crystals. For instance swift crystallization by the high rate cooling might result the formation of needle crystals. Furthermore, impurities in the solution crystallization can inhibit the growth of the crystal in a certain direction. The degree of supersaturation and crystallization from different solvents are also examples of factors effecting on the habit of a crystal [Mul01, Uir06].

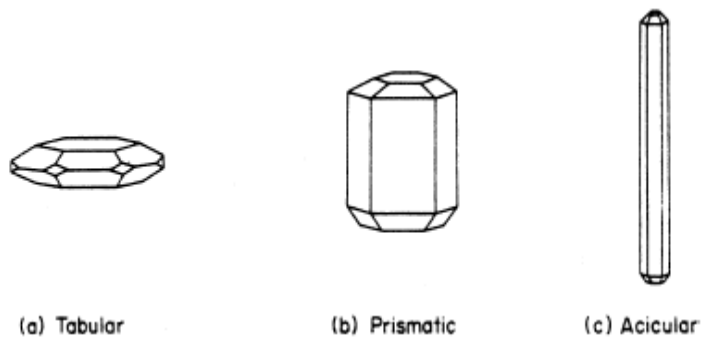


**Fig. 2-3:** presentation of three different habits of belonging to the hexagonal crystal system [Mul01].

### 2.1.5.2 Crystal size

Crystal size is an important factor, especially, in the pharmaceutical industry. Crystals in different ranges of size characterize the crystal size distribution (CSD). The CSD can be represented by the cumulative distribution (number, length, surface area, volume or mass). A narrow CSD shows that the size of crystals is almost uniform while a broad or multimodal CSD has a higher tendency to result in a slow filtration rate, a poor flow ability or a variable dissolution rate [Ber02, Var08].

### 2.1.5.3 Crystalline form

Crystalline materials can have polymorphs, solvates, or hydrates [Hel14].

The impact of solvates and polymorphs on products like foods, especially, however, on chemical and pharmaceutical products is of increasing importance. Polymorphism, in which different crystal lattice arrangements exist for the same chemical compound, can have different physical properties such as crystal shape, solubility, dissolution rate, stability, hardness, color, melting point, density and hygroscopicity (e.g. [Sac06]). Since polymorphs generally are different in the crystal habits, they also show different properties influenced by the shape of the crystal such as flowability and compressibility [Abu10].

The relationship between two polymorphs can be either monotropic or enantiotropic. If two polymorphs are related monotropically, the transformation from the metastable form to the stable form is irreversible in all temperatures and pressures. Only one polymorph has the lowest free energy in different temperature ranges. If two polymorphs are related enantiotropically, the transformation is reversible. In this case, at the temperatures above the transition point, one polymorph is thermodynamically stable while at temperatures below the transition point the other polymorph becomes thermodynamically stable form [Sac06].

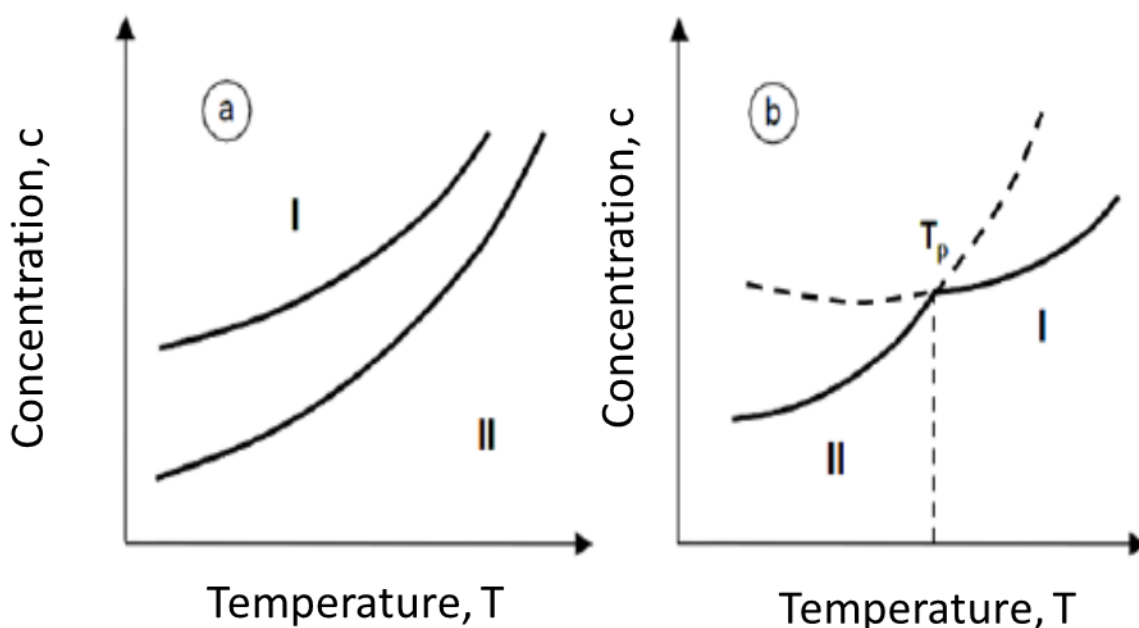


**Fig. 2-4:** (a) Solubility curves of a monotropic system (b) Solubility curve of enantiotropic system. (I) Polymorph form I; II: Polymorph form II;  $T_p$ : transition point [Mul01].

In a monotropic system, the polymorph form II due to a lower solubility (see Fig. 2-4) compared to polymorph form I is the stable form in all temperature range. The phase transition would be exothermic and occurs above the melting temperature of form II (stable form). In an enantiotropic system, polymorph form II is stable at temperatures below the transition point while polymorph form I is stable form at temperatures above the transition point. The phase transition in this system is endothermic [Man09, Sac06].

A Solvate as a crystalline molecular compound in which its molecules are incorporated into the host lattice, containing the unsolvated molecules. A hydrate is a special case of a solvate, when the incorporated solvent is water. The physical and chemical properties of a solvate are different from the unsolvate [Sac06].

The phase transitions between polymorphs and solvates via two processes, the solid-state phase transition or the solvent-mediated phase transition [Car85, Nyv97].

The solid-state phase transition of polymorphs and solvates can occur during some operations like granulation, milling or drying due to change in process condition e.g. temperature and humidity [Zha09].

According to literature [Gav95], the stable polymorphic forms of most organic compounds do not differ much in the lattice energy. For instance the difference in lattice energy of stable polymorphic forms and metastable polymorphic forms of 85% of the organic compounds is approximately only 10%. This implies that the driving force for the several number of solid-state phase transition is small which is proven

by the fact that this phase transition takes long time (weeks or months) [Eli98, Nyv97, Zha09].

The solvent mediated phase transition occurs by immersion of the crystals in a larger volume of the solvent. A metastable form dissolves and creates supersaturation with respect to the stable form and then nucleation and crystal growth of the stable form occurs [Dav02].

Principally, the kinetics of solvent-mediated phase transitions is controlled by the dissolution rate of the dissolved phase and the growth rate occurring phase. The dissolved material immediately crystallizes as a stable form in the dissolution controlled mechanism, while in the growth controlled mechanism, the saturated concentration of the metastable form remains constant until the metastable form is completely dissolved, subsequently a sudden drop in the concentration is followed by nucleation and growth the stable form [Nyv97].

## 2.2 Characterization techniques in the solution crystallization

Many process and product failures can originate from to poor understanding and control of crystallization processes. The understanding of the processes, batch or continuous, is the key to their control. It is essential to gain understanding of the liquid phase as well as the solid phase in crystallization processes. This can be done by on line measuring or characterization techniques.

The term Process Analytical Technology (PAT) became broadly reputed in 2004 when the Food and Drug Administration's (FDA) published the guidance for the industry that represents the basis of the Good Manufacturing Practice (GMP) rules in the pharmaceutical industry [Bee11]. The major motivation behind the PAT invention is defined in the FDA Guidance: PAT- a framework for innovative pharmaceutical development, manufacturing and quality assurance [Fda04]. The quality marks affect the physical (dissolution rate, solubility) and chemical (reactivity) properties of the produced materials but also influences the downstream operations such as filtration and drying. The quality should not be tested at the final product but it is better to have be built in a design including control of the products.

PAT tools as novel technologies being applied to analyze, control and improve processes have obtained significant attraction in academic and industrial research. These tools enable process understanding for scientific purposes, risk management, quality assurance of products and a reduction of risk strategies especially in pharmaceutical industry [Sim15a].

Furthermore, some more potential advantages of the PAT tools in the pharmaceutical manufacturing include:

- (a) Improving process understanding and reducing process failure
- (b) Ensuring quality through optimal design, continuous monitoring, and feedback control
- (c) minimizing the cycle time to improve manufacturing efficiency



(d) understanding the root causes of process deviations

In addition, the Process Analytical Technology supplies data from which relevant process and product information can be extracted. The measured properties can be univariate (scalar) or multivariate (vector or matrix) quantities.

In a PAT environment, real-time process measurements can be divided according to the situation [Fda04]:

In the case of off-line measurement, the samples are removed, isolated and analyzed with analytical equipment in close proximity to the process stream.

In the case of on-line measurements, the samples are not removed from the process stream but temporarily separated, for example via a by-pass system which transports the sample directly through the on-line measurement device where the samples are analyzed in close proximity to the process stream and afterwards the sample returns to the process stream.

In the case of in-line measurements, the sensor is directly immersed into the process flow and the sample is not removed from the stream of the process.

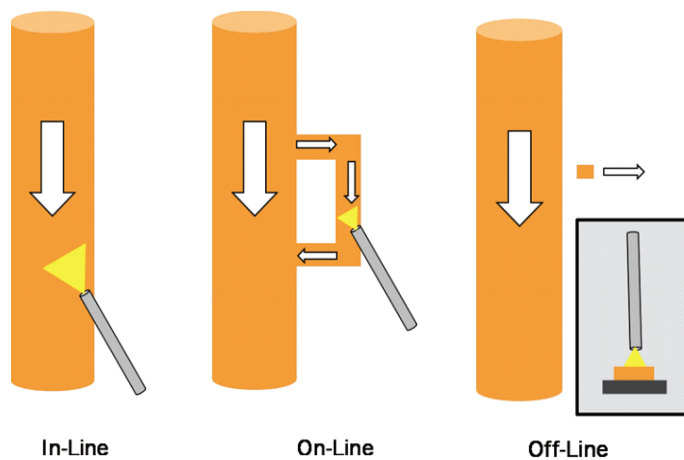


**Fig. 2-5:** Different situations of the PAT tools [Fda04].

The process analytical technology (PAT) tools include on- and in-line equipment, which allow instant measurement to be obtained, avoiding the time delay and errors due to sampling typical in off-line analysis. PAT tools are the most favorable technology to analyze and control critical process variables such as particle size, the particle size distribution (PSD), the crystal shape, and/or the polymorphic or solvate form.

Since crystallization contains the combination of a solid and a liquid phase, these phases have to be investigated. The following section gives an overview on commonly used PAT tools to monitor the crystallization processes.

## 2.2.1 The liquid phase monitoring

Various methods have been used to measure liquid phase concentration in crystallization processes. Supersaturation is one of the essential variables that should be controlled in crystallization processes. This variable has a significant effect on nucleation and growth processes [Sib03]. In the pharmaceutical industry, the bioavailability of active pharmaceutical ingredients (APIs) depends on their solubility. A drug can be ineffective due to too low solubility of APIs and also can have side effects because of high solubility of APIs [Man09].

The methods used for the determination of the concentration are divided in spectroscopic methods, physical methods (e.g. conductivity) and ultrasound technique [Hei12].

### 2.2.1.1 The spectroscopic methods

One of the most common methods for the determination of concentration is a spectroscopy method. Concentration can be obtained from the spectral data using the Beer-Lambert law. The principle of ATR (attenuated total reflection) is shown in Fig. 2-6 and is very intensely described e.g. by [Lew01].

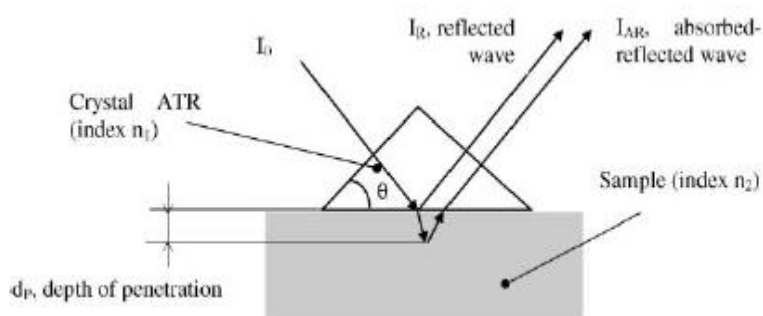


**Fig. 2-6:** ATR measurement principles [Lew01]. When a radiation beam is contacted with a certain angle  $\theta$  via the ATR (attenuated total reflectance) element, the incident beam strikes to the interface of ATR element (crystal) and sample. The absorption of the sample causes the attenuation of the reflected beam that subsequently transferred to the detector to produce a spectrum).

The depth of the penetration of incident beam to the sample is presented by (Eq. 2-1), where  $\lambda$  is the wavelength of the incident radiation,  $n_1$  and  $n_2$  are the refractive indices of the crystal and solution,  $\theta$  is the angle of incidence of the propagating radiation

$$d_p = \frac{\lambda}{2\pi n_1 \sin \theta^2 - \left(\frac{n_2}{n_1}\right)^2}^{1/2} \quad \text{Eq. 2-1}$$

In ATR spectroscopy, the measuring beam becomes reflected at the interface between an auxiliary medium and the sample. This auxiliary medium must be not only infrared transparent but also must have a high refractive index. The penetration depth of the incident beam into the sample is only a few micrometers (0.5-5  $\mu\text{m}$ ), and depends on the refractive indices of the crystals and the solution. The ATR technique can be used to measure exclusively the liquid phase of a crystal slurry without interference of the dispersed crystals [Sch95].

### 2.2.1.1.1 Attenuated total reflectance-fourier transform infrared (ATR-FTIR) spectroscopy

The Attenuated total reflectance Fourier Transform Infrared (ATR-FTIR) spectroscopy has been successfully used to monitor the liquid phase concentration during crystallization processes. The ATR-FTIR spectroscopy is based on the absorption of the light in the mid-infrared region (4000-200  $\text{cm}^{-1}$ ). Since most compounds absorb radiation in the mid infrared region, this technique has a prevalent application. In this technique, the radiated beam impacts on the sample and subsequently the amount of the IR absorbed in different frequency is measured. The frequency in which the absorption occurs indicates the presentation of the different chemical compounds, while the absorption magnitudes determine the concentration of these chemical compounds. The law of Lambert-Beer is commonly used in infrared spectroscopy to relate measured absorbance (A) to the concentration of a sample (c):

$$A = \epsilon l c \quad \text{Eq. 2-2}$$

A is the absorbance of the sample, c is the concentration and  $\epsilon$  is the extinction coefficient. This law is usually valid for low concentrations and in high concentrations it creates problems like increasing in deviation from the intermolecular interactions. The peak height or area of the peak in the IR spectrum can be related to the concentration of solute via the univariate (scalar) or most accurate multivariate (vector and matrix) data analysis in which the whole of the spectrum is considered. The ATR-FTIR spectroscopy is used in the crystallization processes for several objects include [Lin12]:

### 2.2.1.1.1.1 Solubility measurement

The ATR-FTIR spectroscopy can be used to measure the solubility as a function of temperature or solvent composition. Cornel et al. [Cor08] used this technique to measure the solubility of  $\beta$  L-glutamic acid in water as a function of temperature.

### 2.2.1.1.1.2 Determination of the crystal growth rate

The desupersaturation curve can be obtained by using of the ATR-FTIR technique. A method for calculating growth rates using a desupersaturation curve is described by Garside et al. [Gar82] and Chivate et al. [Chi75] as well as Mohan et al. [Moh00] The method only requires calculation of the first two derivatives of the desupersaturation curve evaluated at time zero.

Schöll et al. [Sch07] determined the desupersaturation curve of a seeded batch experiment of  $\alpha$  L-glutamic acid in aqueous solution by using the ATR-FTIR techniques. In this experiment, the IR data can be used in conjunction with additional experimental data such as seed mass and initial particle size distribution to calculate the crystal growth rate of the used case study [Sch07].

### 2.2.1.1.1.3 Polymorphic phase transition

The solvent-mediated phase transition can be distinguished using the ATR-FTIR technique. The solvent-mediated phase transition of the metastable  $\alpha$  into the stable  $\beta$  L- glutamic acid can be monitored using the ATR-FTIR technique. At first, the  $\alpha$  form nucleates from the supersaturated solution. Subsequently the  $\beta$  polymorph nucleated and grows while  $\alpha$  form dissolves. This phase transition can be monitored by the ATR-FTIR technique by a sudden decrease in the solute concentration [Sch06b].

### 2.2.1.1.2 ATR UV/Vis spectroscopy

UV/Vis spectroscopy due to using a radiation beam in the UV/Vis region (200-900 nm), it has some limitations for some compounds that have not the functional groups for the absorption of the UV's wavelength range. Absorbance, obtained from the UV/Vis absorption spectra are directly proportional to the concentration of an absorbed species in the solution according to the Beer-Lambert law [Abu10].

The ATR-UV/Vis spectroscopy has been used for the detection of the nucleation [Sim09], polymorphic phase transition [How09] and measuring of the supersaturation level during the crystallization processes [Abu09, Bil10, Tho05].

### 2.2.1.1.3 Raman spectroscopy

This technique due to considering more scattering rather than absorbing of the radiation beam by the sample is different from other spectroscopic technique. This technique uses a monochromatic radiation beam on a sample and measures the amount of light scattered in different wavelengths. Raman spectroscopy enables to monitor in-line both solid and liquid phases without specific sample preparation. Furthermore, this technique has been successfully used to measure the liquid concentration during the crystallization process [Fal03, Hu05].

The Raman spectroscopy is able to produce information on the composition of the solid phase e.g. in the case of the polymorphism.

The Raman spectroscopy technique needs a model to relate the measured variables (Raman intensity, Raman shift) to the independent variables like concentration or solid phase composition.

The disadvantages of Raman spectroscopy is the sample heating produced by the probe that can degrade the sample and also the presence of strong peaks in the Raman spectra originated from the organic solvents that can interfere with the obtained Raman spectra by the solid phase [Fev07]. Further information on this technique can be found in [Cor12, Sim14b].

### 2.2.1.2 Densitometry and electrical conductivity

Density measurements have been used in the monitoring of the solute concentration (liquid phase) during the crystallization processes. Since this technique needs to be free from the crystals, it has some limitations in solutions which are dense and concentrated [Abu10, Ste13].

The level of the supersaturation during a crystallization process has been determined by measuring the electrical conductivity of the liquid phase with the case study of ammonium chloride [Ses20]. According to Maxwell [Max98], the conductivity of a solution is proportional to the volume fraction of the particles. The presence of the solid particles may change the conductivity value of the solution. Therefore, the correlation between electrical conductivity and concentration is valid only for crystal-free solution. Furthermore, this technique has limitation in the application of the electrically non-conducting solution such as organic systems. These systems are usually not conductors and also these systems are sensitive to impurities [Mul01].

### 2.2.1.3 Ultrasound technique (single frequency)

The single frequency ultrasound technique is proven to be a simple, robust and reliable technique in many cases to monitor the crystallization processes. The principle used in the measurement of the ultrasound velocity is based on the determination of the time required for ultrasound wave to travel through the given medium [Ulr12]. In a given medium, the sound travels with defined ultrasound

velocity ( $v$ ), which depends on the density and adiabatic compressibility of a medium ( $k_{ad}$ ). Besides, the ultrasound velocity also the attenuation of the ultrasound wave can be measured by an ultrasound sensor. The ultrasound sensor contains of two legs.

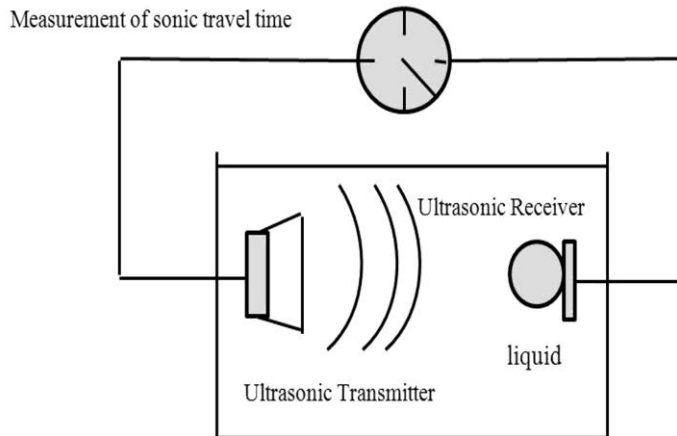


**Fig. 2-7:** Ultrasound measurement principle [Sen03].

At the end of each of the legs a piezo-electric transducer is installed which are facing each other. One of which acts as a transmitter, while the other one serves as a receiver. In periodic time interval, the transmitter emits the ultrasound signals which are identified by the receiver and intensified. The probe emits a very low frequency (2 MHz) ultrasound signal and this energy input to the system does not produce cavitation effects through the media [Gla04, Ulr12].

The ultrasound technique (single frequency) is used for the determination of the metastable zone width (MZW) (see e.g. [Hel15, Oma99, Tit03]), supersaturation [Oma99] and crystal growth kinetics [Gla04, Oma99] by measuring the concentration of the solution using a protected sensor.

### 2.2.1.3.1 Determination the metastable zone width and the concentration of solute

The ultrasound technique (single frequency) can be used for the determination of the metastable zone width for a wide range of materials [Gla04, Hel15, Tit03]. Helmdach et al. [Hel12] analyzed some pharmaceutical and inorganic compounds using the ultrasound technique to specify the concentration of the solute and metastable zone width and evaluated the obtained results. For a large number of inorganic compounds, this technique presents an excellent applicability with respect to the concentration and metastable zone width determination due to the high sensitivity of the ultrasound velocity for these kinds of compounds. The application of this

technique showed some limitations for a number of pharmaceutical compounds with high molecular weight. If the solubility and nucleation points of these compounds cannot be extracted by the ultrasound velocity, the evaluation of the attenuation might supply useful information on the metastable zone width of these compounds [Hel15]. Helmdach et al. [Hel15] divided materials in three groups. The first group includes inorganic and organic compound (non-pharmaceutical compounds) that the ultrasound velocity and temperature have the same trend. In this group, the sensitivity of the ultrasound technique for inorganic compounds with low molecular weight is higher than for organic compounds with a higher molecular weight. The second group involves materials in which the velocity trend changes in the same direction ( $\uparrow, \uparrow$  or  $\downarrow, \downarrow$ ). Within this group two subgroups can be considered. (a) Both trends (ultrasound velocity and temperature) decreasing (b) Both trends (ultrasound velocity and temperature) increasing. The third group includes the materials for which the velocities changes in opposite direction ( $\downarrow, \uparrow$ ) but in contrary to the first group.

The compounds in the second and third group involve organic materials and show some limitations with respect to the measurements of the concentration by the ultrasound technique.

The ultrasound velocity is the square root of the reciprocal product of adiabatic compressibility and density. Both adiabatic compressibility and density depend on temperature, concentration of solute and pressure. For liquids, the pressure dependence can in most cases be ignored [Ulr12]. As mentioned before, temperature and ultrasound velocity change in the same direction in the first group. Therefore, the extent of the change in the ultrasound velocity is maximal. In the third group, the application of the ultrasound velocity is unsatisfactory, since density and adiabatic compressibility change in the opposite direction. In the second group, there is an intermediate position between applicability and non-satisfactory application of ultrasound technique [Hel15]. Furthermore, a direct transferability of the calibration models (solute concentration) from the lab scale into the pilot scale is possible if the effect of gas bubbles in the pilot plant becomes controlled on a low level [Hel15].

Gas bubbles can be produced in the crystallization processes by intensive agitation, addition of seed crystals or pumping of the materials (pilot plant) and can be decreased by deaeration (degassing) in the suspensions to be measured [Mos14a].

Furthermore, Stelzer et al. [Ste13] proved the applicability of the protected sensor for accurate in-line measurements of the liquid concentration during the crystallization processes. The solution in the measuring section of the protected sensor has to be exchanged adequately. By means of the protected sensor, the liquid phase can be measured. The sensor can be protected by a cage with a mesh size which is dependent on the used case study (viscosity of the solution, particle size) and the process condition (mixing) to prevent crystals passing through the measuring section of the sensor. Further explanation can be found in the literatures by Stelzer [Ste13], Omar [Oma99] and Titz-Sargut [Tit03].

Moreover, Pertig et al. [Per15] investigated the effect of seed crystal addition on the measured ultrasound velocity using a protected and an unprotected sensors in a

case study of sucrose-water solution. Since the density of the saturated sugar solution and the density of sugar crystals are similar, the decrease in the solute concentration and the formation of crystals increasing the suspension density and consequently influence the measured ultrasound velocity in the suspension. In this case, the unprotected sensor alone gave no process information. The protected sensor due to decreasing in the solute concentration shows a decrease in the measured ultrasound velocity. Further description can be found in [Per15].

### **2.2.1.3.2 Measuring crystal growth rate**

There are various methods for the determination of crystal growth rates. These methods can be divided into direct and indirect methods. Direct methods are based on the measurement of the change in the size or mass of a crystal, while indirect methods are based on the change in the solution concentration by time. It is demonstrated that the ultrasound technique as one of the indirect methods, has an applicability for the determination of crystal growth kinetics based on the measurement of the desupersaturation curve. Both growth rates for organic and inorganic compounds can be measured from the desupersaturation curve measured by an ultrasound technique [Gla04].

## **2.2.2 The solid phase monitoring**

Several techniques have been used and developed for the in-situ monitoring of the solid phase in the crystallization process. These techniques are able to produce information on the critical product parameters such as particle size, the particle size distribution (PSD), the crystal shape and the polymorphic form and also the crystal purity.

The time dependent particle number and particle size distribution of the concentrated suspension are two critical parameters in crystallization processes. Usually, the suspension densities between 2 and 40 wt% are commonly applied in crystallization processes. Several sizing techniques are used to determine the particle size and particle size distribution. These methods include e.g. coulter counter, laser diffraction and scattering, cascade sieving, optical microscopy, laser scanning and ultrasound spectroscopy. These techniques are different in the capability to measure in-line, on-line or off-line and are different in the covered particle size range.

Some methods such as coulter counter, cascade sieving or laser diffraction require sampling can only be applied for off-line analysis. Sample preparation and sample transport may mainly effect on the measured particle size distribution (PSD) caused by thermal and mechanical stresses of the measured particles [Hei12, Hei13a].

Alternative in-line particle size measuring techniques involve e.g. optical reflectance measurement (ORM) technique, ultrasound attenuation spectroscopy (UAS) [Hip00], single-frequency ultrasound technique (mean particle size) [Per11] or in-situ image analysis [Wan08], Raman spectroscopy [Cor12], Near Infrared spectroscopy,



turbidimetry [Abu10]. There are some limitations in the choice of the in-line particle size analyzers. For instance one of the bottlenecks of using in-line optical microscopy is the evaluation of the low quality images taken from the opaque crystals in the high suspension density [Wan08]. Since not every image is a successful image, the measurement time between two successive images might be long. Therefore, the in-line image analysis is mainly used to detect changes in the morphologies [Hei12]. A main advantage of the 3D ORM as well as UAS over common in-line sizing techniques is the particle characterization over a wide range of the suspension densities (3D ORM: up to 80 vol%; UAS: up to 70 vol%) and the particle size ranges (3D ORM: 0.5-4000  $\mu\text{m}$ ; UAS: 0.01-3000  $\mu\text{m}$ ). A disadvantage of UAS is that due to the lengthy of the measuring time (60s), this device is not suitable for very rapidly changing dynamic systems [Hei13a]. Furthermore, a disadvantages of the UAS is the requirement of lengthy measurement times (60s), making it unsuitable for very fast changing dynamic systems. Also UAS is limited regarding the complexity in analyzing the obtained data. The analysis of the attenuation spectra by means of mathematical models to calculate the crystal size distribution (CSD) and hence the mean crystal size is difficult. More explanations on the commonly used in-line sizing techniques are presented in the following section.

### 2.2.2.1 Image analysis

Image analysis is used to monitor the crystal size and shape in the crystallization processes. A Particle Vision Measurement (PVM) system as in-situ video microscope could be applied to provide images of crystals and crystal structures during the crystallization processes by using laser light [Gil06, Sch06a].

The limitation of this technique is that every image is not a successful image and consequently the measurement time between two successful images can become long. Furthermore, the evolution of the low quality images is strongly dependent on the suspension density and type of the crystals (transparent or opaque) [Cal05, Lar07, Kem08, Wan08].

### 2.2.2.2 Ultrasound technique (multi frequency)

Ultrasonic extinction (multi frequency) is applied for in-line particle size analysis. Ultrasonic extinction is dependent on the acoustic properties of the product to be analyzed. Information related to frequency dependent ultrasonic extinction can be converted into a particle size distribution. This technique can be used to measure particle sizes in the range of 0.1 to 3000  $\mu\text{m}$  in opaque liquids with high solid concentrations (e.g. up to 50%Vol).

An electrical high frequency generator is connected to a piezoelectric ultrasonic transducer. The generated ultrasonic waves are distributed into the suspension and interact with the suspended particles. An ultrasonic detector receives the ultrasonic waves after passing the measuring zone and converted them into an electrical signal. The extinction of the ultrasonic waves is calculated from the ratio of the signal

magnitude on the generator and detector sides. Further information on this technique can be found in [Gee03, Smi10, Sym15].

Furthermore, this technique has been successfully applied for the on-line crystal size measurement by Mougin et al. [Mou02] for the case study of L-glutamic acid. This technique is based on the measurement of attenuation of ultrasonic waves as a function of frequency (in the range of 1 to 150 MHz). The crystal size distribution can be achieved using mathematical model that relates attenuation of sound through a suspension to the particle size distribution of the suspension.

### 2.2.2.3 Turbidimetry

Since the presence of the solid particles in a liquid phase changes the optical properties of the solution, the optical instrument such as turbidimetry can be used for the detection of solid particles [Abu10]. The turbidity technique is able to provide information on the clear and cloud points related to the solubility and nucleation points. The turbidity sensor measures the weakness of the light which is increasing with higher suspension density and decrease in the particle size [Helm13a].

Furthermore, Howard et al. [How09] used this technique along with the FBRM technique for monitoring and detection of polymorphic transformations during the anti-solvent crystallization of sodium benzoate from an isopropanol (IPA)/water mixture. Further description on this research can be found by Howard et al. [How09].

### 2.2.2.4 Ultrasound technique (single- frequency)

Pertig et al. [Per11] have shown that the solid state (suspension density and particle size) can be evaluated by using a single frequency ultrasound technique as a comparatively new, robust and inexpensive Process Analytical Technology (PAT) tool in dense and opaque systems without diluting. The single- frequency ultrasound technique measures ultrasound velocity as well as attenuation. These measured parameters are applied to calculate the most important solid phase variables such as suspension density ( $\varphi$ ) and mean crystal size ( $d_{50}$ ) by applying simple mathematical models based on the equation of Urick [Pov97, Ste13]. Pertig et al. [Per11] used different suspension densities and particle size ranges of case studies of ammonium sulfate and urea and recorded ultrasound velocity and attenuation by the single frequency ultrasound technique. They expressed the measured ultrasound signals as a function of suspension density ( $\varphi$ ) and mean crystal size ( $d_{50}$ ) by mathematical models. Simple mathematical models (partially based on the Urick equation) are used to calculate the mean particle size ( $d_{50}$ ) and the suspension density ( $\varphi$ ) [Pin95]. Furthermore, this technique differs from UAS (Ultrasonic Attenuation Spectroscopy). An advantage of the UAS technology is the possible determination of particle size distributions. A disadvantage of UAS is the requirement of lengthy measurement times (60 s) making it unsuitable for very fast changing systems. Also UAS are limited regarding the complexity in analyzing the obtained data. The analysis of the

attenuation spectra by means of mathematical models to calculate the CSD and hence the mean crystal size is intensely intricate [Mou03], [Ste13].

Sayan et al. [Say02] investigated the change of the ultrasound velocity as a function of particle size or suspension densities, respectively, for the case studies of the NaCl, KNO<sub>3</sub>, K<sub>2</sub>SO<sub>4</sub> and MgSO<sub>4</sub>\*7H<sub>2</sub>O. Measurements were performed in different suspension densities (from 0-60%wt) and particle size range (from 250-500 µm). The ultrasound velocity of different suspension densities and different particle size ranges were determined by single-frequency ultrasound measurement technique. It was found that variations in parameters such as particle size and solid concentration can have a significant effect on the ultrasound velocity measurement.

### **2.2.2.5 Three dimensional optical reflectance measurement (3D ORM (advanced particle analyzing system (APAS) with multi capture signal technology (MCST))**

The 3D ORM (Three Dimensional Optical Reflectance Measurement) is based on the physical effect of reflection.

The light from a highly stabilized a 10-mW laser diode is coupled in a 4-µm single-mode fiber passing the optical mechanical dynamic selective focus system of the beam wave guide. The focus is moving in a dynamic depth into the suspension. Crystals which are inside the center of the focus are measured concerning their exposed particle surface area. Only if the focus is in alignment with the system, as shown in Fig. 2-8. Where only those particles are measured which are in the focal point, these signals are taken into account. The 3D ORM technique works with a self-selective dynamical focal point which guaranties the highest resolution of the particles [Seq13]. When the focal point is able to detect particles from 0.5 up to 600 µm. Furthermore, the focal point can optically broaden and selectively detect larger particles up to 2000, and also in special cases up to 4000 µm. Consequently, the position of the focal point mainly depends on the used particle size (distribution) during the process. The optimal distance of the focal point from the probe window is half of the size of the studied particles [Hel13a].

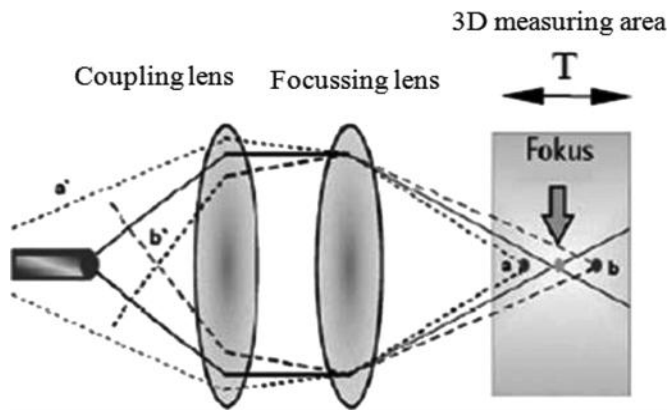


**Fig. 2-8:** Measurement principle of the 3D ORM instrument [Hei12]. A moving light beam is focused into a flowing solution and particles are detected by their reflection as they pass through the moving laser focus. If the particles are not in the measuring zone, the reflected light will not be collected by the sensor [Seq13].

The alignment of the focal point with the system (see Fig. 2-8), is one property which is based on the fact that the system is using only one fiber for in and out going energy/signals. This technology can only work as long as  $1\mu\text{s}$  is between two signals [Mos14b].

Depending on the process and application, suspension densities from 2 to 40 wt% are commonly applied. The outcome of the measurement is to determine the average length (D50) or the mean particle size and particle number [Hel13a]. Table 2-1 shows the characteristics related to the used 3D ORM (APAS with MCST) in this study.

**Table 2-1:** The features of the used 3D ORM (APAS with MCST) [Hel13a].

Features	3D ORM (APAS with MCST)
Rotation of optical lens	No
Focal point	Dynamic (max. 600 $\mu\text{m}$ outside window system)
Fiber optic	One single-mode 4 $\mu\text{m}$ fiber (fiber-optical coupler)
Laser intensity	10 mW (modular laser systems up to 30 mW)
Laser wavelength	785 nm
Extraction of raw reflection signals	Yes , Multi Capture Signal Technology (MCST)
Measurement range	0.5-2000 $\mu\text{m}$

As can be seen in Fig. 2-9 the 3D ORM (APAS with MCST) represents different height of signals for different particle shapes.

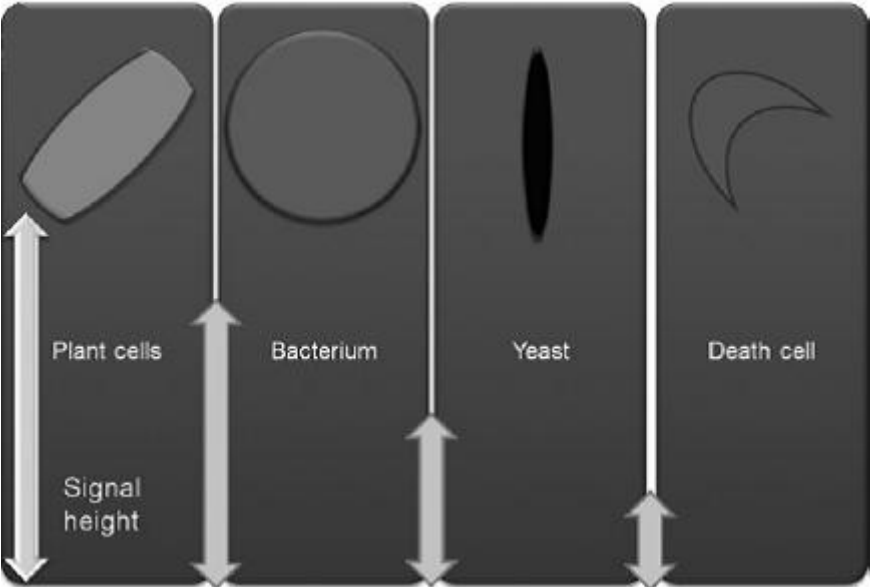


**Fig. 2-9:** Schematics of different particle shapes and their signal heights measured by the 3D ORM (APAS with MCST) [Hel13a].

In addition to OBF, other factor called COP (Coincidence Probability) indicates how close the particles are to each other that is defined by the following equation, where D is the distance between particles and n is number of particles.

$$\text{COP} = D/n \qquad \text{Eq. 2-3}$$

The presented results by Helmdach et al. [Hel13a] and Mostafavi et al. [Mos14b] clearly indicate the possibility of this technique for in-line particle analysis in terms of the size, number and the shape of the particles in various fields of the application. Diverse application possibilities of the 3D ORM (APAS with MCST) make this device highly favorable in the academic research.

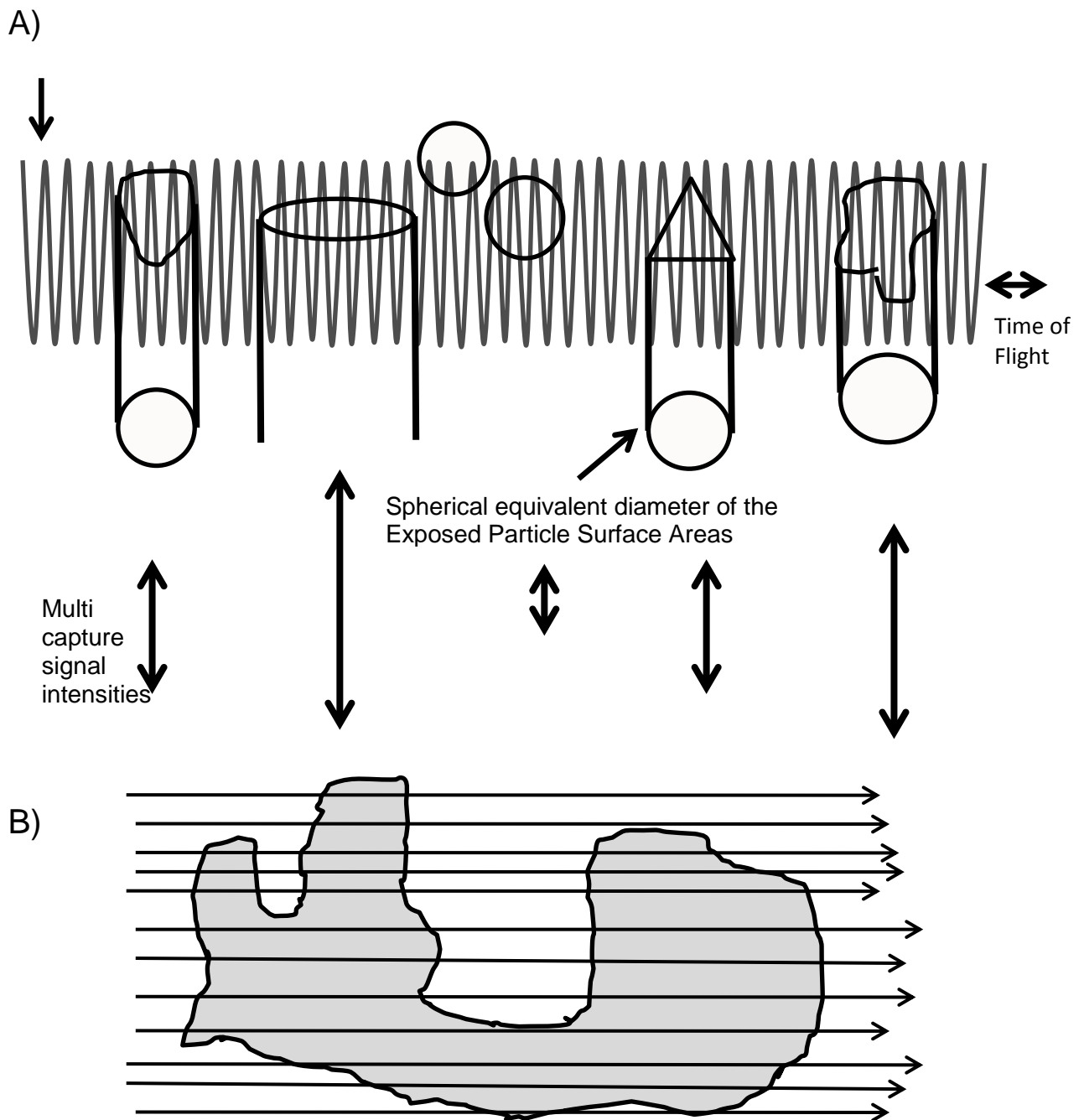


**Fig. 2-10:** In situ particle size analysis by a 3D ORM technique [Sch12b]. (A) The 3D ORM technique provides information on the Exposed Particle Surface area (EPSA) by application of the pulsed laser beam focus. By laser pulsation, this focus laser point moves up and down. The actual surface of a particle (area), not just the edge of the particles (one dimension as recorded by the FBRM measurement technique), can be measured. The particle size is determined by the time the particle is positioned inside the pulsed laser beam focus (time of flight) and the signal intensity. During the time of flight, laser and particle are interacting and the laser light is reflected back. (B) The 3D ORM technique measures not only the time of one signal (one dimension), but an Exposed Particle Surface Area (EPSA) which is related to the actual surface of the particle. This technique allows the interpretation of shapes due to different height of signal derived by the measured Exposed Particle Surface Area (EPSA) [Hel13a, Mos14b].

### 2.2.2.6 FBRM (focused beam reflectance measurement)

In the Focused Beam Reflectance Measurement (FBRM), a laser light source produces a continuous beam of monochromatic light focused to a small spot on the surface of the probe window. A pneumatic or electrical motor rotates the optics in such a way that the rotating focused beam of laser light is continuously scanning over particles that are passing in front of the probe.

Studies [Wyn03, Li05, Ru00, Sch12a, Wor05, Kem08, Yu08] have been performed for the determination of the Particle Size Distribution from the measured chord length distribution, CLD.

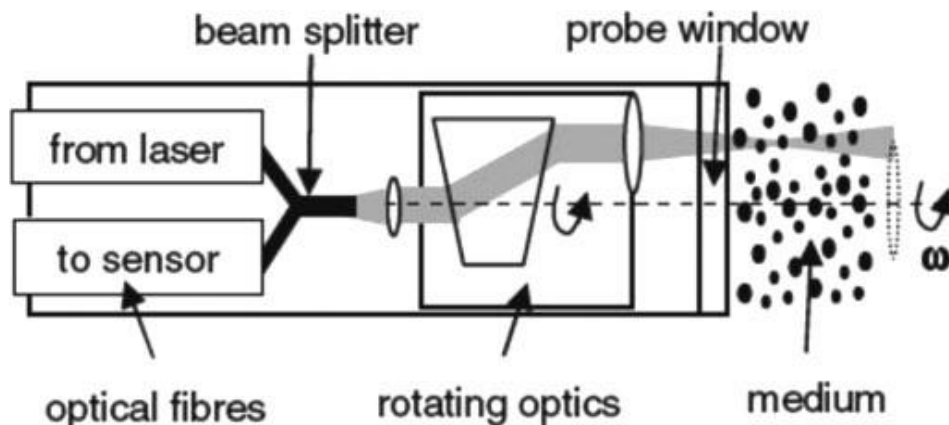


**Fig. 2-11:** Measurement principle of the laser scanner (FBRM instrument) [Hei12].

The suspended particles scatter the laser light back to the probe where the reflected light is detected. From the duration of each back scatter of light and the rotation velocity of the optics, the chord length can be determined [Mos14b].

The measured chord length distribution, CLD, is a function of the number and dimension of the particles in the suspension [Sch12]. Due to the random orientation of the suspended particles and the position where the laser beam can hit each of these particles, the particle size distribution (PSD) cannot be directly extracted from CLD [Sch12].

From these measurements (FBRM and 3D ORM), the total counts, which enable to define the suspension density in case the overall sample volume does not change, and the chord lengths, which can be used to define the size of the particles, can be defined. Table 2-2 presents the characteristics of the used FBRM instruments. Using FBRM, a focal point position of the laser is chosen at +20  $\mu\text{m}$  from the probe window.

**Table 2-2:** The features of the used FBRM techniques **[Hel13a]**.

Features	FBRM
Rotation of optical lens	Yes, with $2 \text{ ms}^{-1}$
Focal point	Fixed, (+20 $\mu\text{m}$ inside sapphire window)
Fiber optic	Two multimode 105/125 $\mu\text{m}$ fibers (beam splitter)
Laser intensity	0.9 mW at the probe window
Laser wavelength	780 nm
Extraction of raw reflection signals	yes
Measurement particle size range	0.5-2000 $\mu\text{m}$
Suspension density <b>[Hel14]</b>	SD: $\leq 80 \text{ wt}\%$

The FBRM as well as 3D ORM technique is based on the physical effect of the reflection. From one edge to the other edge (one-dimension) can be measured by the FBRM technique. The time of flight (TOF) only translated to the chord length using the FBRM technique **[Hel13a, Mos14b]**.



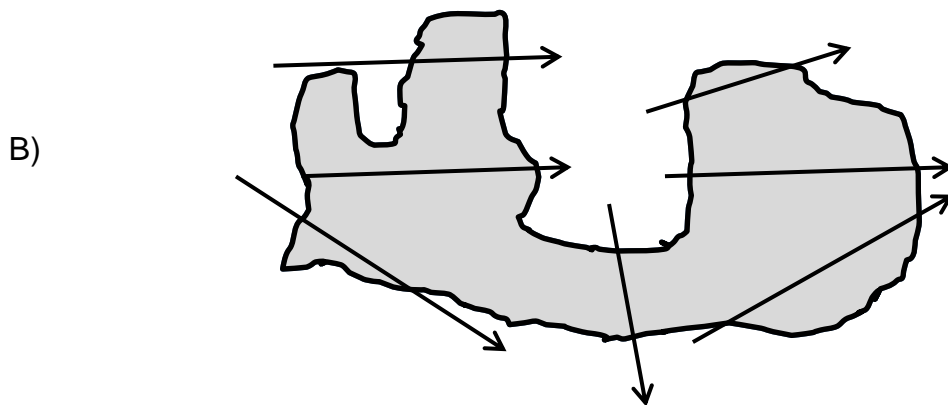
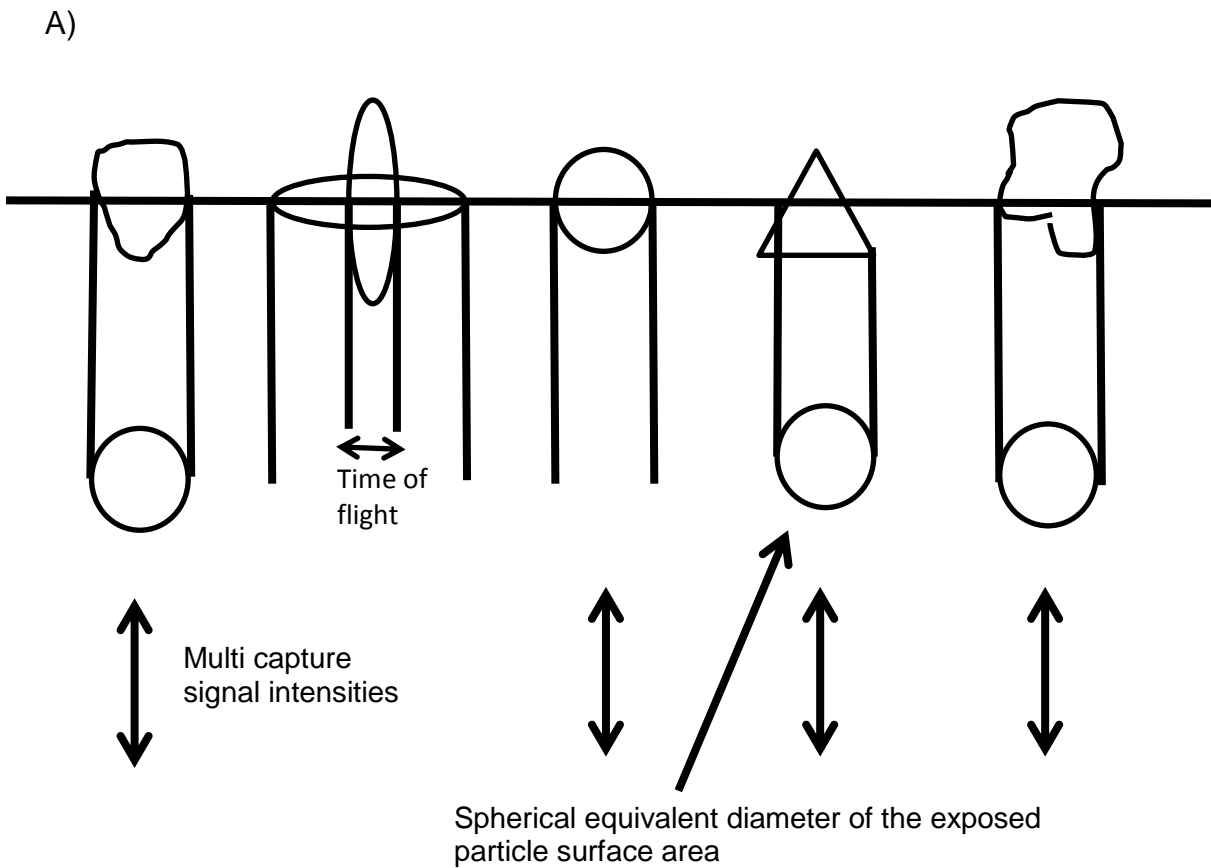


**Fig. 2-12:** In situ particle size analysis by the FBRM technique [Sch12b]. (A) In the FBRM technique, the pulse (time of flight) is detected by the FBRM probe and translated into a chord length (CL). The FBRM device provides information related to the chord length measurement which can be subsequently converted by the user if desired to a spherical equivalent diameter. A chord length (CL) is simply defined as the straight line distance from one edge of the particle to the other edge. Since a random distance of a particle surface is measured, the measured chord length is not necessarily the particle diameter. (B) The FBRM technique measures only from one edge to the other edge of the particle (one dimension) [Sch12b]

### **2.2.2.6.1 Determination of the solubility and metastable zone width by the FBRM technique**

Besides particle size measurements, one of the applications of the FBRM technique can be to determine the fundamental parameters of a crystallization process, including solubility and metastable zone width (MZW) [Bar02]. The focused beam reflectance measurement (FBRM) is one of the in situ instruments that have been applied extensively in the crystallization processes to provide qualitative as well as quantitative information about nucleation and crystal growth. Since the FBRM technique can only measure newly formed particles with detectable size, it can provide information on the nucleation and growth phenomena during the crystallization process by evaluation of the measured counts or chord length distribution [Abu09b].

Schoell et al. [Sch06b] showed that the combination of the ATR-FTIR spectroscopy with the FBRM techniques can be used to precise determination of the induction time that is the time span between attainment of a homogeneous supersaturation level throughout the reactor and the detection of particle formation. Furthermore, the FBRM technique has been used to determine the accurate induction time measurement as a function of supersaturation [Sch12].

### **2.2.2.6.2 Polymorphic or solvate phase transformation**

Different polymorphic or solvate forms are often different in the crystal shape. Schoell et al. [Sch06a] showed in situ measurement techniques such as FBRM or in-line microscopy can be used to monitor the polymorphic transformation in case studies of L-Glutamic acid during a crystallization process. The FBRM technique can detect the polymorphic phase transition of the L-Glutamic acid by exhibiting different chord length distribution (CLD) for  $\alpha$  - L-Glutamic acid and  $\beta$ -L-Glutamic acid. Furthermore, in situ microscopy along with ATR-FTIR and Raman spectroscopy also can be used to show the polymorphic phase transition of L-Glutamic acid [Sch06a]. A morphology change, which can be due to polymorph or solvate transformation, is directly exhibited in the measured CLD data.

### **2.2.2.6.3 Advantages and limitations in the FBRM technique**

One of the main advantages of the FBRM technique is its high statistical robustness, due to counting up to several hundreds of thousands of particles per second, depending on the suspension density and particle size. Furthermore, the FBRM technique can be applied in a wide range of process condition such as temperature, pressure and solid concentration. In principle, there is no upper limit of suspension density that can be measured through the FBRM technique. However, the measured CLDs do not correlate with particle concentration in a linear way at higher suspension densities. The FBRM technique is also sensitive to the counting of the fine particles and consequently it can monitor some events like nucleation, breakage and dissolution which can have a major impact on the final product quality. Consequently,

the FBRM technique can be considered as a process characterization and optimization tool, appropriate for monitoring the particle system dynamics in terms of rate and degree of change in particle number and dimension. This permits the user to study different process parameters on the particulate product.

The difficulties in the calculation of the Particle Size Distribution from the Chord Length Distribution (CLD) are one of the limitations of the FBRM technique. The measured CLD can be influenced by the stirring conditions in the crystallizer and the flow field around the probe. For instance, Yu et al. [Yu05] used the FBRM technique in the anti-solvent crystallization of paracetamol from water-acetone mixture and found elevated agitation decreases the measured chord length by the FBRM technique and consequently reduces the agglomeration degree of the big particles. Further information on this research can be found in [Yu05].

Furthermore, the size, shape, and number of particles in the suspension can influence the CLD [Kai07]. However, an absolute conclusion concerning the particle shape is not possible by this technique [Mos14b].

## **2.2.3 The polymorphic or solvate forms monitoring**

In industries, especially, in the pharmaceutical industry, it is essential to obtain understanding conditions of the formation of different solvates or polymorphic forms as well as their specifications by using characterization techniques.

Different polymorphic or solvate forms based on the change in the shape or size can be identified using many characterization techniques. These techniques can be categorized as off-line and in-line techniques.

Typical off-line techniques for identification of different polymorphic or solvate forms include:

### **2.2.3.1 Microscopy**

#### **2.2.3.1.1 Optical microscopy**

This technique generates information on the morphology of crystals, which can be applied to distinguish between different polymorphic or solvate forms of a substance [Rod04].

#### **2.2.3.1.2 Scanning electron microscopy (SEM)**

Provides a two-dimensional morphological image with higher resolution compared to the optical microscopy and similar to the optical microscopy is used to differentiate between different polymorphic or solvate forms [Yu98].

Some in-line techniques to identify the polymorphic transition are:

### **2.2.3.2 Spectroscopic analysis**

#### **2.2.3.2.1 Fourier transform infrared (FTIR) spectroscopy**

The measurement principle of the Fourier Transform Infrared spectroscopy is explained in the 2.2.1.1 section. The different polymorphic or solvates forms due to possessing different functional groups produce different spectrum. It is proved that this technique is able to identify different polymorphic forms by comparing the spectra of the sample with the reference [Alz02].

#### **2.2.3.2.2 Raman spectroscopy**

Contrary to the infrared spectroscopy, a monochromatic light is used to irradiate a sample in Raman spectroscopy. This technique is able to identify different polymorphic forms by providing characteristic peaks for different polymorphic forms. It is shown by Caillet et al. [Cai06], [Cai07], [Cai08] that Raman spectroscopy is a useful tool to monitor the solvent-mediated phase transition in a case study with citric acid due to producing specific spectra for monohydrate and anhydrate of citric acid.

The Raman spectroscopy has been developed to determine the relative concentrations of different polymorphic or solvate forms of a pharmaceutical compound Helmdach et al. [Hel13b] have demonstrated that Raman spectroscopy is applied to determine the polymorphic form content in a case study with L- Glutamic acid in water. More explanation in this study can be found in the literature of [Hel13b]. Generally, Raman spectroscopy is used to monitor the solid composition and solid concentration as well as liquid concentration. Various factors such as crystal size, temperature, solute and solid concentration on the Raman spectra were analyzed by Simon et al. [Sim14a] in order to design a good calibration strategy for polymorphic form quantification of a case study with O-Amino Benzoic Acid (OABA) in the solution of isopropyl alcohol (10%) and water (90%).

It was found that Raman spectroscopy is a useful tool for in-situ characterization of complex polymorphic slurry systems, especially for the determination of transformation rates and elucidation of the phase transition of the different polymorphic or solvate forms.

### **2.2.3.3 Ultrasound technique (single-frequency)**

Application of the ultrasound technique (single frequency) in the crystallization processes of polymorphs and solvates can be great benefit. Strege [Str04] has shown that the ultrasound technique (single frequency) can successfully be applied to monitor the phase transformation of inorganic substances as well as organic substances. The polymorphic phase transition can be monitored by change in the ultrasound velocity and temperature. Since temperature and concentration changes during the polymorphic or solvate phase transition and ultrasound velocity depends on these parameters, the change in the ultrasound velocity and temperature can be seen during the polymorphic phase transition.

### **2.2.3.4 FBRM techniques**

The FBRM technique is used as an in-line technique to monitor the polymorphic phase transition.

Sathe et al. [Sat10] have used the FBRM technique to monitor the polymorphic phase transition of acitretin form III to form II in the alcoholic slurry. This polymorphic transition can be monitored by the change in the chord length distribution. Furthermore, the Particle Vision Monitoring (PVM) technique is applied to monitor the change in the particle shape during the polymorphic phase transition of this mentioned case study.

### **2.2.3.5 3D ORM (APAS with MCST) technique**

The 3D ORM (APAS with MCST) as well as FBRM techniques are in-line techniques to monitor the polymorphic phase transition.

This technique shows sensitivity (change in the measured length) with respect to the variation in the particle shape during the polymorphic phase transition and consequently this technique can monitor the polymorphic or solvate phase transition. Helmdach et al. **[Hel13a]** demonstrated the use of this technique to monitor the polymorphic or solvate transition in a case study with L-glutamic acid. The polymorphic phase transition of L-glutamic acid from  $\alpha$  form to  $\beta$  form can be monitored by the change in the measured D90 (weighted by number) **[Hel13a]**.

### 3. Aim of the present work

It is important to control crystallization processes based on the information out of the running process (liquid and solid phase) in order to produce products with required high quality (purity and certain crystal size as well as crystal size distribution (CSD)). Crystallization processes from solution are usually performed in suspension densities of 10 to 40 Vol-% and with crystal sizes of 50 to 500  $\mu\text{m}$ . There are only few measuring techniques which can be used under those conditions. The liquid phase (solute concentration and supersaturation) has to be controlled to maintain the process within the metastable zone and to prevent primary homogenous (spontaneous) nucleation and also to achieve the optimal crystal growth rate for the suspended crystals. The solid phase (the crystal size as well as suspension density) has also to be monitored in order to obtain information related to the progress of the crystallization process (see **[Ste13]**).

Furthermore, crystalline phases can exist in different lattice arrangements (polymorphs) and also can incorporate solvents (solvates). Since polymorphic or solvate forms may have different functionalities and physical properties, such as bioavailability, solubility, melting point, crystal shape, hardness, density and stability, it is necessary to investigate the appropriate existing conditions for each polymorphic or solvate form and the probability of a transformation between them. In the pharmaceutical industry, this phase transition can lead to an additional complexity with regard to the processability and bioavailability of drugs. Furthermore, a phase transition can generate a severe risk to patients. Consequently, pharmaceutical manufacturers have to select a polymorphic or solvate form that has desirable characteristics that will assist in the efficient performance of the drug products **[Abu10, Sch13]** and the whole crystallization process must be monitored to ensure that the desired polymorph or solvate is produced.

For these mentioned purposes, appropriate analytical techniques are required to monitor in-line process parameters (liquid and solid phases) or polymorphic phase transition during a crystallization process to ensure the preferred product properties.

Although extensive studies have been conducted in order to control in-line or on-line process parameters including the liquid phase **[Abu09, Abu10, Bil10, Gla04, Hel15, Lew01, Oma99, Sch95, Sch07, Sim09, Tho05, Tit03]**, the solid phase **[Abu10, Gee03, Smi10, Mou02, Pin95, Per11, Say02, Sch12, Ste13]** or polymorphic phase transition **[Cai06, Cai07, Cai08, Hel13a, Hel13b, How09, Sat10, Str04, Yu05]** using appropriate analytical techniques, further investigation with respect to this subject (measuring techniques) have to be carried out. For instance, since not all matters related to the applicability of these measuring techniques in the pilot scale are clear up to date, further studies need to be performed.

The transferability of measuring techniques from lab scale into pilot scale is one of the topics needed to be more investigated. Helmdach et al. **[Hel15]** found that a direct transfer of the calibration models (solute concentration) from lab scale into

pilot-plant scale is possible if the influence of air bubble in the pilot plant is low. Measuring techniques do not show correct results with respect to the examined parameters in the presence of air bubbles in a process. For instance, Helmdach et al. [Hel12a] evaluated the influence of air bubbles on the outcome of some sizing techniques including FBRM, 3D ORM and the ultrasound technique and found that air bubble can influence the measured number of crystals especially, in high-viscose suspensions. This work will also focus on the influence of air bubbles on the measurement of different crystal sizes in different suspension densities.

The selected measuring techniques which are capable to give results under to processes conditions for crystallization processes from solution are: ultrasound, 3D ORM, FBRM techniques. Those techniques will be examined here.

The question of the influence of particle shape on the signals measured by the different measuring techniques and whether they lead to big errors or could be used to monitor phase transition is an open point. In addition to the purity, stability or particle size of a compound, features like morphology influence the quality of the product and are of great importance. Furthermore, the shape of a crystal is as a significant parameter in the pharmaceutical crystallization processes, since the surface area of a crystal influence the dissolution rate of drugs. Moreover, the shape, e.g. needles of crystalline material can modify the recorded result of some sizing techniques in a way that wrong values may be calculated from the signals. Most measuring techniques assume a spherical shape for the suspended particles. However, this assumption is in most cases not true [Ahu78]. This work also will focus on the effect of the particle shape on the result of different measuring techniques in the crystallization process.

As mentioned before, it is required to investigate the exact stability conditions (temperature or concentration) of a desired polymorphic or solvate in different case studies using new characterization techniques. Moreover, the combined results of these new measuring techniques show the capability to provide a unique insight into the polymorphic phase transition. The last objective of this research is a full understanding of the ability to monitor the phase transition in some case studies using simultaneously two rather new PAT tools, the ultrasound (single frequency) and 3D ORM techniques.

Since different measuring techniques have different outcomes due to their variety in the measuring principles, it is necessary to select different measuring techniques in order to test their applicability in a crystallization process or a polymorphic phase transition. Furthermore, different case studies including organic or inorganic substances will be used to investigate the robustness or limitations of these measuring techniques.



## **4. Materials, methods and procedures**

### **4.1 Materials**

The materials are considered according to aims defined in each part of this research. Not the crystallization but rather the measuring techniques are in the focus of the research. For instance, in order to investigate the effect of the particle shape on outcome of the in-line sizing techniques, two substances (ammonium chloride and L-threonine) with different shapes (cubic and needle like) were selected.

**Table 4-1:** Some characteristics of the used substances in different experiments

Material	Supplier	Purity	Solubility curve																
Sugar	Super market	≥99 %	<p>[Bub95a]</p> <table border="1"> <caption>Data for Sugar Solubility Curve</caption> <thead> <tr> <th>Temperature [°C]</th> <th>Concentration (g sucrose/g water)</th> </tr> </thead> <tbody> <tr><td>0</td><td>1.8</td></tr> <tr><td>20</td><td>2.0</td></tr> <tr><td>40</td><td>2.5</td></tr> <tr><td>60</td><td>3.2</td></tr> <tr><td>80</td><td>4.0</td></tr> <tr><td>100</td><td>5.0</td></tr> <tr><td>110</td><td>5.2</td></tr> </tbody> </table>	Temperature [°C]	Concentration (g sucrose/g water)	0	1.8	20	2.0	40	2.5	60	3.2	80	4.0	100	5.0	110	5.2
Temperature [°C]	Concentration (g sucrose/g water)																		
0	1.8																		
20	2.0																		
40	2.5																		
60	3.2																		
80	4.0																		
100	5.0																		
110	5.2																		
L-Threonine	Carl Roth	≥99 %	<p>[Daw59]</p> <table border="1"> <caption>Data for L-Threonine Solubility Curve</caption> <thead> <tr> <th>Temperature [°C]</th> <th>Concentration [g/100g water]</th> </tr> </thead> <tbody> <tr><td>20</td><td>9</td></tr> <tr><td>30</td><td>10.5</td></tr> <tr><td>50</td><td>14</td></tr> <tr><td>60</td><td>19</td></tr> </tbody> </table>	Temperature [°C]	Concentration [g/100g water]	20	9	30	10.5	50	14	60	19						
Temperature [°C]	Concentration [g/100g water]																		
20	9																		
30	10.5																		
50	14																		
60	19																		
Ammonium Chloride	Carl Roth	≥99 %	<p>[Zap02]</p> <table border="1"> <caption>Data for Ammonium Chloride Solubility Curve</caption> <thead> <tr> <th>Temperature [K]</th> <th>Concentration [g/100 g solution]</th> </tr> </thead> <tbody> <tr><td>270</td><td>23</td></tr> <tr><td>300</td><td>29</td></tr> <tr><td>330</td><td>35</td></tr> <tr><td>360</td><td>41</td></tr> <tr><td>390</td><td>47</td></tr> </tbody> </table>	Temperature [K]	Concentration [g/100 g solution]	270	23	300	29	330	35	360	41	390	47				
Temperature [K]	Concentration [g/100 g solution]																		
270	23																		
300	29																		
330	35																		
360	41																		
390	47																		
Magnesium sulfate hexahydrate	Carl Roth	≥99 %	See chapter 4.2.4.1																
di-sodium tetraborate pentahydrate	Alfa Aesar	≥99 %	See chapter 4.2.4.2																
Sulfathiazole	Alfa Aesar	≥99 %	See chapter 4.2.4.3																

## 4.2 Methods and procedures

### 4.2.1 Study of the sucrose crystallization using ultrasound technique

Studying the sucrose crystallization, needed the following steps:

- I. The saturation and the nucleation points of sugar solution were determined by means of the ultrasound technique in order to ensure that the metastable zone is wide enough and its limits are known for the desupersaturation measurements within the metastable zone. The measurement of the metastable zone width was performed in a jacketed crystallizing vessel. The experimental steps for determination of the metastable zone width of a sucrose solution involve:
  - (a) Heating the saturated solution of sucrose 10°C above the saturation temperature and keeping it at this temperature for 3 h until all of the crystals dissolved.
  - (b) Cooling the saturated solution of sucrose by a constant cooling rate (e.g. 5K/h) until nucleation occurred.
  - (c) Heating the saturated solution of sucrose by the same rate (e.g. 5K/h) until all of the crystals are dissolved again. (As described e.g. by Titz-Sargut et al. [Tit03]).
- II. In order to determine the concentration of a solution from the measurement of the ultrasound velocity and temperature, the correlation between these parameters were determined. The experimental procedures include:
  - (a) Preparing the different experimental solutions of sucrose with addition of defined amounts of sucrose in distilled water in a closed vessel (crystallizer) and stirring strongly using a magnetic stirrer.
  - (b) Cooling the solutions with constant a cooling rate (3K/h) from 65°C to 58°C.
  - (c) Measuring the change in the ultrasound velocity with temperature at in each case with defined concentration by a single frequency ultrasound technique.
- III. The supersaturation curve of sucrose solution was measured in seeded isothermal batch crystallization experiment. The experimental steps for the determining of the desupersturation curve involve:
  - (a) Cooling the saturated solution of sucrose by slow cooling rate (5K/h) until half of the metastable zone width is reached (the value must be known).
  - (b) Addition of a defined amount of seed crystals with specified particle size range.

- (c) Decreasing in the supersaturation after seeding due to crystal growth. The ultrasound velocity was measured versus time at constant temperature by means of the emerged protected ultrasound sensor. The mesh of the protective jacket should be fine enough to keep the particles out of the measuring section. Furthermore, the solution must flow sufficiently through the measuring section.

#### **4.2.2 The influence of air bubbles on the measurement of different crystal sizes and suspension densities by the 3D ORM measurement technique**

Saturated sucrose-water solution was prepared according to the solubility data. Each experiment was started with a saturated solution at 25 °C [Mat95].

During the isothermal experiments, defined amounts of crystals with different size ranges of sucrose, separated by sieving, were added to the saturated solutions. Three different suspension densities (5-10-15 Vol-%) each with particle size ranges of 20-200 µm were measured by 3D ORM probe.

These experiments started with a suspension density of 15 Vol-% and were subsequently diluted, step by step for each measured suspension density, by adding defined amounts of saturated solution [Per11]. These experiments were performed in a jacketed glass vessel and an external thermostat was used to control temperature (isotherm at 25°C). The crystallizer was equipped with a propeller stirrer and 3D ORM. The stirring speed in these experiments was 500 rpm. A 3D ORM 523 PsyA CSD Particle Analyzer is used for these experiments. The laser (860 nm, 0.85 Mw; Laesr class I) beam focus rotates with a constant speed of 2 ms<sup>-1</sup>. The diameter of the ORM focal point is 5-10 µm. The measurements were performed using the software Win-ORM 6.7 (Sequip S&E GmbH, Germany) [Seq13].

In next step, the surfactant Tween 20 (polyoxyethylene sorbitan monolaurate) was added to a saturated solution of sucrose and defined amounts of particles. The Tween 20 concentration in the saturated sucrose solution was 0.005 Vol.-%. After adding the surfactant, the solution was moderately stirred for 5 h at low speed stirring (200 rpm) to remove the air bubbles/ for degassing.

## **4.2.3 Effect of particle shape on inline particle size measurement technique**

### **4.2.3.1 Ultrasound probe**

For the investigation of particle shape two systems with different shapes are selected:

a: sugar-water (substance shape [Bub95b]: hexagonal prism)

b: L-Threonine-water (substance shape [Lek04]: needle like)

First, defined amount of L-Threonine with sieved particle size ranges of 80-200  $\mu\text{m}$  was considered and by taking in consideration that the particle number and the volume of each particle in both mentioned systems remain the same, the amount and the size of sugar particles were calculated. During the isothermal experiments, defined amounts of these mentioned substances were added to saturated solution and the single frequency ultrasound technique was used to measure the ultrasound velocity of these two systems.

### **4.2.3.2 Laser backscattering probes**

For investigation of the effect of particle shape on the measured results two systems were selected. The first: Ammonium Chloride-water (distilled) as a substance that has a cubic shape and the second: L-Threonine-water (distilled) as a substance that has a needle like shape.

Saturated L-Threonine-water and Ammonium Chloride-water solutions were prepared according to the solubility data [Daw59, Zap02]. Each experiment was started with a saturated solution at 20 °C.

During the isothermal experiments, defined amounts of particles with different size ranges of L-Threonine and Ammonium Chloride, separated by sieving, were added to the saturated solutions. Two different suspension densities (10-15Vol-%) each of them with sieved particle size ranges of (80-200  $\mu\text{m}$ ), were measured by the FBRM and 3D ORM (APAS with MCST) probes.

These experiments started with a suspension density of 15 Vol-% and were subsequently changed, for each measured suspension density, by adding defined amounts of saturated solution in order avoid undesired air intake during addition of solids [Per11].

## **4.2.4 The phase transition of crystals in-line**

Three compounds (two inorganic and one organic) were considered in order to measure in-line the solvent mediated phase transition.

#### 4.2.4.1 Magnesium sulfate

Magnesium sulfate forms various hydrates in aqueous solution. Experiments have been performed with two types of these hydrates, the magnesium sulfate heptahydrate and magnesium sulfate hexahydrate known as epsomite and hexahydrate.

According to drawings depicted in the literatures [Str04], the crystal system of magnesium sulfate hexahydrate is monoclinic prismatic, while magnesium sulfate heptahydrate belongs to the orthorhombic –disphenoidal crystal class. Photos of both modifications are given by Strege [Str04].

According to Otto [Ott02], the transition temperature between epsomite and hexahydrate is approximately 48.1°C (see Fig. 4-1). At higher temperatures than this transition point, hexahydrate is the stable form while epsomite is the stable form at temperatures below this transition point.

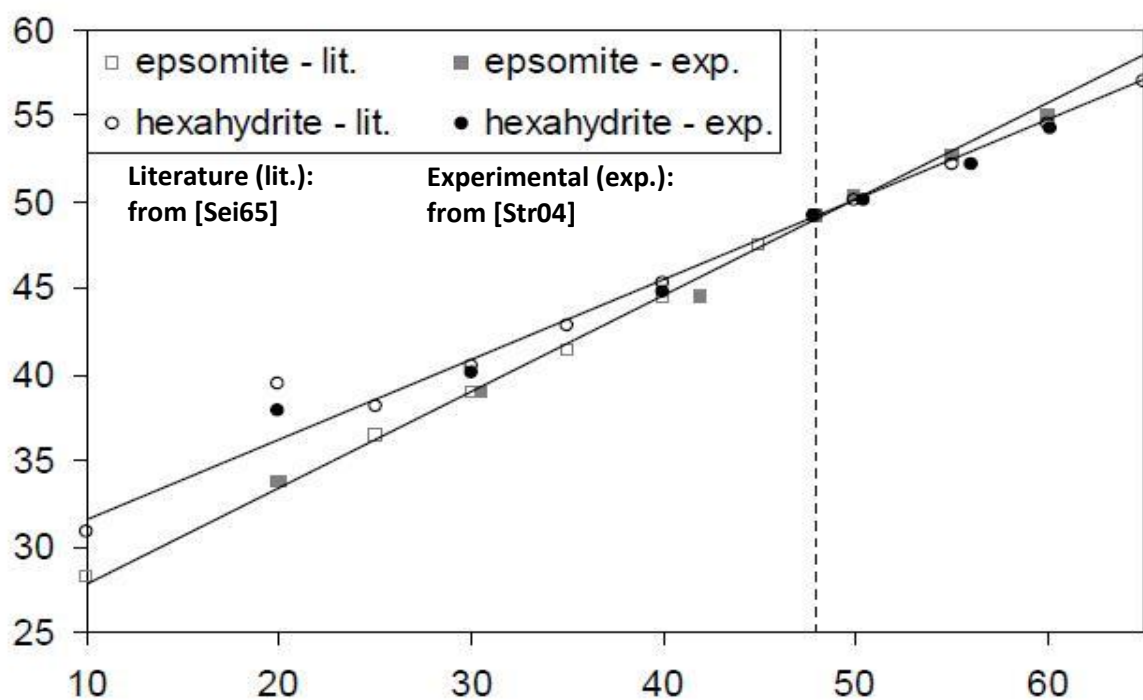


**Fig. 4-1:** Solubility of magnesium sulfate heptahydrate and hexahydrate in an aqueous solution at different temperatures. Filled signs show experimental solubility data from [Str04] and unfilled signs show solubility data from [Sei65].

The experimental steps for the phase transition experiments include:

- Cooling of a saturated solution of magnesium sulfate hexahydrate until the onset of hexahydrate nucleation.

- (b) Keeping the temperature constant to decrease the supersaturation by growth of the nucleated magnesium sulfate hexahydrate.
- (c) Further cooling to dissolve the magnesium sulfate hexahydrate and a subsequent nucleation and growth of epsomite.

#### 4.2.4.2 Di-sodium tetraborate pentahydrate

The second substance applied in this study is di-sodium tetraborate pentahydrate that can be transformed to di-sodium tetraborate decahydrate at 60.8°C [Smi02]. According to Smith [Smi02], above this transition point, pentahydrate is the stable form, while decahydrate is the more stable form at temperatures below this transition point (see Fig. 4-2).

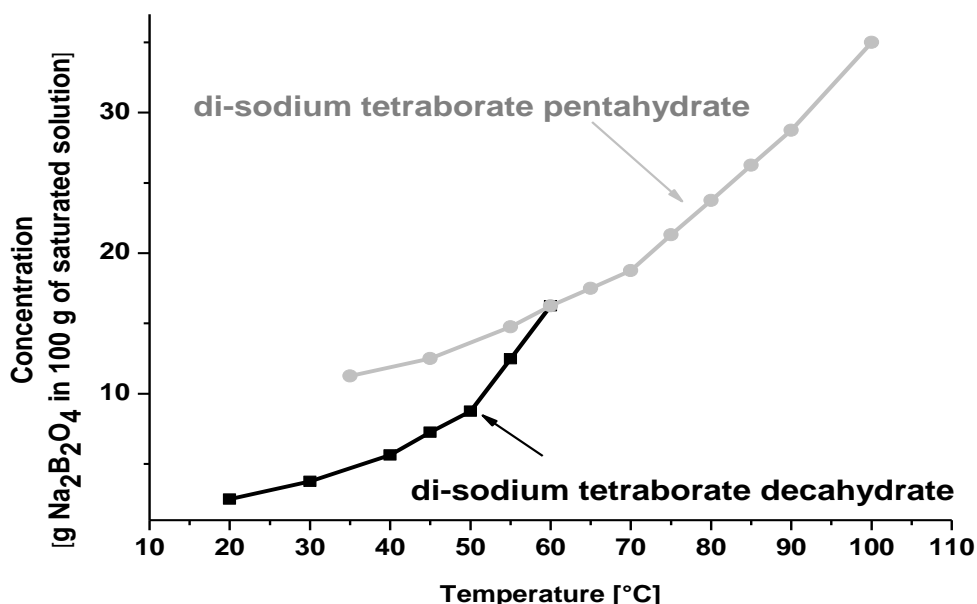


**Fig. 4-2:** Solubility curve of di-sodium tetraborate pentahydrate and decahydrate in water at different temperatures. Data derived from [Smi02].

The habits of di-sodium tetraborate pentahydrate crystals are hexagonal-rhombohedral, while decahydrate crystals belong to the monoclinic prismatic class [Gem73, Lev78]. The photos of di-sodium tetraborate pentahydrate and decahydrate are presented by Strege [Str04].

The experimental steps for the phase transition experiments involve:

- (a) Cooling of a saturated solution of di-sodium tetraborate pentahydrate until the start of pentahydrate nucleation.
- (b) Keeping the temperature constant in order to decrease in the supersaturation by growth of the nucleated pentahydrate.
- (c) Further cooling for a dissolution of the pentahydrate and subsequently nucleation and growth of the decahydrate.

### 4.2.4.3 Sulfathiazole

Sulfathiazole (4-amino-N-(1, 3-thiazol-2-yl) benzene sulfonamide), an antimicrobial agent, has been chosen as the third compound applied in this study. According to Abu Bakar et.al. [Abu08a], it has four polymorphs (form I, II, III and IV) all with different morphologies. The microscopic images of the different polymorphic forms of sulfathiazole are shown in Fig. 4-3.

Form I is needle or rod like shaped (see Fig. 4-3) and was used in this study and was prepared by natural cooling from 80 °C to 20 °C of a saturated solution of sulfathiazole in pure n-propanol (7.2 g sulfathiazole in 300 g of n-propanol) [Abu09a].

All of the crystallized solids produced by this method were vacuum filtered and were dried at 70 °C for 24 hours. All of the crystallized form can be dried in the hot air oven.

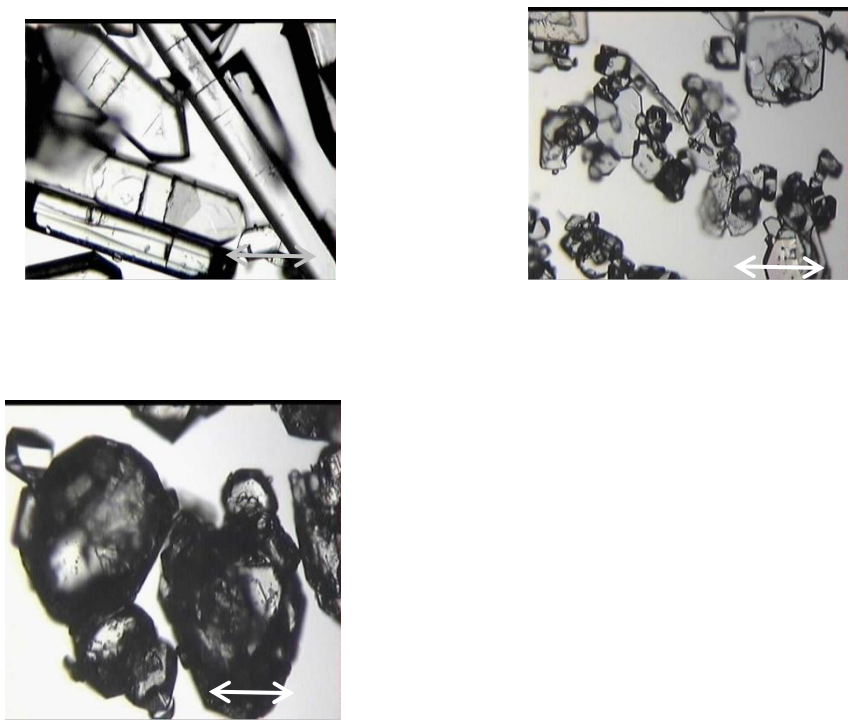


**Fig. 4-3:** Microscopic images of different polymorphic forms of sulfathiazole. a) form I b) form II c) form III. The scale bar represents 200  $\mu\text{m}$  for all of the microscopic images [Abu08a]. Regarding to the morphology, some of these represented crystals seem to be in agreement with those of pure polymorphs reported in the literature [Abu08a]. According to the literature [Abu08], form I has needle-like shape, form II is a cuboid, and form III is a truncated hexagon.

Although the polymorphic forms of sulfathiazole have been comprehensively investigated, it is according to some authors (e.g. Abu Bakar et al. [Abu09a, Abu11]) difficult to produce pure polymorphs as crystalline products. Most of the time, the



desired polymorphic forms include impurities from at least one other form. For instance, traces of form II and III can be observed during the crystallization of sulfathiazole in n-propanol –if not totally dry– from which form I should be obtained.

The solubility of form I and III in water is presented in Fig. 4-4 [Kho93]. Due to the lower solubility of form III compared to form I (see Fig. 4-4) at different temperatures, this form is more stable than form I in water.

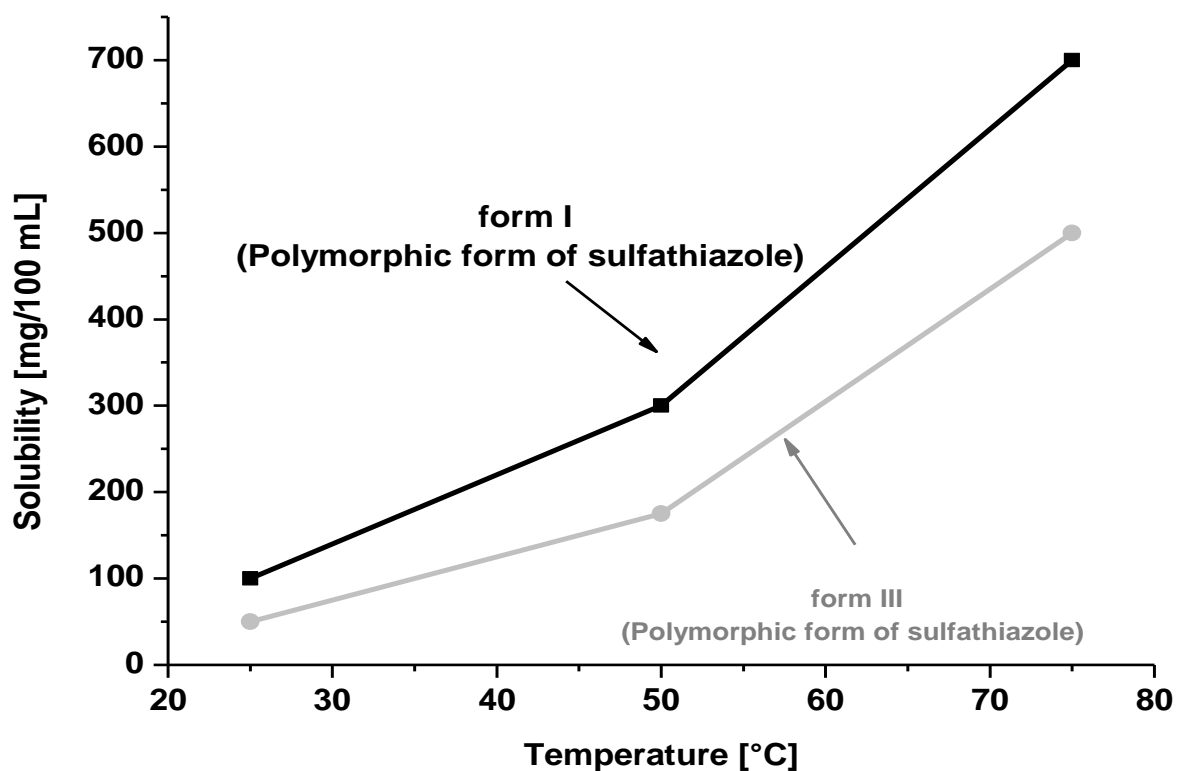


**Fig. 4-4:** The solubility of sulfathiazole polymorphic form I and form III as a function of temperature in water [Kho93].

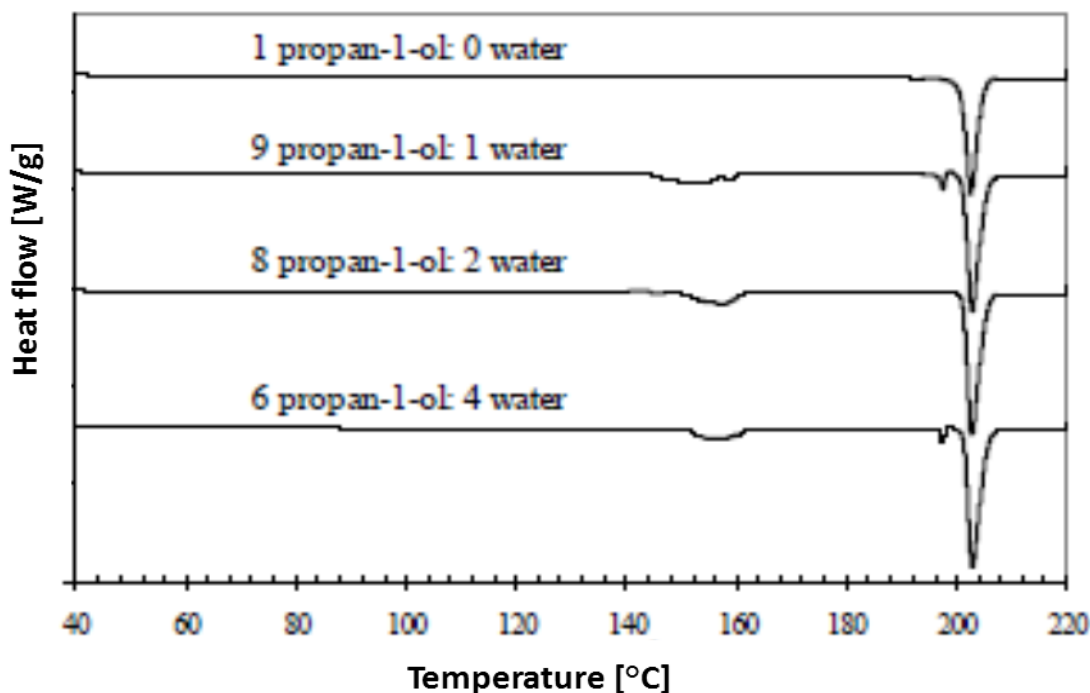


**Fig. 4-5:** DSC thermograms of the crystals formed at different mixture of n-propanol: water [Abu08b].

Fig. 4-5 illustrates the DSC thermograms of the crystals acquired from different mixtures of solvents (water: n-propanol). Lagas et al. [Lag81] have shown that a complete melting of form II at its melting temperature of 197°C can only be observed if the crystals are pure form II. If only a little amount of form I ( $T_m = 203^\circ\text{C}$ ) is present melting together with form II it melts at 198°C. Furthermore, a form III transformation into form I in the temperature range of 150-170 °C happens without presenting any melting point of form III at 175°C.

As proved by DSC analysis [Abu08b], the crystals obtained from pure n-propanol are form I since they produce only one melting peak at 202 °C related to the melting point of form I.

Furthermore, crystals acquired from different mixtures of n-propanol and water are mixtures of form I, II and III since they generated melting peaks at 203°C corresponding to the melting point of form I, 198°C related to the melting point of form II in the presence of form I and peaks in the range temperature of 150-170°C represented the polymorphic transition of form III into form I. Consequently, the results achieved by DSC analysis technique suggest that only crystals obtained from pure n-propanol are form I and crystals taken from different mixtures of n-propanol: water are mixtures of form I, II and III [Abu08b].

## **6. Results**

In this chapter, the results focusing on the benefits, problems and limitation in application of the examined in-line measuring techniques such as ultrasound (single frequency) technique, 3D ORM and FBRM are presented. For these studies different experimental set-ups and case studies have been used. Furthermore, some off-line techniques such as optical microscopy are used to evaluate some of the results obtained by the in-line measuring techniques.

### **6.1 The ultrasound technique: here the example of sucrose crystallization**

It is essential to determine the metastable zone width as well as the level of the actual supersaturation to control the crystallization process and achieve a high quality product. As explained in the chapter 2, the ultrasound technique is one of the robust techniques which enables to determine supersaturation as well as the metastable zone width.

#### **6.1.1 Determination of the metastable zone width using the single frequency ultrasound technique (case study: sucrose)**

The response of the ultrasound technique during this cycle (cooling and heating of the saturated solution) can be used to specify nucleation and saturation temperatures (see Fig. 6-1). The ultrasound velocity and temperature of the prepared solutions were measured using a LiquiSonic 30 immersion sensor. This procedure has been carried out for other substances e.g. glycine, ibuprofen, citric acid, paracetamol, artemesinic acid [Hel15], copper sulfate pentahydrate and potash alum [Gla04].

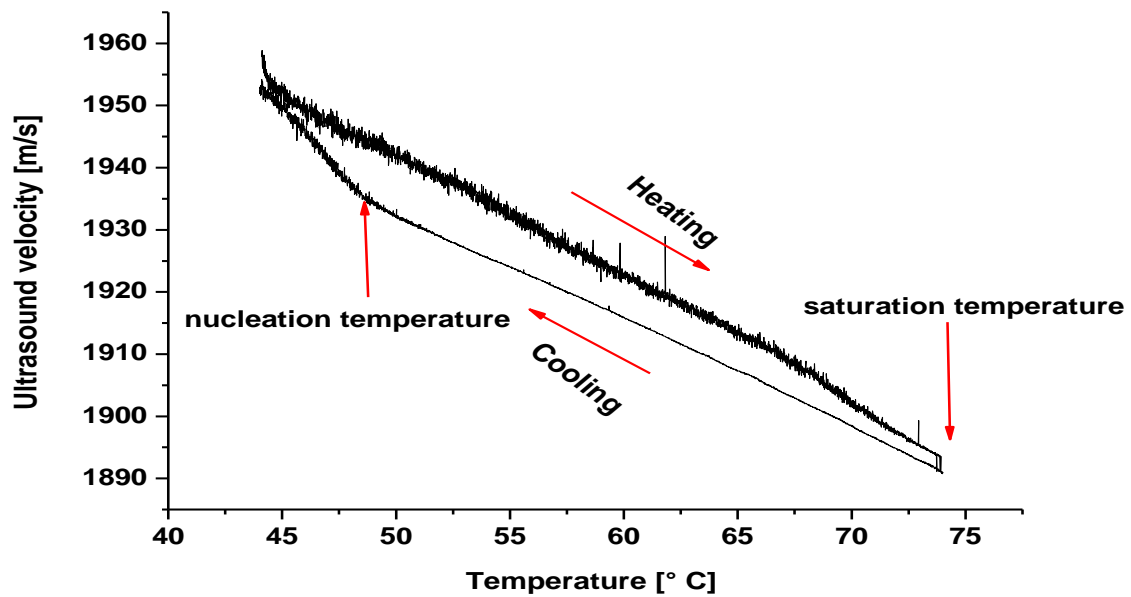


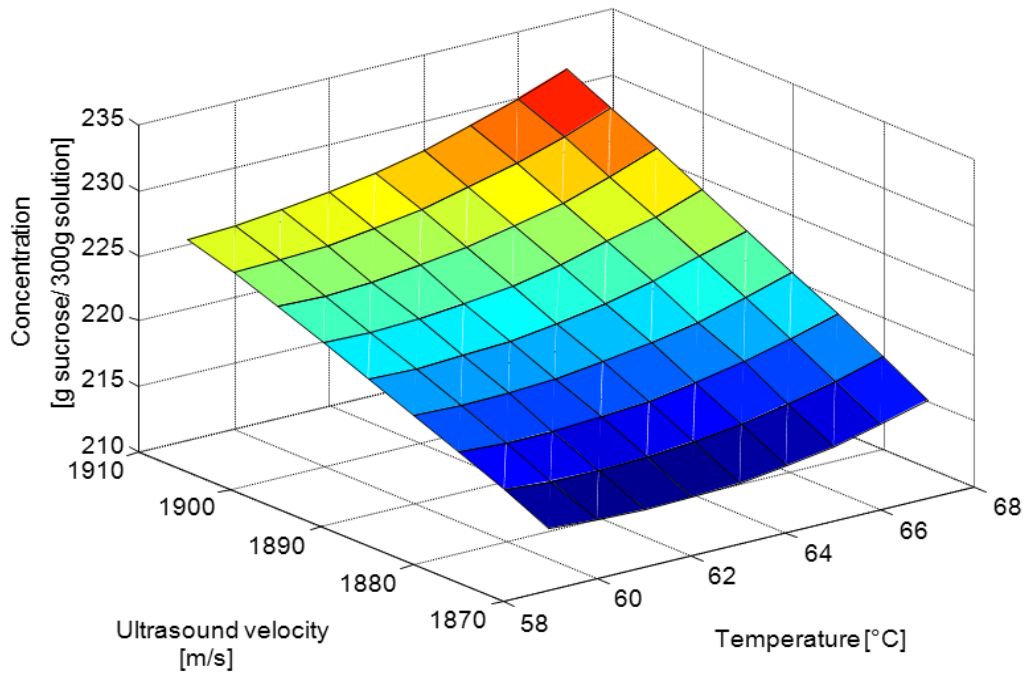
**Fig. 6-1:** Determination of the limits of the metastable zone width of sucrose solution by means of the single frequency ultrasound technique.

As can be seen in the Fig. 6-1, the ultrasound velocity (measured data in Fig.6-1) increases linearly with decreasing in temperature. When nucleation occurs, the increase in the ultrasound velocity is not anymore linear and a sudden acceleration in the increase in the ultrasound velocity with decrease in temperature occurs (see Fig. 6-1). This point is specified as the nucleation temperature. During the heating cycle, the ultrasound velocity decreases with increase temperature and intersects the cooling curve when all crystals are dissolved. The point of intersection is determined as saturation temperature. The temperature difference between the nucleation point and the saturation point represents the width of the metastable zone.

### **6.1.2 Measurement of the ultrasound velocity versus concentration and temperature using the single frequency ultrasound technique (case study: sucrose)**

The experimental procedure for this measurement is explained in chapter 5. The change in the ultrasound velocity with temperature at each concentration are measured by a single frequency ultrasound technique and are presented in Fig. 6-2.

(a)



(b)

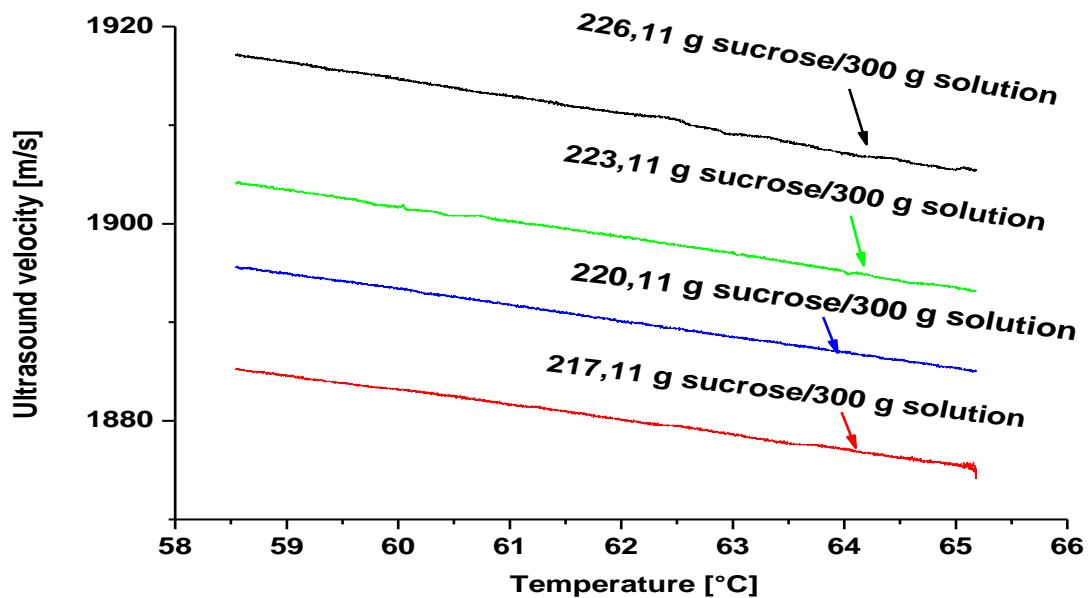


**Fig. 6-2:** Ultrasound velocity versus temperature for different concentration of sucrose. (a) This is plotted by the MATLAB software (the variation of three parameters, ultrasound velocity, temperature and concentration). (b) (Black line: 226,11 g sucrose/300 g solution, green line: 223,11 g sucrose/300 g solution, blue line: 220,11 g sucrose/300 g solution, red line: 217,11 g sucrose/300 g solution).

The ultrasound velocity through the liquid media depends on the density and adiabatic compressibility of the medium. In order to define the concentration of sucrose in water using the ultrasound sensor, it is essential to develop a correlation where the concentration can be directly obtained from the measured ultrasound velocity and temperature by means of the ultrasound probe. The dependence of the ultrasound velocity and temperature at different concentrations of sucrose in water as illustrated in Fig. 6-2. This figure shows a linear dependence of the ultrasound velocity on the temperature at constant concentration of solute (sucrose). With increasing concentration the ultrasound velocity will increase to higher values of the concentration. The recorded ultrasound velocity and temperature were correlated to the solute concentration and applied to identify a polynomial model. This measurement can be correlated in the following expression:

$$c = -1844 - 30.08 * T + 2.864 * v + 0.09213 * T^2 + 0.01006 * T * v - 0.0008444 v^2$$

Where c is the concentration in g sucrose/300 g water, T is the temperature in degree Celsius and v is the ultrasound velocity in m/s.

### 6.1.3 Desupersaturation curve determination by means of the single frequency ultrasound technique (case study: sucrose)

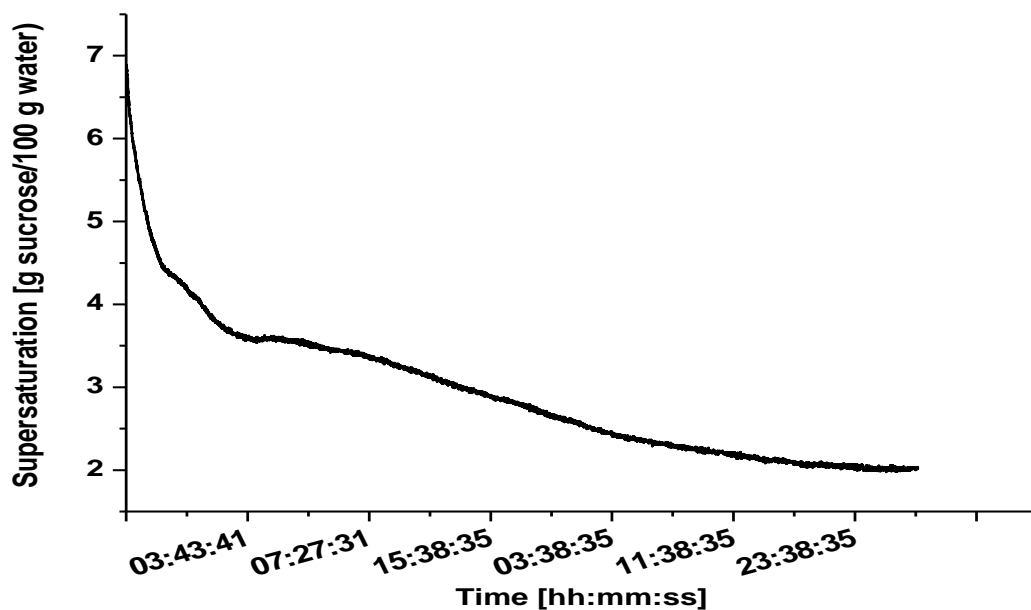


**Fig. 6-3:** Measured desupersaturation curve for the sucrose-water solution by means of the ultrasound single frequency technique.

Fig. 6-3 shows measured desupersturation curve of sucrose solution obtained from experimental data and equation. The measured decrease in the concentration during the batch cycle represents a reasonable growth rate during the batch cycle. The determination of the solute sucrose content by the ultrasound technique was already

shown by Bubnik et al. [Bub03]. In this study, however, an overall monitoring including the solid state and liquid state was performed.

## **6.2 The influence of air bubbles on the measurement of different crystal sizes and suspension densities by the 3D ORM (523 PsyA CSD Particle Analyzer)**

As explained in chapter 2, the mean crystal size and the suspension density are the key factors to evaluate the improvement in industrial crystallization processes [Fro14]. The measuring technique used to control these two mentioned variables are described in chapter 5. The 3D ORM is one of these techniques that is widely used in different industries such as crystallization, bio processes and polymerization. The measurement principle of this technique is explained in detail in chapter 2.

The chord length measured by the 3D ORM technique can be used to measure the size distribution or just the mean chord length as an important regulation value. Only reliable measurement of crystal sizes lead to an efficient control of processes. Air bubbles lead to generate incorrect measured crystal sizes. The false measurement of crystal sizes causes the generation of incorrect experimental data and an inefficient control of the processes. Air bubbles are caused in the crystallization processes by intensive agitation and addition of seed crystals. The aim of this part is to investigate the effect of air bubble on the measurement of different crystal size ranges in different volume suspension densities using a 3D ORM measurement technique [Mos14a].

## 6.2.1 Influence of the volume suspension density on the measured mean chord length

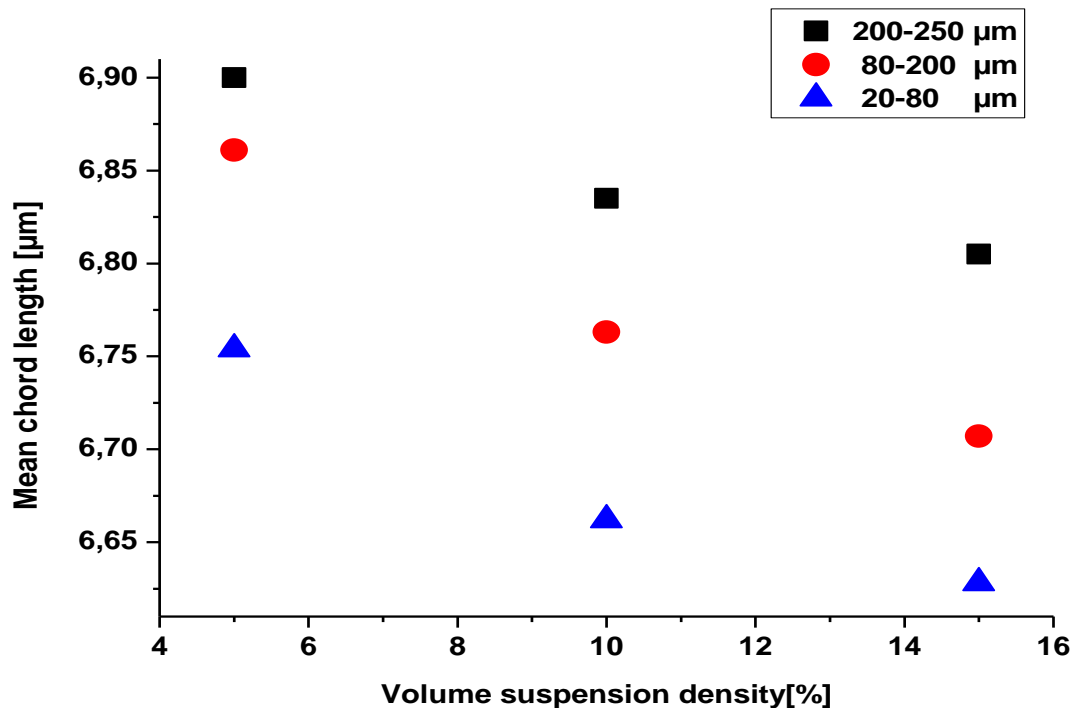


**Fig. 6-4:** Variation of the measured mean chord length versus volume suspension density for different particle size ranges (without surfactant) [Mos14a].

In Fig. 6-4, the effect of the volume suspension density on the recorded mean chord length is presented which was measured by means of the 3D ORM technique.

In an ideal case, by adding a constant sieve fraction of crystals in a saturated solution, the same mean chord length should be obtained. However, for sucrose and various other substances, a shift of the mean chord length toward smaller sizes is observed (see [Hei12]). Based on the presented result, the question arises what phenomenon is responsible for this effect. This question will be replied in chapter 7 (7-1).

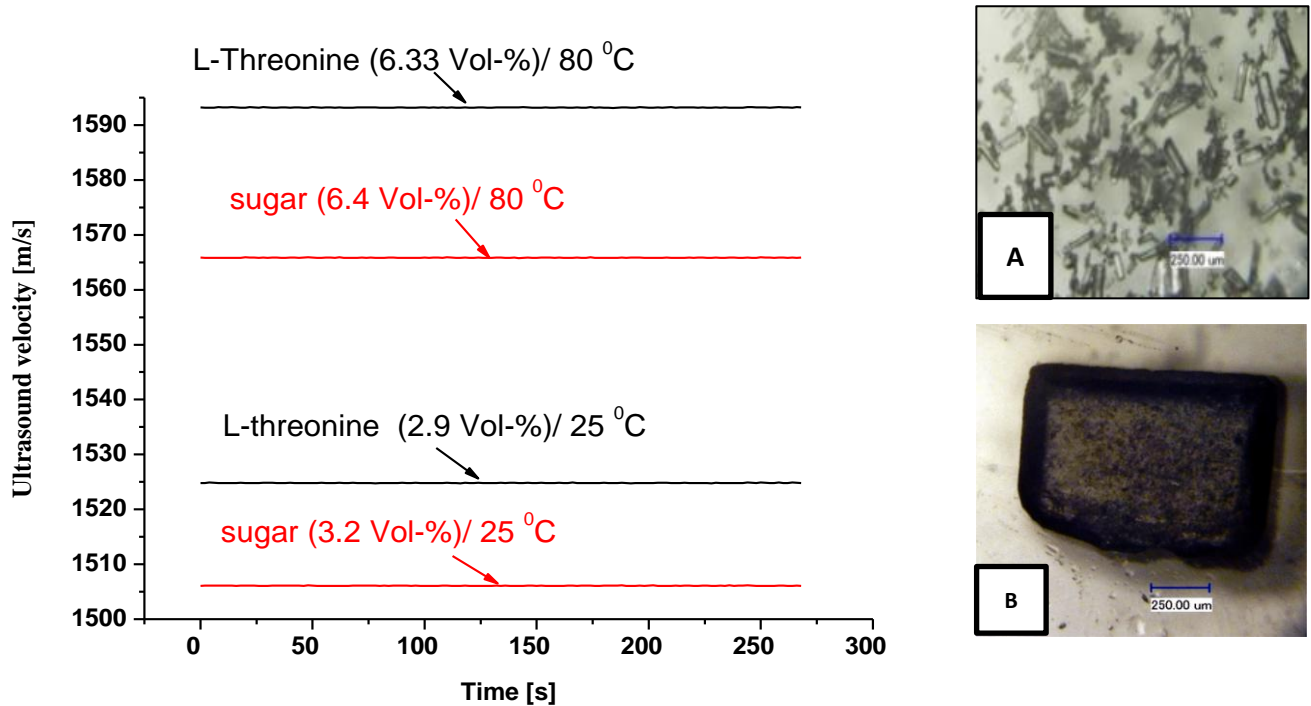
## 6.3 Effect of particle shape on inline particle size measurement technique

Crystallization is a unique, indispensable process step in many industrial production lines such as pharmaceuticals, and agrochemicals. Features like morphology and particle size are important parameters especially in the pharmaceutical crystallization processes [Bar05]. For instance, the efficiency (bioavailability) of an active



pharmaceutical ingredient (API) is strongly modified by the dissolution rate of crystals and depends also on crystal size and the crystal size distribution (CSD) [Ste02].

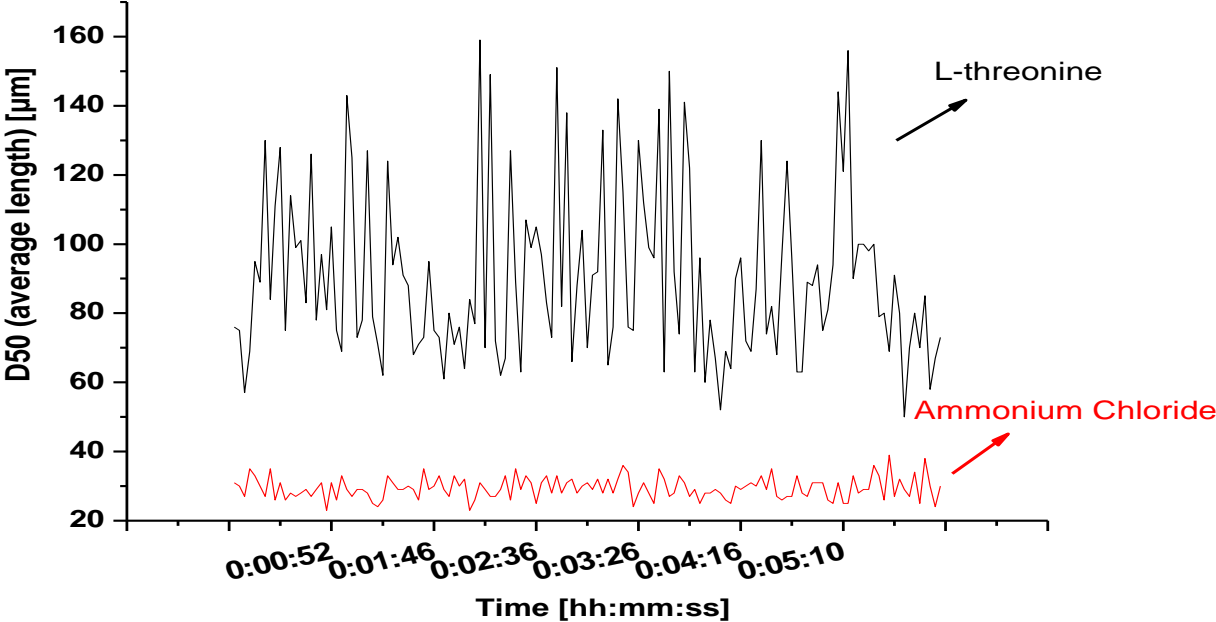
### 6.3.1 Ultrasound device: Measurement of the ultrasound velocity in L-threonine and sugar suspensions



**Fig. 6-5:** Ultrasonic velocity versus time, sugar (20-80  $\mu\text{m}$ , red line), L- Threonine (20-80  $\mu\text{m}$ , black line), the photos on the right side are: A: L-Threonine, B: Sugar. The photos of the crystals are taken off-line by a microscope [Mos14b].

Tests with the same number and volume of each particle (two mentioned considerations) were carried out at constant temperature in each case to prove the effect of the particle shape on the ultrasonic measurement technique in two systems: (a) sugar-water (substance shape: non-needle like shape), (b): L-Threonine-water (substance shape: needle like shape). The inline monitored results of these two systems each at different temperature levels are presented in Fig. 6-5. It is obvious from Fig. 6-5 that the ultrasound technique is capable to measure accurately inline as a function of time at constant temperatures. A constant signal was achieved for both systems that means the different physical properties of the liquid phase do not influence the signal for the solid phase.

### 6.3.2 3D ORM (APAS) device: Measurement of the particle size (average length) in L-threonine and ammonium chloride suspensions



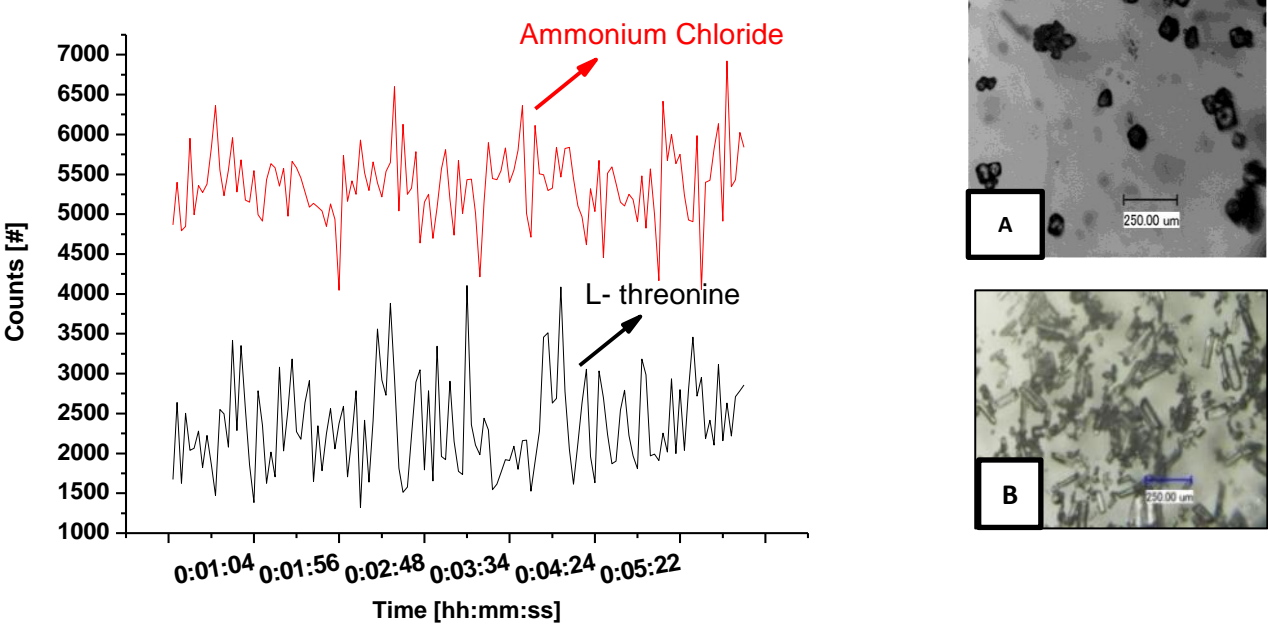
**Fig. 6-6:** Variation of mean chord length versus time; ammonium chloride (15Vol-%, 80-200 μm, red signals), L-Threonine (15 Vol-%, 80-200 μm, black signals) [Mos14b].

Fig. 6-6 shows the measured average length of two substances by the 3D ORM measurement technique obtained from exposed particle surface area (EPSA). The 3D ORM measurement technique does not measure directly particle size. The outline measurement of this sizing technique needs to be deconvoluted and converted into a particle size.

### 6.3.3 3D ORM (APAS) device: Measurement of the counts (number of particles) in L-threonine and ammonium chloride suspensions

Based on the two mentioned considerations (same suspension density and particle size range), experiments were performed at constant temperature to prove the effect of particle shape on the 3D ORM (APAS with MCST) measurement technique in the two systems: (a) ammonium chloride-water (substance shape: cubic), (b) L-Threonine –water (substance shape: needle like).

In Fig.6-7, the counts of two substances are presented which were measured by means of 3D ORM (APAS with MCST) device.



**Fig. 6-7:** Variation of particle number (counts) versus time; Ammonium Chloride (15 Vol-%, 80-200 μm, red signals), L-Threonine (15 Vol-%, 80-200 μm, black signals), the photos on the right side are: A: Ammonium Chloride, B: L-Threonine [Mos14b].

### 6.3.4 FBRM device: Measurement of the mean chord length in L-threonine and ammonium chloride suspensions

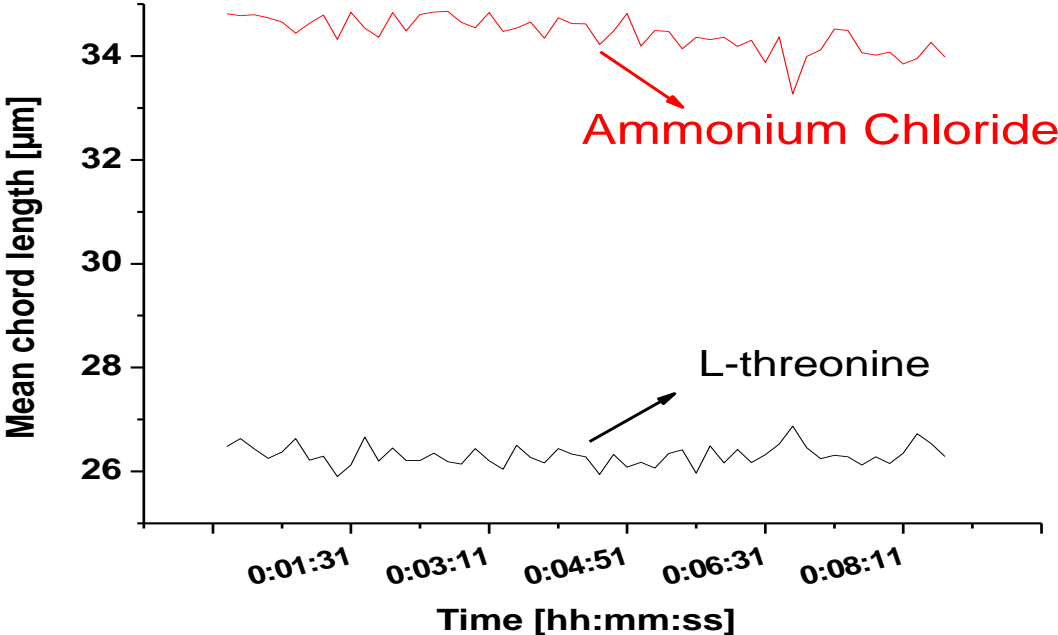


**Fig. 6-8:** Variation of mean chord length versus time (primary mode); ammonium chloride (15 Vol-%, 80-200 µm, red signals); L-Threonine (15 Vol-%, 80-200 µm, black signals) [Mos14b].

Comparing the two signals (Fig. 6-8), a constant signal was achieved for both systems. It is obvious from Fig. 6-8, that the FBRM can measure the mean chord length of different particle shapes over time. This measured mean chord length generated from straight line measurement (from one edge to the other edge of a particle).

### 6.3.5 FBRM device: Measurement of the counts (number of particles) in L-threonine and ammonium chloride suspensions

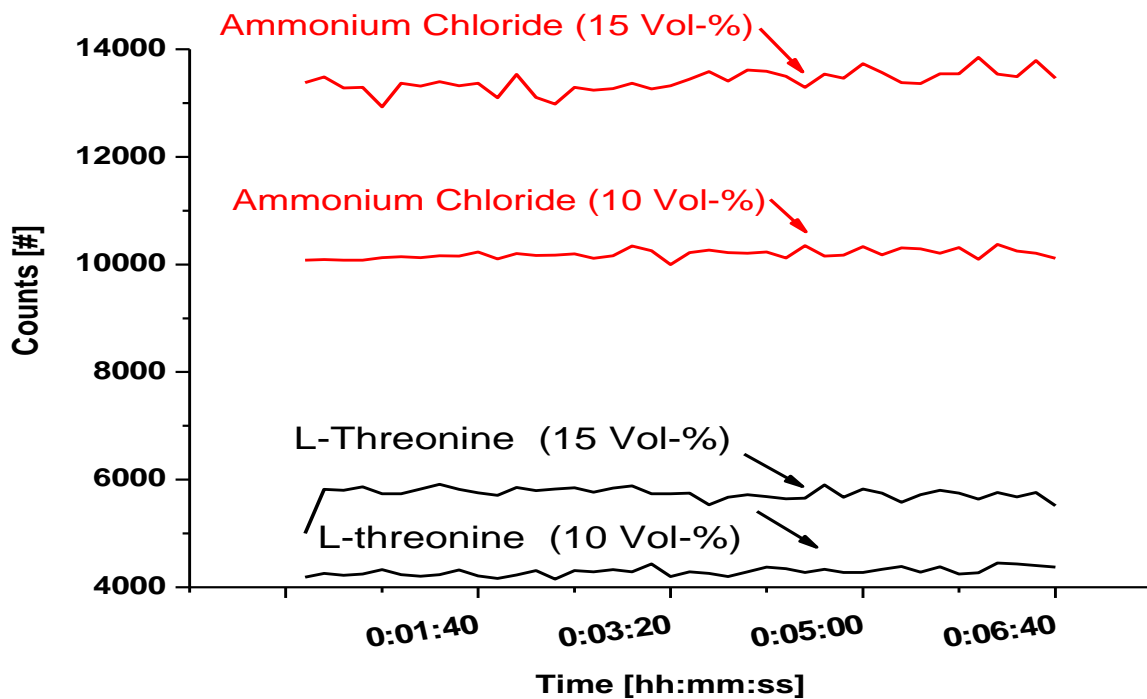


**Fig. 6-9:** Variation of particle number (counts) versus time (primary mode): ammonium chloride (80-200  $\mu\text{m}$ , red signals), L-Threonine (80-200  $\mu\text{m}$ , black signals) [Mos14b].

Based on the two mentioned considerations (same volume suspension density and particle size range), experiments were performed in constant temperature to prove the effect of particle shape on the results of the FBRM measurement technique in the two systems: (a) ammonium chloride-water (substance shape: cubic), (b) L-Threonine-water (substance shape: needle like). Fig. 6-9 presents the number of particles (counts) for two systems and two different suspension densities. As can be concluded, the number of the particles (counts) increases with increase in volume suspension density in these solutions.

## 6.4 The phase transition of crystals in-line

In industries, especially, in the pharmaceutical industry, it is essential to obtain an understanding concerning conditions of the formation of different solvates or polymorphic forms as well as their specifications by using characterization techniques. These techniques have been extensively noted in the literature [Abu10]. Several off-line analyzing tools including microscopy (optical and scanning electron microscopy (SEM)), thermal analysis (differential scanning calorimetry (DSC), thermogravimetry (TG)), vibrational spectroscopy (Fourier transform infrared (FT-IR), Raman, solid state nuclear magnetic resonance (ssNMR) and X-ray diffractometry (XRD)) can be used for the characterization of different polymorphic forms [Abu10]. These analytic techniques require sample preparation which can lead to a time delay in the recognizing of the polymorphic forms. As explained in chapter 2 process analytical technology (PAT) tools are probe-based methods that can be utilized for the monitoring of a crystallization process and a polymorphic phase transition.

The Raman spectroscopy, FBRM, FTIR, NIR, Mid-IR, ATR-UV/Vis, turbidimetry techniques are common PAT analysis techniques exerted to distinguish different polymorphic forms of a compound and provide useful information on conditions under which different polymorphic forms can exist [Sim14, How09].

The objective of this section is a full understanding of the ability to monitor phase transitions by using the 3D ORM and the ultrasound (single frequency) techniques. Microscopy is used to confirm the polymorphic phase transition and identify the shape of the different polymorphic form. The measurement principles of the used techniques are explained in detail in chapter 2.

### 6.4.1 Solvent mediated phase transition of magnesium sulfate hexahydrate to magnesium sulfate heptahydrate

Controlling the crystallization process to produce the desired crystal form is indispensable in order to increase the probability to prohibit failed batches. This can be achieved by using measurement techniques for identifying different polymorphic forms of a compound and the situations under which the desired polymorphic forms are able to exist [How09].

The solvent-mediated phase transition of magnesium sulfate hexahydrate to heptahydrate was monitored by means of ultrasound and 3D ORM (APAS) techniques. The saturated solution of hexahydrate was cooled until the nucleation of hexahydrate happened. The noticeable change in the 3D ORM signals related to the measured lengths (D 10, D 50, D 90 (length weighted)) and slightly increase in the ultrasound velocity indicates the nucleation of hexahydrate at 60 °C. Afterwards the temperature of the suspension was kept constant for a while to assure that supersaturation was completely decreased by nucleation and subsequent growth of the nucleated hexahydrate. Finally, the suspension was further cooled (up to 45 °C) until nucleation of epsomite happened. The solvent mediated phase transition of

hexahydrate into epsomite can be identified by an increase in temperature (at time 04:29:44 in Fig. 6-10) and drastic increase in the ultrasound velocity and also by significant change in the measured lengths by using the 3D ORM technique.

Fig. 6-10 presents the results of the solvent mediated phase transition of magnesium sulfate hexahydrate to epsomite monitored by ultrasound and 3D ORM techniques simultaneously.

Moreover, the solvent mediated phase transition of hexahydrate to epsomite is also proved by taking microscopic images from samples removed from the crystallizing vessel in the specified points, shown in Fig. 6-10. The microscopic images related to magnesium sulfate hexahydrate and heptahydrate (see Fig. 6-10) are confirmed by those of Strega **[Str04]** (see chapter 4.4.1).

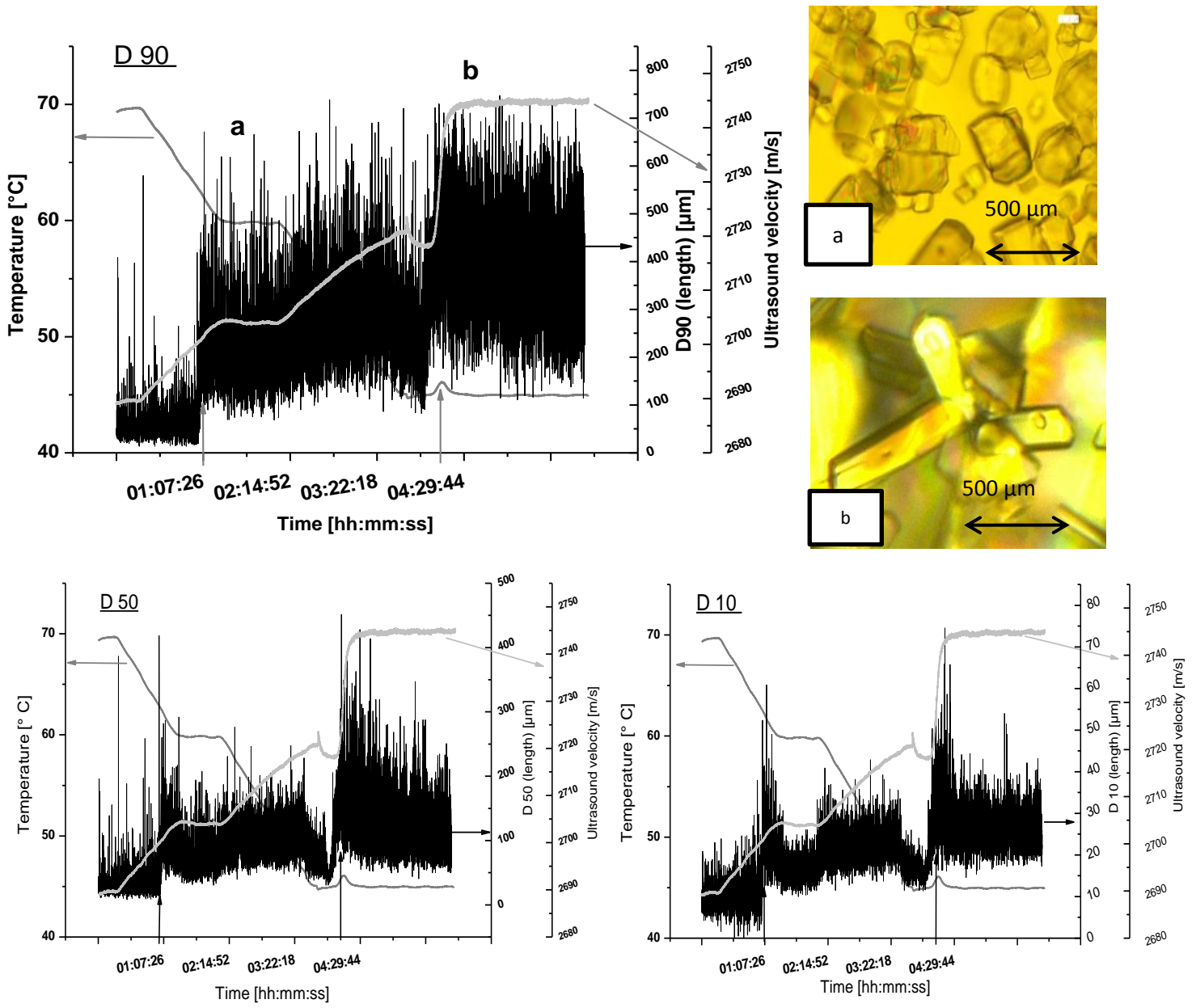


**Fig. 6-10:** Monitoring of solvent mediated phase transition of hexahydrate to epsomite by ultrasound and 3D ORM technique. (Ultrasound velocity: light gray signals, temperature: dark gray signals, measured length signals (D10, 50, 90 (length)): black signals). (a) Microscopic image of magnesium sulfate hexahydrate, (b) microscopic image of magnesium sulfate heptahydrate. The scale bar represent 500 µm for all of the microscopic images [Mos15].



## 6.4.2 Solvent mediated phase transition of di-sodium tetraborate pentahydrate to di-sodium tetraborate decahydrate

The sensitivity of the ultrasound and the 3D ORM (APAS) techniques to the solvent mediated phase transition from di-sodium tetraborate pentahydrate to decahydrate is presented in Fig. 6-11. The two mentioned techniques were simultaneously used to observe the solvent mediated phase transition.

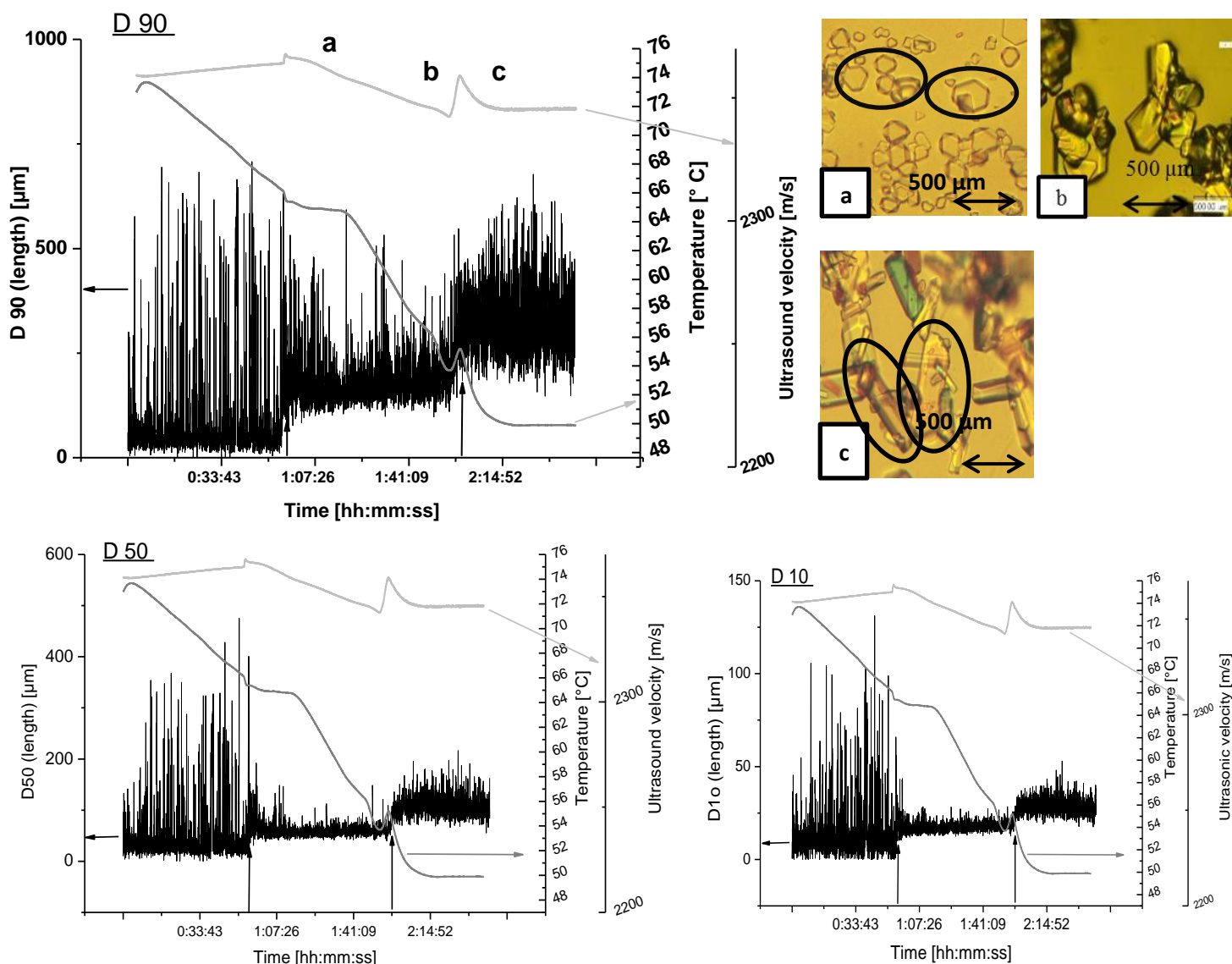


**Fig. 6-11:** Monitoring of solvent mediated phase transition of di-sodium tetraborate pentahydrate to decahydrate by ultrasound and 3D ORM technique. (Ultrasound velocity: light gray signals, temperature: dark gray signals, measured length signals (D10, 50, 90 (length)): black signals). (a) Microscopic images of di-sodium tetraborate pentahydrate, (b) microscopic image of phase transition of di-sodium tetraborate pentahydrate to decahydrate

and (c) microscopic image of di-sodium tetraborate decahydrate. The scale bar represent 500  $\mu\text{m}$  for all of the microscopic images [Mos15].

First, the saturated solution of di-sodium tetraborate pentahydrate was cooled until nucleation of pentahydrate occurred. The nucleation of pentahydrate can be observed by an increase in the ultrasound velocity and slightly decrease in the temperature (at time 00:53:45 in Fig. 6-11) by using the ultrasound technique. Furthermore, the nucleation of pentahydrate can be recognized by the remarkable change in the measured lengths (D10, 50, 90 (weighted by length)) by the 3D ORM (APAS) technique. After nucleation of pentahydrate, the temperature was maintained constant in order to reduce the supersaturation by growth of the nucleated pentahydrate. Therefore, a further cooling of the suspension was performed until the phase transition of pentahydrate to decahydrate happened (at time 01:52:55 in Fig. 6-11). This solvent mediated phase transition can be identified in the ultrasound technique by increase in the ultrasound velocity signal and temperature. Furthermore, the 3D ORM technique is able to recognize this phase transition by increase in the recorded lengths (D10, D50, and D90 (weighted by length)).

The microscopic pictures of samples taken from the specified points in Fig. 3-26 confirm the solvent mediated phase transition of di-sodium tetraborate pentahydrate to decahydrate. The photos given in Fig. 6-11 illustrated the crystals (placed in the plotted ellipses in Fig. 6-11) are in agreement of the crystal shapes referred to the chapter 4.4.2.

### **6.4.3 Solvent mediated phase transition of sulfathiazole polymorphic forms**

Sulfathiazole, an antimicrobial agent, as an organic compound applied to investigate the polymorphic phase transition of different polymorphic forms of it in different solvents by using the ultrasound and the 3D ORM techniques.

Saturated solution of sulfathiazole polymorphic form I in n-propanol was prepared according to the solubility data [Kho93]. This experiment was started with saturated solution at 20°C. During the isothermal experiments, defined amounts of sulfathiazole polymorphic form I were added to the saturated solution. Subsequently, defined amounts of distilled water were added to the prepared suspensions. Due to the addition of the distilled water to the suspension, a polymorphic phase transition from the sulfathiazole polymorphic form I into forms II and III occurred. The results of the polymorphic phase transition by the 3D ORM (APAS) technique is to be seen in Fig. 6-12.

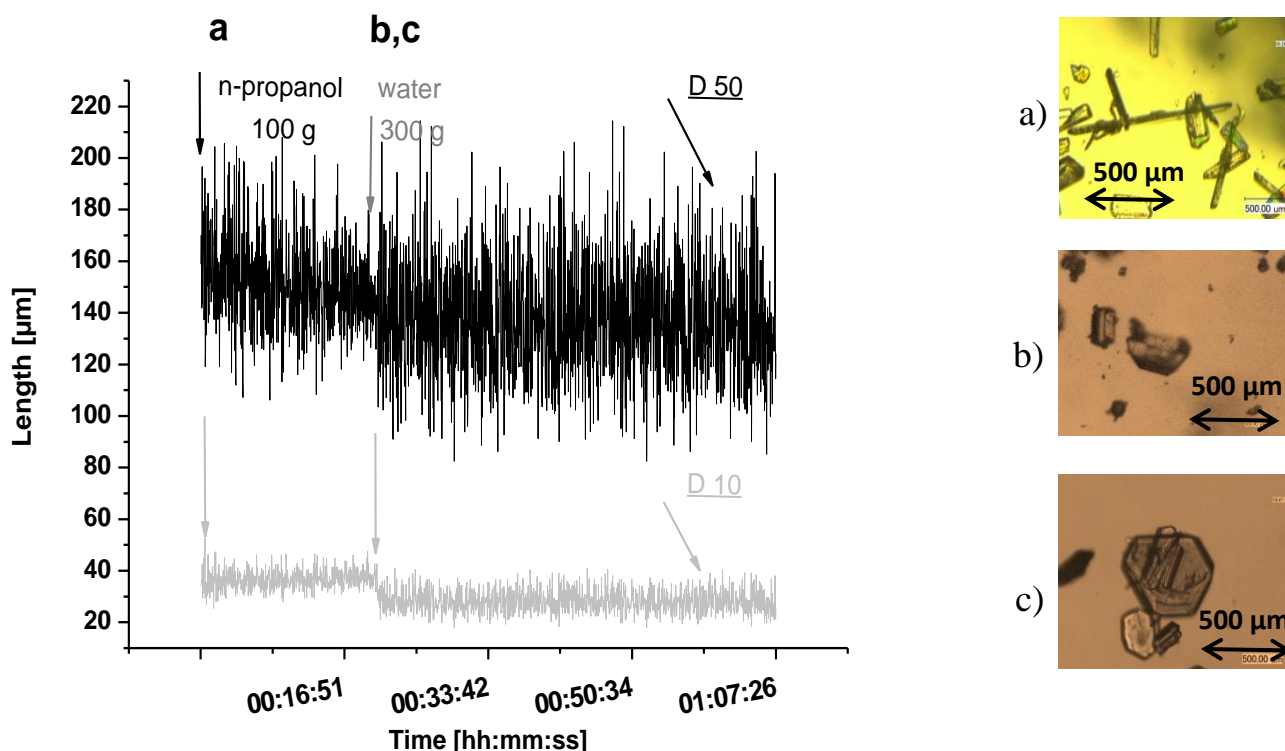


**Fig. 6-12:** Monitoring of the polymorphic phase transition of sulfathiazole polymorphic form I into forms II and III due to addition of distilled water into the suspension of form I in pure n-propanol, shown are D10 and D50. Change in D90 is similar to D50 and not shown here. (a) Microscopic images of sulfathiazole polymorphic form I (needle like) (b) Microscopic images of sulfathiazole polymorphic form II (cuboid) (c) Microscopic images of sulfathiazole polymorphic form III (truncated hexagon). All scale bars represents 500  $\mu\text{m}$  [Mos15].

The ultrasound technique does not show any sensitivity to this polymorphic phase transition according to the measured signals (ultrasound velocity and attenuation).

Variation in the particle shape due to the phase transition of sulfathiazole polymorphic form I (needle like) into forms II (cuboid) and III (truncated hexagon) by addition of water can be monitored by change in the measured length D10, D50 and D90 (weighted by length) by the 3D ORM technique. The change in D90 (weighted by length) due to polymorphic transition of sulfathiazole polymorphic form I into polymorphic forms II and III is similar to D50 (weighted by length) change and is not shown here.

The microscopic pictures taken from samples at defined points shown in Fig. 6-12 prove the phase transition of sulfathiazole polymorphs in this experiment. The crystal shapes of the images (see Fig. 6-12) are in agreement with images taken from the work of Abu Bakar [Abu08a] to be seen in Fig. 4-3.

## 7. Discussion

In this chapter, the results presented in chapter 6 will be discussed and compared to literature data.

### 7.1 The influence of air bubbles on the measurement of different crystal sizes and suspension densities by the 3D ORM technique

As shown in chapter 6 (Fig. 6-4), the measured mean chord length by means of the 3D ORM technique based on case study with sucrose decreases with an increase in the volume suspension density. However, a constant sieve fraction should result from the measurement of the same mean chord length in different volume suspension densities. Furthermore, for various substances with a constant sieve fraction, a shift of the Chord Length Distribution (CLD) toward smaller size with increase in volume suspension density is observed [All88, Giu03, Hea02, Hei12, Kai08]. To investigate the reason for this phenomenon the following procedures were carried out.

#### 7.1.1 Effect of the viscosity during in-line measurement by the means of the 3D ORM technique

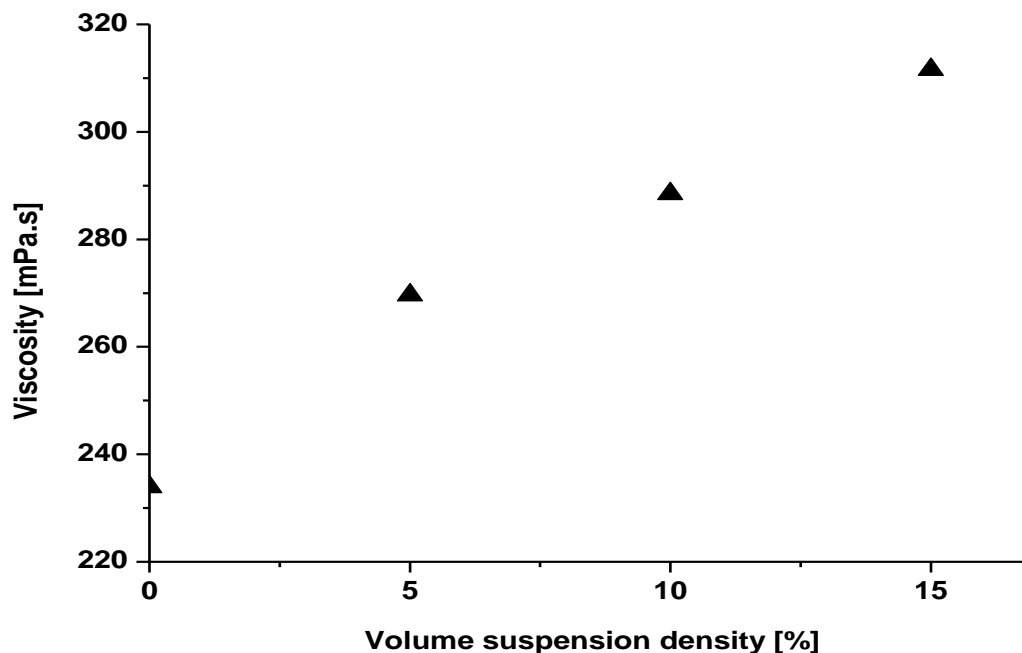


**Fig. 7-1:** Variation of the viscosity versus volume suspension density (temperature: 23 °C; rotation speed: 70 1/s) [Mos14a].

In order to prove the influence of the solution viscosity, an experiment using different suspension densities of sucrose was carried out. As can be seen in figure 7-1 the measured viscosity increases in a linear trend, within a limited volume suspension density range. The high viscose solution tends to accommodate gas bubbles stronger compared to the low viscose solution [Hel12a].

Consequently, the entrained gas might lead only to the generation of false results in respect to be measured crystals.

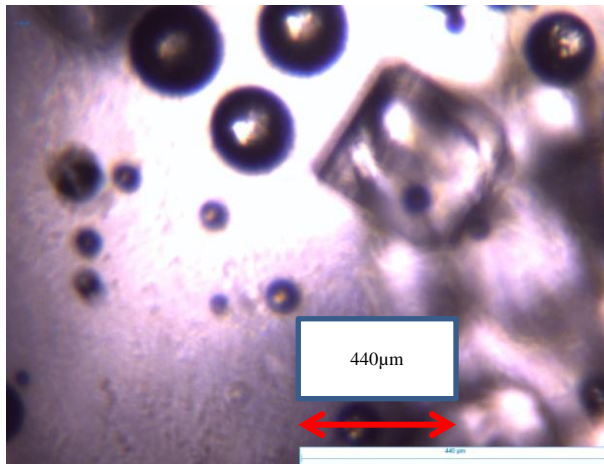


**Fig. 7-2:** In-line microscopic image of sucrose crystals along with gas bubbles at higher volume suspension density (15 Vol-%) [Mos14a].

The presence of bubbles, especially, small bubbles in higher volume suspension can be observed in Fig. 7-2. A propeller stirrer used in the glass vessel is breaking the bubbles down to very small sizes (see Fig. 7-2). Due to the high viscosity, the bubbles, especially very small gas bubbles, remain for a long time in the suspension. The used measurement device is not able to distinguish between gas bubbles and crystals.

A transfer of the gas free results from the lab to the pilot plant where gas inclusions are unavoidable shows that the technology in principle is able to measure the important parameters but the effect of air bubble should be considered during the measuring.

### **7.1.2 Investigation of the behavior of the 3D ORM measurement technique with three volume suspension densities and different particle size ranges**

A comparison of the results of the 3D ORM (523 PsyA CSD Particle Analyzer) measurement technique for three different volume suspension densities and the crystal range of 80-200 µm, with and without surfactant was carried out. The results are presented in Fig. 7-3. Furthermore, these results are summarized for three different crystal size fractions between 20-250 µm (200-250, 80-200 and 20-80 µm) in Table 7-1.

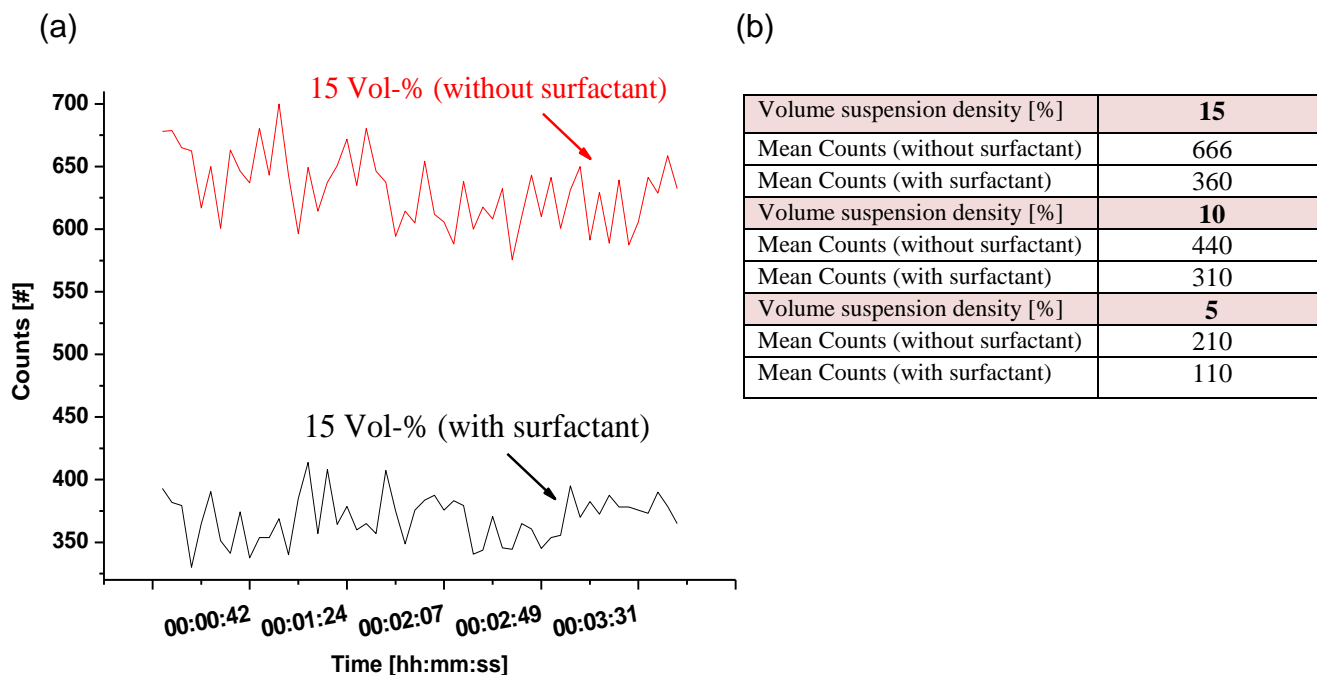


**Fig. 7-3:** (a) Variation of the crystal numbers (counts) versus time for the crystal size range (80-200  $\mu\text{m}$ ); (b) summarized mean counts in different volume suspension densities for the mentioned crystal size range **[Mos14a]**.

**Table 7-1:** Comparison of the mean crystal numbers within different volume suspension densities and crystal size ranges with surfactant and without surfactant measured by the 3D ORM technique **[Mos14a]**.

	Volume suspension density		
	15%	10%	5%
<b>200-250 <math>\mu\text{m}</math></b>	Mean crystal number (mean counts)		
Without surfactant	470	310	120
With surfactant	340	220	75
<b>Difference</b>	<b>130</b>	<b>90</b>	<b>45</b>
	Volume suspension density		
	15%	10%	5%
<b>80-200 <math>\mu\text{m}</math></b>	Mean crystal number (mean counts)		
Without surfactant	666	440	210
With surfactant	360	310	110
<b>Difference</b>	<b>306</b>	<b>130</b>	<b>100</b>
	Volume suspension density		
	15%	10%	5%
<b>20-80 <math>\mu\text{m}</math></b>	Mean crystal number (mean counts)		
Without surfactant	750	525	300
With surfactant	370	325	175
<b>Difference</b>	<b>380</b>	<b>200</b>	<b>125</b>

As can be seen in the Table 7-1 and Fig. 7-3, the measured mean crystal numbers (counts) increases with increase in volume suspension density, as expected. Experimental result illustrates that the surface tension of saturated solution of sucrose (211 g sucrose in 100 g water) can be decreased from 71.4 mN m<sup>-1</sup> to 34.1 mN m<sup>-1</sup> by addition of the surfactant Tween 20 (0.005 Vol.-%. ) at 22°C. By adding this surfactant to a saturated solution of sucrose and consequently decrease in the surface tension of the saturated solution, a great difference between the mean crystal number measured with surfactant and without surfactant, especially, in higher volume suspension density is evident. Therefore, the non-neglectable role of gas bubbles on the solid phase measurement in crystallizers could be concluded in this mentioned volume suspension density.

Furthermore, Helmdach et al. [Hel12a] showed in a seeded cooling crystallization experiment with sucrose solution experiment, that the number of crystals (counts) in the suspension with surfactant is too low in comparison to the suspension without surfactant. Further information can be found in [Hel12a].

### 7.1.3 Influence of the volume suspension density on the mean chord length measured by mean of the 3D ORM (523 PsyA CSD Particle Analyzer) (with surfactant)

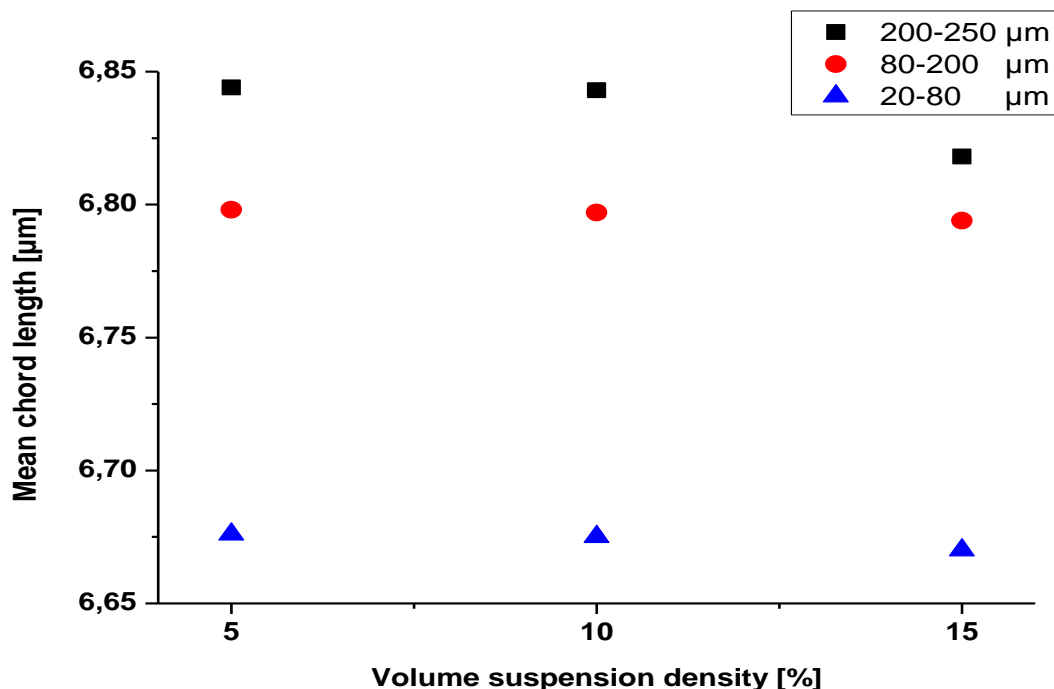


Fig. 7-4: Influence of the volume suspension density on the recorded mean chord length [Mos14a].

The surfactant Tween 20 added to the saturated sucrose solution reduces the surface tension of the solution and hence, after 5h gentle stirring almost all of the gas bubbles could be removed (degassing). The result is an approximately constant mean chord length for the used constant sieve fractions (see Fig. 7-4). Since the probability of the presence of air bubbles in the high viscosity of the sucrose suspension with a larger crystal size range (200-250  $\mu\text{m}$ ) is high (low decrease in crystal number after addition of surfactant compared to other crystal size ranges), only a small decrease in the mean chord length after addition of surfactant is observed in this mentioned crystal size range. Consequently, the decrease in the mean chord length in high viscose suspensions without surfactant is resulting from the presence of air bubbles.

The surfactant was used to prove the effect of the gas bubbles but they are not the solution for the problem due to the presence of the gas bubbles. The measuring technique is only reliable if the liquid phase is gas bubble free!

## **7.2 Effect of particle shape on inline particle size measurement technique**

In the following, discussion on some of the results related to measured signals (counts and particle size) by different sizing techniques using substances with different shapes is presented.

### **7.2.1 Ultrasound device: Measurement of the ultrasound velocity in L-threonine and sugar suspensions**

An effect of the particle shape on the measured signals by this measuring technique is not visible (see Fig. 6-5). Although the used ultrasonic technique is apparently insensitive to the particle shape, the ultrasonic velocity, however, is clearly sensitive to particle size.



## 7.2.2 3D ORM (APAS) device: Measurement of the particle size (average length) in L-threonine and ammonium chloride suspensions

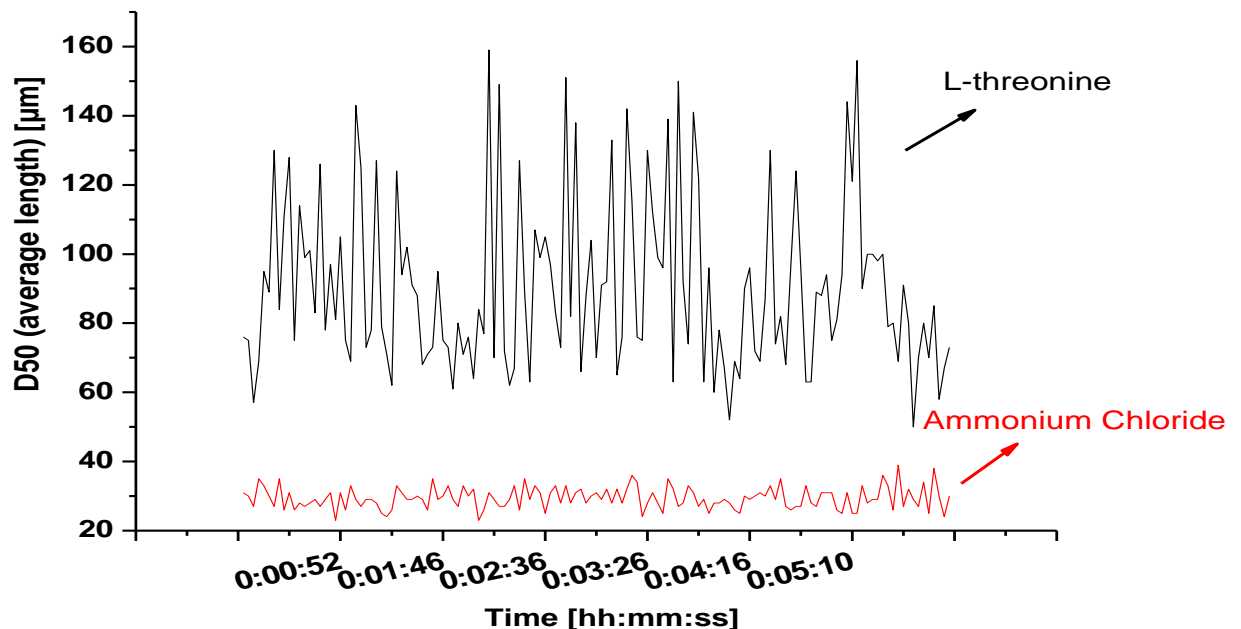


**Fig. 7-5:** Variation of average length versus time; ammonium chloride (15Vol-%, 80-200 μm, red signals), L-Threonine (15 Vol-%, 80-200 μm, black signals) [Mos14b].

The D50 (average length out of area measurement) recorded by this device (see Fig.7-5) is different from the sieved particle size range (80-200 μm). For instance, this measurement technique shows this parameter for L-Threonine particles between 65 and 140 μm and for ammonium chloride particles at approximately 30 μm (see Fig. 7-5). The reason can be described by the fact that the physical principle of measuring the size of particles is not the same. The measurement principle of the FBRM and 3D ORM techniques are based on the physical effect of reflection of light. The extent of back reflected light in the 3D ORM and FBRM measurement techniques depends on the optical properties of particles and solution, e.g. refractive index, morphology, roughness of the particles. Since the used substances have not the same mentioned properties, the measured average length of L-Threonine and ammonium chloride particles are not the same, even though the used particles result from the same sieve fraction. The presented results in Fig. 7-5 show, however, that the particles size measurement is relatively constant with time and is reproducible.

In real multi-phase systems, however, often different particle shapes are present which are difficult to distinguish by only one geometrical dimension. The APAS provides information on the exposed particle surface area (EPSA) with a further geometrical dimension (two dimensions) as can be seen in Fig. 2-10 by the

application of a pulsed laser point. Average length signals in the 3D ORM measurement technique are derived from the measured exposed surface area (EPSA).

Furthermore, needle like particles can be detected because of different orientations to the focal point by their length or diameter in this measurement technique. Consequently, the average length signals for needle like particles in this measurement technique have more fluctuations compared to non-needle like particles. Comparison of average length signals for needle like particles and non-needle like particles demonstrate that it is possible from the 3D ORM measurement technique to differentiate particles with different shapes (see Fig. 7-5) based on the fluctuation intensity of the signals. Furthermore, this difference between average length signals of two different shapes is still present after normalization of this graph (chord length/counts versus time) (see Fig. 7-6).

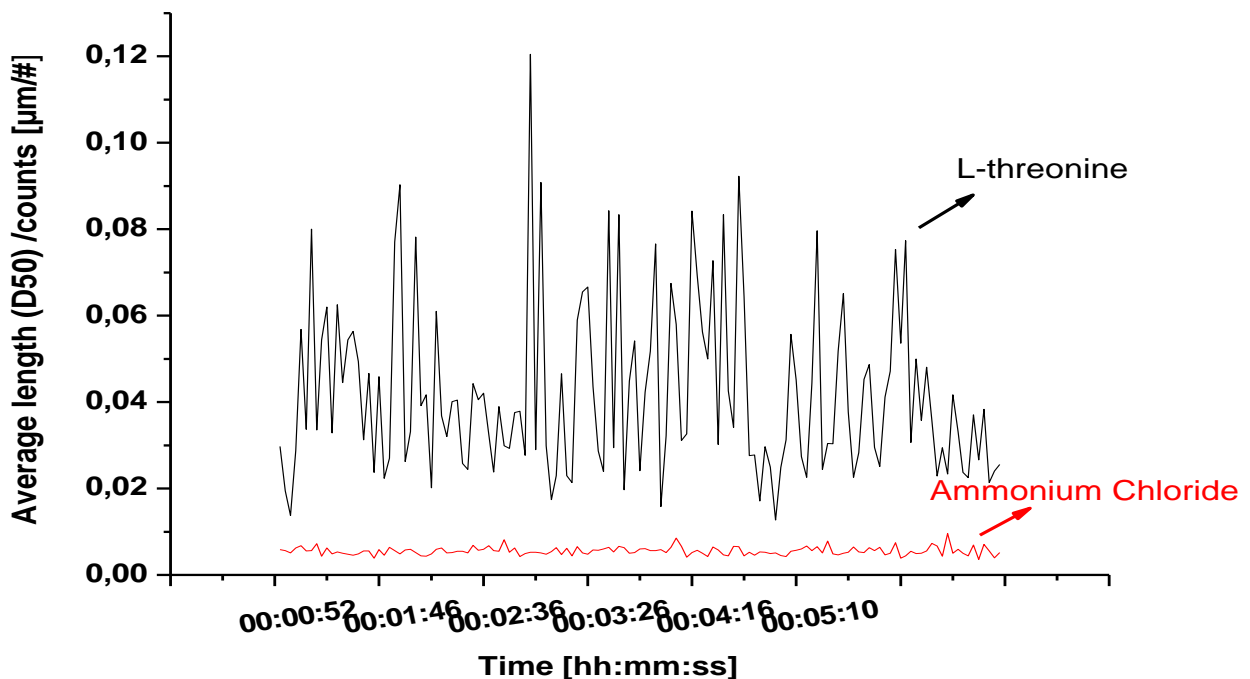


**Fig. 7-6:** Variation of average length (D50)/counts versus time; ammonium chloride (15Vol-%, 80-200 µm, red signals), L-Threonine (15 Vol-%, 80-200 µm, black signals).

As can be mentioned in chapter 2 (see Fig. 2-10), particles with different shape deliver signals with different intensity in the diagram. Comparing the signals resulting from different particle shapes, it can be observed that needlelike particles have higher signal intensity and these particles can be detected by their length (see Fig. 2-10 A). The 3D ORM measurement technique is also able to detect different morphologies of particles. That allows e.g. to follow a polymorphic transformation which is extremely important in many applications, e.g. pharmaceuticals. In real time and inline, a shape discrimination technique gains many advantages such as no sampling needed, measuring in original concentration without dilution. It can give useful extra information on several important events in a crystallizer, e.g. crystal growth and crystal breakage [**Hel13a**, **Lem13**].

### 7.2.3 3D ORM (APAS) device: Measurement of the counts (number of particles) in L-threonine and ammonium chloride suspensions

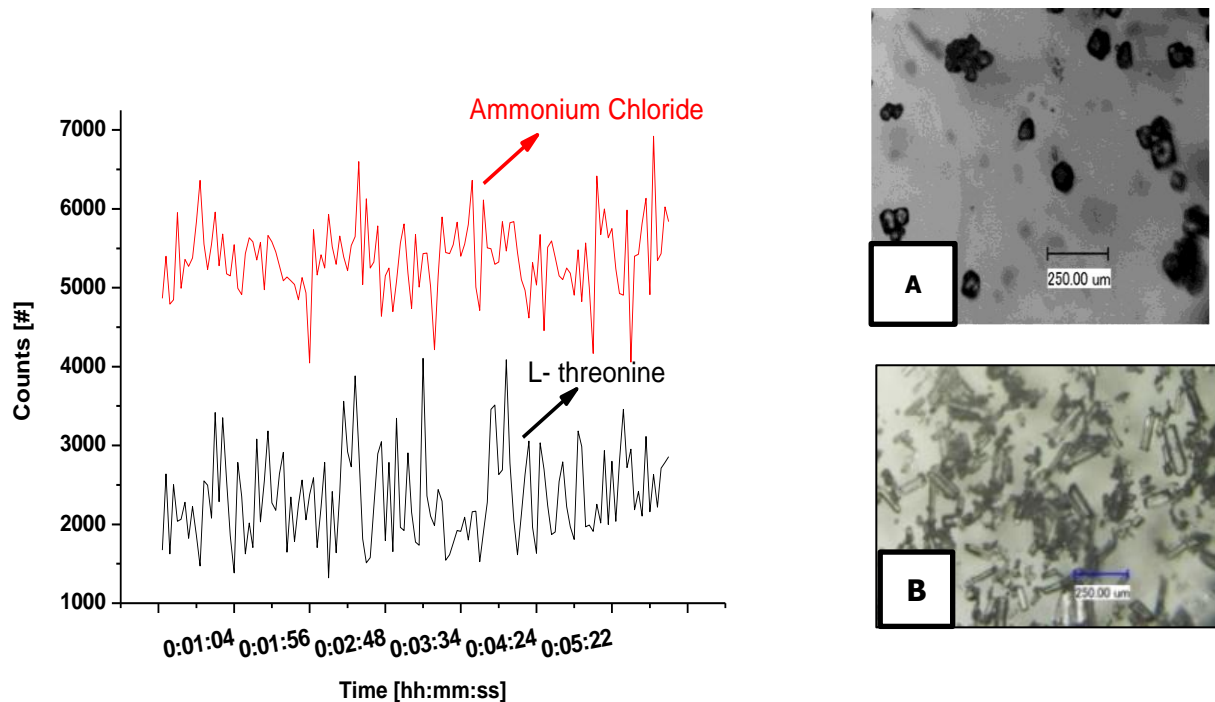


**Fig. 7-7:** Variation of particle number (counts) versus time; Ammonium Chloride (15 Vol-%, 80-200 μm, red signals), L-Threonine (15 Vol-%, 80-200 μm, black signals), the photos on the right side are: A: Ammonium Chloride, B: L-Threonine [Mos14b].

In Fig.7-7, the counts of two substances (ammonium chloride & L-threonine) are presented which were measured by means of 3D ORM (APAS with MCST) device.

In these two systems, there is a strong difference between the count numbers of two systems with the same volume suspension density. This difference is related to different reflection intensities of two substances. These reflection intensities of the particles can be analyzed using the obscuration factor (OBF) (see Fig. 7-8) which indicates the average reflection intensities of particles in the focus of the laser [Hel13a]. This parameter was measured by the 3D ORM (APAS with MCST) measurement technique during the experiments.

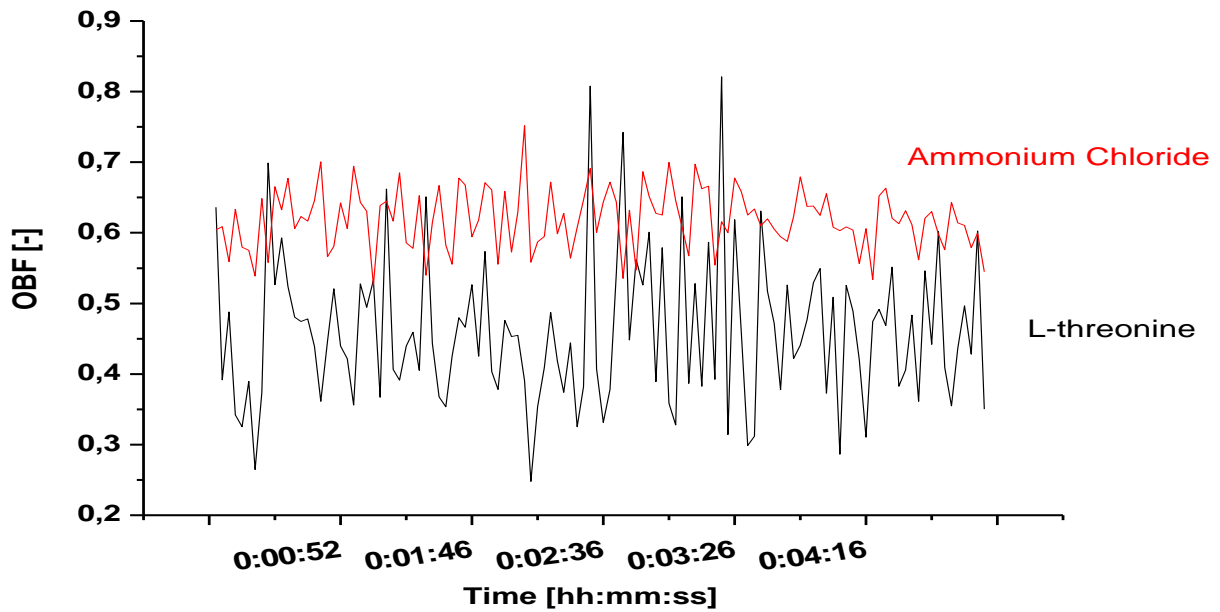


**Fig. 7-8:** Variation of Obscuration Factor (OBF) versus time; Ammonium Chloride (15 Vol-%, 80-200  $\mu\text{m}$ , red signals), L-Threonine (15 Vol-%, 80-200  $\mu\text{m}$ , black signals) [Mos14b].

As can be concluded from Fig. 7-8, the obscuration factor (OBF) for ammonium chloride particles has a higher value compared to L-Threonine particles. It was found from experiments that the smaller this mentioned factor is, the lower is the absolute value of the measured counts. Therefore, more ammonium chloride particles can be counted. The obscuration factor (OBF) is also influenced by particle properties such as roughness, impurities, etc.. Consequently, the difference in refractive index between particles and solution was considered.

The refractive index at a solid phase and particle-solvent system of substances like ammonium chloride, ascorbic acid and  $\alpha$ - glycine were determined by Heinrich [Hei12] and it was found that the smaller the difference in refractive index between particle and solution, the lower the absolute value of the measured counts [Hei12]. The refractive indices for the substances used within this work are summarized in table 7-2.

**Table 7-2:** The refractive indices for the substances used within this work (selected refractive indices at  $\lambda=589\text{ nm}$ ).

Substance	Refractive index (solid) [-]	Refractive index (solution) [-]
ammonium chloride	1.64 [Che13]	1.38 (20 °C; sat.s.) (own measurement)
L-Threonine	1.52 [Rod03]	1.35 (20 °C; sat.s.) (own measurement)

As can be concluded from these experiments, the obscuration factor (OBF) as well as difference in refractive index between particle and solution is critical factor affecting on the measured particle number (counts). Particles with higher value of these mentioned parameters will be counted more. The 3D ORM (APAS) technique is able to present the information on the OBF factor and substances with different reflection intensities, diffusivity, roughness and or purity can be distinguished in this

technique. For instance, Helmdach et al. [Hel13a] found that OBF factor of living cancer cell measured by this technique is more than dead cancer cell after a chemotherapeutic agent. Consequently, this technique is able to distinguish between living cancer cell and dead cancer cell by presenting measured OBF.

#### 7.2.4 FBRM device: Measurement of the mean chord length in L-threonine and ammonium chloride suspensions

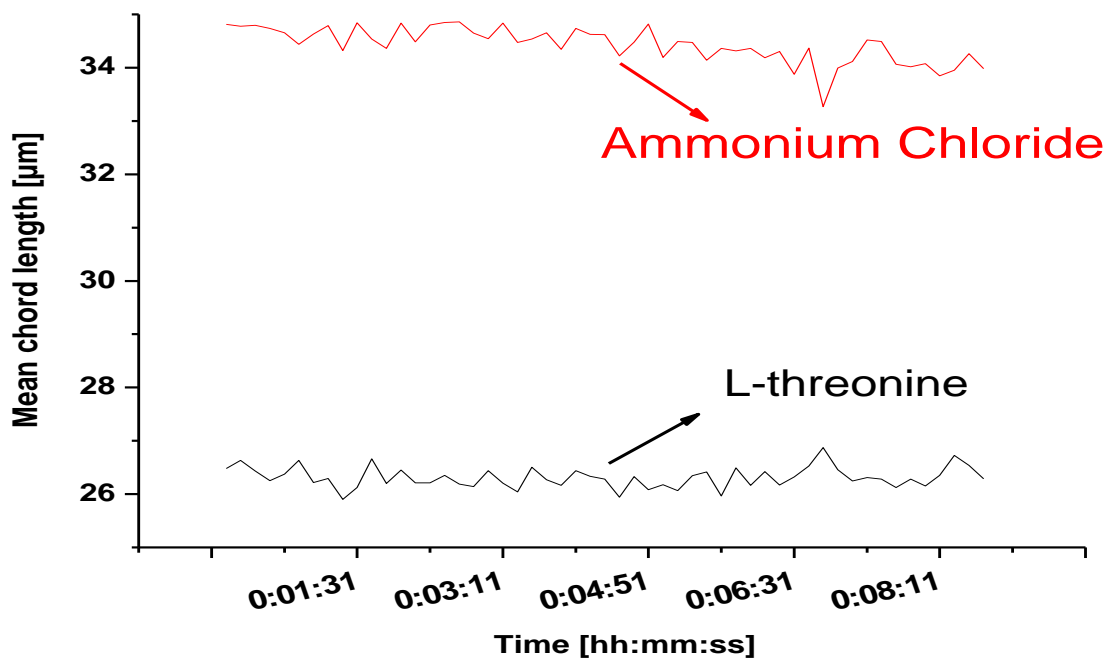


**Fig. 7-9:** Variation of mean chord length versus time (primary mode); ammonium chloride (15 Vol-%, 80-200 µm, red signals); L-Threonine (15 Vol-%, 80-200 µm, black signals) [Mos14b].

As described in the previous section (7.2.2) for the 3D ORM measurement technique, the measured mean chord length by the FBRM measurement technique is different from the sieved particle size range, too. The measurement technique gives the size (mean chord length) of L-Threonine particles of approximately 26 µm and of Ammonium Chloride particles approximately at 35 µm (see Fig. 7-9). Furthermore, this difference between average length signals of two different shapes is still present after the normalization of this graph (chord length/counts versus time) (see Fig. 7-10).

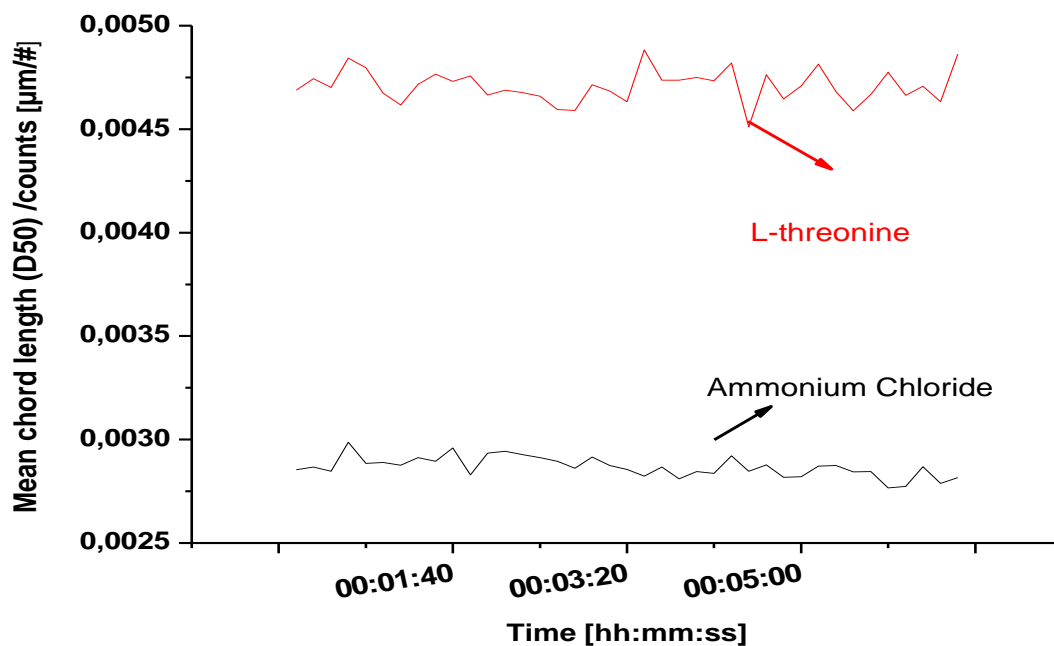


**Fig. 7-10:** Variation of mean chord length/counts versus time (primary mode); L-Threonine (15 Vol-%, 80-200 µm, red signals); ammonium chloride (15 Vol-%, 80-200 µm, black signals).

A one dimensional measuring technique such as the FBRM does not allow to distinguish different morphologies.

The FBRM technique provides information related to the chord length measurement which can be subsequently converted by the user if desired to a spherical equivalent diameter. The orientation of a particle at the probe window plays an important role in determining characteristic length from the measured chord length. The chord length measured by this technique in a suspension of needle like particles is a strong function of the needle width. The results in Fig. 7-9 supports that the width of the needle like particles has a higher probability than the length to be measured by the FBRM measurement technique. For needle like shaped particles, however, there cannot be a similar high fluctuation observed as to be seen with the 3D ORM measurement technique (see Fig. 7-9). The FBRM measurement technique has been established to show polymorphic transformation by monitoring the change in chord length distribution or variation in the mean chord length signals or particle number (counts) of different particle size, respectively. The changes in these mentioned signals state changes in the shape or in the size. It is, however, never clear that the mentioned signals belong to a specified particle shape [Osu05, Su10]. Also the FBRM technique is one of the probe-based measurement tools which is installed directly in the crystallizer without the need for sample dilution or manipulation. The FBRM has also been successfully applied as a useful tool for detecting a nucleation event and characterization the metastable zone width [Bar05].

## 7.2.5 FBRM device: Measurement of the counts (number of particles) in L-threonine and ammonium chloride suspensions

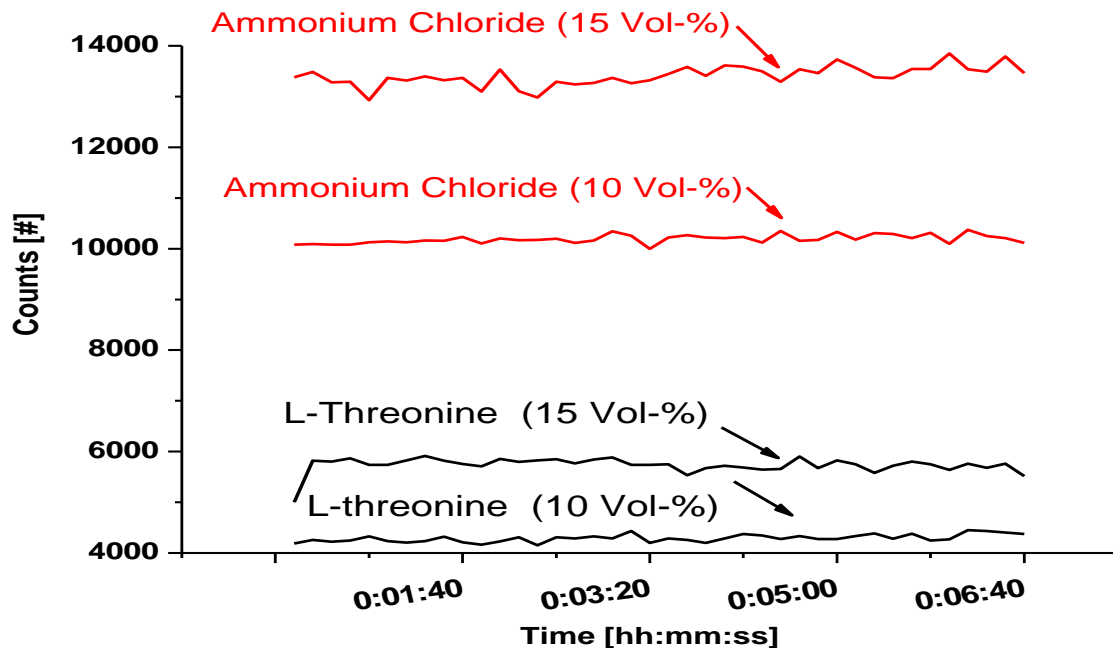


**Fig. 7-11:** Variation of particle number (counts) versus time (primary mode): ammonium chloride (80-200  $\mu\text{m}$ , red signals), L-Threonine (80-200  $\mu\text{m}$ , black signals) [Mos14b].

Fig. 7-11 presents the number of particles (counts) for two systems and two different suspension densities. As can be concluded, the number of the particles (counts) increases with increase in volume suspension density in these solutions. Since the FBRM measurement principle is based on the detected backward reflected laser light, the amount of backward collected light is a function of the optical properties of particles and solution, size and shape of the considered particles. Due to difference in these mentioned properties, difference in the particle numbers (counts) can be observed in these two mentioned systems.

Furthermore, the orientation of a particle at the probe window plays an important role in determining of the measured data (counts and mean chord length). Further information on this subject can be found in [Hei12].

The FBRM technique is one of the frequently used in-line particle characterization (particle number and particle size) techniques that can be used to provide information on the nucleation and growth phenomena during a crystallization process by



evaluation of the measured counts or chord length distribution and also to track a polymorphic transformation from the metastable to the stable form by assessment of the change in the crystal counts and the chord length distribution data [Abu09b, Osu05].

### 7.3 The phase transition of crystals in-line

The solvent-mediated phase transition of magnesium sulfate hexahydrate to magnesium sulfate heptahydrate, di-sodium tetraborate pentahydrate to di-sodium tetraborate decahydrate, polymorphic form I of sulfathiazole to polymorphic form II and III of sulfathiazole was monitored by means of ultrasound and 3D ORM techniques. The solvent mediated phase transition two of these mentioned case studies (magnesium sulfate and di-sodium tetraborate) can be identified by an increase in temperature and drastic increase in the ultrasound velocity in the ultrasound measurement technique.

Since variables such as concentration of solute and temperature affecting the measured ultrasound velocity are not the same for magnesium sulfate hexahydrate and magnesium sulfate heptahydrate/di-sodium tetraborate pentahydrate and di-sodium tetraborate decahydrate, an intense change in the ultrasound velocity signal during the phase transition can be observed (at time 04:29:44 in Fig. 6-10 & at time 01:52:55 in Fig. 6-11). Concerning the ultrasound technique the results confirm the findings by Strege [Str04, Uir12]. Strege et al. [Str04] has shown that the ultrasound technique (single frequency) can successfully be applied to monitor the phase transformation of inorganic substance as well as organic substances.

During transformation of the metastable form (magnesium sulfate hexahydrate/di-sodium tetraborate pentahydrate) to the stable form (magnesium sulfate heptahydrate/di-sodium tetraborate decahydrate), energy is reduced and heat is released. Consequently a slight increase in temperature can be observed during this transformation (at time 04:29:44 in Fig. 6-10 & at time 01:52:55 in Fig. 6-11) [Mos15].

Since change in the morphology of particles happens during the solvent mediated phase transition of these mentioned case studies change in the 3D ORM readings (D10, D50, D90 (weighted by length)) can be detected (at time 04:29:44 in Fig. 6-10, at time 01:52:55 in Fig. 6-11 & at time 00:16:51 in Fig. 6-12) [Mos15].

Helmdach et al. [Hel13a] have demonstrated the use of this technique to detect the polymorphic transition in a case study with L-glutamic acid.

As can be concluded from this section, at least one of the used measuring techniques such as ultrasound single frequency and 3D ORM (APAS) techniques based on their measurement principles is able to detect the solvent-mediated phase transition of the used case studies. For instance, the change in the concentration and temperature during the solvent-mediated phase transition of the some used case studies can be successfully in-situ monitored using the ultrasound single frequency

technique and also change in the morphology of all of the used case studies during this phase transition can be detected using the 3D ORM technique.

During the polymorphic transformation if the change in the particle shape is noticeable, application of the 3D ORM (APAS) technique due to its measurement principle can be suggested. The different solvate or polymorphic forms can be distinguished by the use of ultrasound single frequency and 3D ORM techniques, however, the application of these techniques does not work in all cases, but always at least one is working. There are limitations with respect to the nature of the examined materials.

## 8. Conclusion

The final conclusion of the main results with respect to the aims described in chapter 3 can be presented as following.

First, the feasibility of a simple, less complex, universal applicable and robust technique ultrasound single frequency technique for measurement of supersaturation and metastable zone width determination (MZW) based of the case study with sucrose was tested. It has been found this technique is able to measure supersaturation on-line using the protected ultrasound sensor within the metastable zone. The effect of the particle size and/or suspension density on the measured ultrasound velocity can be eliminated using the protected sensor. The measurement of concentration by means of the ultrasound technique is possible by finding the relationship between ultrasound velocity, temperature and concentration.

Second, the effect of air bubbles on the measurement of different crystal size ranges of sucrose in different suspension densities using the 3D ORM measurement technique is evaluated. With regard to high viscosities of sucrose suspensions, bubbles, especially, very small air bubbles have long retention times in these suspensions. The used measurement device is not able to differentiate between air bubbles and crystals. The bubbles lead to the generation of false results (mean chord length) with respect to the crystals as wanted to be measured objects. By addition of a surfactant and a subsequent degassing step, approximately constant mean chord length can be achieved for constant sieve fractions in different suspension densities. Addition of the surfactant in the suspension was performed in order to proof the presence of air bubbles influencing the measured length and it is not applicable in the industry. Thus, it is required if a control of processes should be efficient carried out, that gas bubbles have to be minimized (e.g. by deaeration in the suspensions to be measured) **[Mos14a]**.

Third, the sensitivity of the ultrasound (single frequency), 3D ORM, and FBRM techniques with respect to the shape of the particle is investigated. It is illustrated that the sensitivity of these mentioned techniques is different.

The ultrasound technique (single frequency) does not exhibit sensitivity to the particle shape for the case studies conducted here according to the measured signals (see Fig. 6-5) but the ultrasound velocity is sensitive to particle size and suspension densities.

As mentioned in chapter 7, the 3D ORM technique gives information on the exposed particle area and from these data allows for calculation of particle size. Particles with varying shapes produce different height of signals in the diagram (see Fig. 2-10 & 6-6). Since needle like particles based on their orientations to the focal point can be detected either by their length or width, the 3D ORM measurement technique shows a noticeable fluctuation in the signals of average length. Therefore, a significant effect of the particle shape on the measured signals can be observed by this

measurement technique. It is therefore possible to detect different morphologies of particles. That could allow e.g. to follow polymorphic transformations if it goes in line with a shape change of the particles which is in most cases the point. This is extremely important for a number of applications.

The FBRM device provides information related to chord length measurements which can be subsequently converted by the user if desired to a spherical equivalent diameter. Stable signals of the mean chord length for needle like particles (L-Threonine) can be recorded by the FBRM measurement technique. In the FBRM measurement technique, needle like particles can be detected due to the flow pattern more often by their width than the length.

The 3D ORM measurement technique can supply an average length of particles generated from the exposed particle surface area of the particles. The FBRM measurement technique can give the mean chord length of particles derived from straight line signal from one edge to the other edge of a particle. However, these measured lengths of particles in 3D ORM and FBRM measurement techniques are different from sieved particle size fractions since the measurement principles are not identical. For example, the measurement principle of the FBRM and 3D ORM measurement techniques are based on the physical effect of the reflection of light. The extent of back reflected light in the 3D ORM and FBRM measurement techniques depends on the optical properties of particles and solution, e.g. refractive index, morphology, roughness and purity of the particles. Since these mentioned properties are not the same for the various substances, accordingly the measured lengths are different, but reproducible **[Mos14b]**.

In a various cases, crystallization leads to the formation of a metastable solvate or a polymorphic form, of a crystalline substance, which might transform into a more stable form. Solvates and polymorphs have a critical aspect in industrial production, especially, in food and pharmaceutical industries. Since different polymorphic forms display different physical properties such as bioavailability, dissolution rate and crystal habit. Furthermore, the different forms could have a significant effect on the downstream processing. Controlling and having the knowledge of crystallization processes to produce desired solvates or polymorphic forms is required in order to achieve a high quality final product. PAT tools have already been used in some studies to monitor morphological phase transitions. The application of the PAT tools leads to significant product quality improvement.

Finally, the sensitivity of the rather new PAT tools such as ultrasound single frequency and 3D ORM techniques concerning the solvent mediated phase transition is investigated in three case studies during this research.

It is found that application of these mentioned tools in the crystallization processes of polymorphs and solvates can be of great benefit.

The solvent mediated phase transition of magnesium sulfate hexahydrate to heptahydrate and di-sodium tetraborate pentahydrate to decahydrate measured in-

situ using ultrasound shows a clear response (change, increase) in the ultrasound velocity and temperature. Ultrasound, however, does not show any usable response in the case of the polymorphic phase transition of sulfathiazole.

The solvent mediated phase transition could be detected by clear changes in the recorded lengths (D10, 50, 90 (weighted by length)) in the 3D ORM technique. Since changes in the morphology of particles (confirmed by optical microscopy) occur during the polymorphic phase transition in case of the used substances, changes in the 3D ORM readings (D10, 50, 90 (weighted by length)) due to the measuring principle of this technique regarding to different particle shapes could be detected **[Mos15]**.

Furthermore, this study demonstrates the power of these tools to track and control in-line the solvate and polymorphic phase transformations. One of the two sensors could catch a change either in the solution concentration or the solid content or the shape of crystals. This is extremely important for many applications, especially, in the pharmaceutical industry.

## 9. Summary

The properties of crystalline products have to possess defined characteristics such as purity, crystal size, crystal size distribution and polymorphic form. These properties can be controlled using the process analytical technology (PAT) tools. These tools can provide effective and efficient means for acquiring information to facilitate process understanding, continuous improvement, and development of risk-abatement strategies. PAT tools can be situated in the process stream and provide information on the process e.g. concentration of solute and the product e.g. polymorph content in real-time [Hel14]. The measured properties can be univariate (scalar) quantities or multivariate (vector and matrix) [Sim14b].

PAT tools must be capable to deal with the conditions of the suspension crystallization (e.g. a size range of 50 to 500  $\mu\text{m}$  and a suspension density of 10 to 40 Vol %).

Ultrasound single frequency, 3D ORM (523 PsyA CSD Particle Analyzer & APAS) and FBRM techniques are examples of these PAT tools in principle capable of dealing with the conditions of suspension crystallization and are therefore used in this research. The ultrasound single frequency technique is an ideal method for in-situ determination of the crystallization parameters in the liquid phase (concentration, supersaturation) and the solid phase (suspension density and mean particle size). This technique has a high reliability and belongs to the series of new inexpensive PAT developments [Ste13]. The 3D ORM technique as well as FBRM technique are established techniques for the measurement of the mean particle size, the mean chord length, or the particle size distribution and the suspension densities in-line and in-real time [Hel13a], but where are the limits of these tools in a crystallization process?

The effect of gas bubbles on the outcome (measured mean chord length) of the 3D ORM technique (523 PsyA CSD Particle Analyzer) is investigated in this research. This measurement technique could produce on the first view incorrect mean chord lengths for constant sieve fractions of added crystals. To investigate the reason for this phenomenon some procedures described as following were carried out.

Based on the resulting data derived from measuring the viscosity of different volume suspension densities, the measured viscosity increases in a linear trend, within a limited volume suspension density range (see Fig. 7-1). Because of a high viscosity of sucrose suspensions -here the case study-, the probability of a presence of gas bubbles, especially, in the higher volume suspension densities, is high.

Furthermore, the presence of gas bubbles, especially, small bubbles in higher volume suspension densities can be observed using in-line microscopic image (see Fig. 7-2).

Moreover, a comparison of the results of the 3D ORM (523 PsyA CSD Particle Analyzer) technique for three different volume suspension densities and crystal size

ranges, with and without surfactant was carried out. The measured mean crystal number (counts) increases with increase in the volume suspension density. In addition, a great difference between the mean crystal number measured with surfactant and without surfactant, especially, in higher volume suspension density is evident (see Fig. 7-3 & Table 7-1). By adding the surfactant Tween 20 to a saturated solution of sucrose, a decrease in the surface tension of this solution takes place and the gas bubbles leave the solution. Consequently, the non-neglectable role of gas bubbles on the solid phase measurement could be concluded in higher volume suspension density.

Furthermore, the influence of the particle shape on the result of different measuring techniques including ultrasound single frequency, FBRM and 3D ORM (APAS) techniques is evaluated. Advantages and shortcomings of these techniques are compared and discussed. The ultrasound technique, however, does not show any sensitivity to the particle shape for the used case studies-here sucrose and L-threonine suspensions-according to the measured ultrasound velocity signals (see Fig. 6-5).

The 3D ORM (APAS) measurement technique indicates a noticeable fluctuation in the measured signals (average length) of the needle-like particles compared to non-needle-like particles (see Fig. 7-5). Furthermore, this difference between average length signals of two different shapes of the particles (needle and non-needle like) is still present after normalization (see Fig. 7-6). Needle-like particles can be detected either by their length or width based on their orientations to the focal point. Therefore, a significant effect of the particle shape on the measured signals (average length) can be detected in this measurement technique. The 3D ORM technique is able to measure the exposed particle surface area which is related to the actual surface of a particle using the laser pulsation. This technique allows the explication of shapes due to the different height of signals derived by the measured exposed particle surface area [Hel13a, Sch12b].

In addition, an absolute conclusion regarding the particle shape is not possible by the FBRM technique. The width of the needle like particles has a higher probability than the length to be measured by the FBRM technique. For needle-like shaped particles, however, there cannot be a similar high fluctuation that can be observed in the 3D ORM technique (see Fig. 7-9). Furthermore, this difference between average length signals of two different shapes of particles (needle-like and non-needle like) is still present after the normalization (see Fig. 7-10). The FBRM measurement technique is able to present the mean chord length of particles derived from the straight line signal from one edge to the other edge of a particle.

Furthermore, the measured lengths of particles in the 3D ORM and FBRM techniques are different from the sieved particle size fractions since the measurement principle of these techniques are different (see Fig. 7-5 & Fig. 7-9).

A strong difference between the particle number (counts) of two used systems (ammonium chloride and L-threonine) with the same volume suspension density can be observed (see Fig. 7-7). This difference is related to difference in the reflection intensities of particles and solution, shape, roughness, purity of the particles. The reflection intensities can be analyzed using the obscuration factor (OBF) (see Fig. 7-8) using the 3D ORM (APAS) technique. It is found from the experiments that the smaller this mentioned factor is, the lower is the absolute value of the measured counts (compare Fig. 7-7 & Fig. 7-8)

An online control in production of crystalline substances with respect to their morphology or a solvent mediated phase transfer is of key importance in many industries. In this work, monitoring of solvent mediated phase transition by ultrasound single frequency and 3D ORM (APAS) techniques is evaluated based on case studies with magnesium sulfate, di-sodium tetraborate and sulfathiazole. The solvent mediated phase transition of magnesium sulfate hexahydrate/di-sodium tetraborate pentahydrate into magnesium sulfate heptahydrate/di-sodium tetraborate decahydrate can be identified by an increase in temperature and drastic increase in the ultrasound velocity (at time 04:29:44 in Fig. 6-10 & at time 01:52:55 in Fig. 6-11) using the ultrasound technique and also by significant change in the measured lengths (D10, D50, D90 (length weighted)) (at time 04:29:44 in Fig. 6-10, at time 01:52:55 in Fig. 6-11 & at time 00:16:51 in Fig. 6-12) using the 3D ORM technique. The ultrasound technique does not show any sensitivity to the polymorphic phase transition based on the case study with sulfathiazole according to the measured signals (ultrasound velocity and attenuation). However, the polymorphic phase transition of sulfathiazole polymorphic form I into forms II and III can be monitored by change in the measured length D10, D50 and D90 (weighted by length) using the 3D ORM technique. The achieved results by the in-line PAT tools are also proven by the optical microscopy.

## **10. Zusammenfassung**

Die Eigenschaften kristalliner Produkte müssen definierte Merkmale wie Reinheit, Kristallgröße, Kristallgrößenverteilung und polymorphe Form aufweisen. Diese Eigenschaften können mithilfe von Process Analytical Technology (PAT) -



Werkzeugen kontrolliert werden. Diese Werkzeuge können ein wirksames und effizientes Mittel zur Informationsgewinnung darstellen, um das Prozessverständnis, die kontinuierliche Optimierung und die Entwicklung von Risikovermeidungsstrategien zu erleichtern. PAT-Werkzeuge können sich im Prozessstrom befinden und in Echtzeit Informationen zum Prozess z. B. Konzentration an gelöstem Stoff sowie zum Produkt z. B. polymorpher Anteil liefern **[Hel14]**. Die gemessenen Eigenschaften können univariate (skalare) Größen oder multivariat (Vektor und Matrix) sein **[Sim14b]**.

Die PAT-Werkzeuge müssen in der Lage sein, auf die Zustände der Suspensionskristallisation einzugehen (z. B. einen Größenbereich von 50 bis 500  $\mu\text{m}$  und einer Suspensionsdichte von 10 bis 40 Vol %).

Ultraschall-Einzelfrequenz-, 3D-ORM- (523 PsyA CSD Particle Analyzer & APAS)- und FBRM-Methoden sind Beispiele für PAT-Werkzeuge, welche prinzipiell in der Lage sind, auf die Zustände der Suspensionskristallisation einzugehen. Daher werden diese in dieser Forschungsarbeit genutzt. Die Ultraschall-Einzelfrequenz-Methode ist eine ideale Methode zur In-situ-Bestimmung von Kristallisationsparametern in der flüssigen Phase (Konzentration, Übersättigung) und in der festen Phase (Suspensionsdichte und mittlere Partikelgröße). Diese Methode bietet eine hohe Zuverlässigkeit und gehört zur Reihe der neuen preiswerten PAT-Entwicklungen **[Ste13]**. Die 3D-ORM-Methode sowie die FBRM-Methode sind etablierte Methoden zum Messen der mittleren Partikelgröße, der mittleren Sehnenlänge oder der Partikelgrößenverteilung und der Suspensionsdichten inline und in Echtzeit **[Hel13a]**. Aber wo liegen die Grenzen dieser Werkzeuge in einem Kristallisationsprozess?

In dieser Forschungsarbeit wird die Auswirkung von Gasblasen auf das Ergebnis (gemessene mittlere Sehnenlänge) der 3D-ORM-Methode (523 PsyA CSD Particle Analyzer) untersucht. Auf den ersten Blick könnte diese Messmethode für konstante Siebfraktionen zugefügter Kristalle falsche mittlere Sehnenlängen erzeugen. Um den Grund für dieses Phänomen zu ermitteln, wurden einige der im Folgenden beschriebenen Verfahren durchgeführt.

Beruhend auf den resultierenden Daten, welche aus der Messung der Viskosität bei verschiedenen Kristall-Suspensionsdichten abgeleitet wurden, steigt die gemessene Viskosität innerhalb eines begrenzten Bereichs der Kristall-Suspensionsdichte linear an (siehe Abb. 7-1). Aufgrund der hohen Viskosität von Saccharosesuspensionen - hier die Fallstudie – besteht eine hohe Wahrscheinlichkeit, dass insbesondere bei höheren Kristall-Suspensionsdichten Gasblasen auftreten.

Darüber hinaus können mithilfe mikroskopischer Aufnahmen (inline) Gasblasen, insbesondere kleine Blasen bei höheren Kristall-Suspensionsdichten beobachtet werden (siehe Abb. 7-2).

Außerdem wurde ein Vergleich der Ergebnisse der 3D-ORM (523 PsyA CSD Particle Analyzer) Methode für drei verschiedene Kristall-Suspensionsdichten- und

Kristallgrößenbereiche mit und ohne Netzmittel durchgeführt. Die gemessene mittlere Kristallzahl (Anzahl) nimmt mit Zunahme der Kristall-Suspensionsdichte zu. Außerdem ist insbesondere bei höherer Volumen-Suspensionsdichte ein großer Unterschied zwischen der mit Netzmittel und der ohne Netzmittel gemessenen mittleren Kristallzahl offensichtlich (siehe Abb. 7-3 und Tabelle 7-1). Durch Hinzufügen des Netzmittels Tween 20 zu einer gesättigten Saccharoselösung erfolgt die Abnahme der Grenz-flächenspannung dieser Lösung und es treten Gasblasen aus der Lösung aus. Folglich kann bei höherer Kristall-Suspensionsdichte davon ausgegangen werden, dass Gasblasen bei der Messung der festen Phase eine nicht zu vernachlässigende Rolle spielen.

Außerdem wird der Einfluss der Partikelform auf das Ergebnis verschiedener Messmethoden einschließlich der Ultraschall-Einzelfrequenz-, FBRM- und 3D-ORM (APAS) –Methode bewertet. Es werden Vor- und Nachteile dieser Methoden verglichen und diskutiert. Gemäß den gemessenen Ultraschallgeschwindigkeitssignalen in den verwendeten Fallstudien - hier Saccharose- und L-Threonin-Suspensionen – zeigt die Ultraschall-Methode jedoch keine Empfindlichkeit bezüglich der Partikelform (siehe Abb. 6-5).

Die 3D-ORM-(APAS)-Messmethode zeigt bei nadelförmigen Partikeln im Vergleich zu nicht nadelförmigen Partikeln eine deutliche Schwankung der gemessenen Signale (durchschnittliche Länge) an (siehe Abb. 7-5). Darüber hinaus bleibt dieser Unterschied zwischen den Signalen von durchschnittlicher Länge für die beiden unterschiedlichen Partikelformen (nadelförmig und nicht nadelförmig) auch noch nach der Normalisierung erhalten (siehe Abb. 7-6). Nadelförmige Partikeln können je nach ihrer Orientierung zum Fokuspunkt entweder über ihre Länge oder ihre Breite aufgespürt werden. Daher kann in dieser Messmethode ein signifikanter Effekt der Partikelform auf die gemessenen Signale (durchschnittliche Länge) festgestellt werden. Die 3D-ORM-Methode ist mithilfe der Pulsation des Lasers in der Lage, die exponierte Partikeloberfläche zu messen, die mit der tatsächlichen Oberfläche des Partikels in Beziehung steht. Infolge der unterschiedlichen Höhe der von der gemessenen exponierten Partikeloberfläche abgeleiteten Signale ermöglicht diese Methode die Formen zu erklären **[Hel13a, Sch12b]**.

Darüber hinaus ist mit der FBRM-Methode keine endgültige Aussage bezüglich der Partikelform möglich. Mit der FBRM-Methode wird mit höherer Wahrscheinlichkeit die Breite der nadelförmigen Partikel als deren Länge gemessen. Bei nadelförmigen Partikeln kann es jedoch keine ähnlich hohe Schwankung geben, wie sie bei der 3D-ORM-Methode beobachtet werden kann (siehe Abb. 7-9). Darüber hinaus bleibt dieser Unterschied zwischen den Signalen von durchschnittlicher Länge für die beiden unterschiedlichen Partikelformen (nadelförmig und nicht nadelförmig) auch noch nach der Normalisierung erhalten (siehe Abb. 7-10). Die FBRM-Messmethode ist in der Lage, die durch das geradlinige Signal von einer zur anderen Kante eines Partikels abgeleitete mittlere Sehnenlänge der Partikel darzustellen.

Außerdem unterscheiden sich die mit der 3D-ORM- und FBRM-Methode gemessenen Partikellängen von den ausgesiebten Partikelgrößenfraktionen, da die Messprinzipien dieser Methoden unterschiedlich sind (siehe Abb. 7-5 und Abb. 7-9).

Es kann ein deutlicher Unterschied bei der Partikelzahl (Anzahl) der beiden verwendeten Systeme (Ammoniumchlorid und L-Threonin) bei gleicher Volumen-Suspensionsdichte beobachtet werden (siehe Abb. 7-7). Dieser Unterschied steht mit den unterschiedlichen Reflexionsintensitäten der Partikel und der Lösung sowie der Form, der Rauheit und der Reinheit der Partikel in Verbindung. Die Reflexionsintensitäten können mithilfe des Verdunklungsfaktors (OBF) (siehe Abb. 7-8) mit der 3D-ORM-(APAS)-Methode analysiert werden. Bei den Experimenten stellte sich heraus, dass je kleiner dieser erwähnte Faktor ist, umso geringer auch der absolute Wert der gemessenen Anzahl ist (vergleiche Abb. 7-7 und Abb. 7-8).

Eine Online-Kontrolle bei der Produktion kristalliner Substanzen bezüglich ihrer Morphologie oder des solvensvermittelten Phasentransfers ist in vielen Industrien von wesentlicher Bedeutung. In dieser Arbeit wird die Überwachung des solvensvermittelten Phasentransfers durch die Ultraschall-Einzelfrequenz- und die 3D-ORM-(APAS)-Methode beruhend auf Fallstudien mit Magnesiumsulfat, Dinatriumtetraborat und Sulfathiazol untersucht. Der solvensvermittelte Phasentransfer von Magnesiumsulfat-Hexahydrat/Dinatriumtetraborat-Pentahydrat zu Magnesiumsulfat-Heptahydrat/Dinatriumtetraborat-Decahydrat kann bei Verwendung der Ultraschall-Methode durch eine Zunahme der Temperatur und eine drastische Zunahme der Ultraschall-Geschwindigkeit (zum Zeitpunkt 04:29:44 in Abb. 6-10 und zum Zeitpunkt 01:52:55 in Abb. 6-11) sowie ebenso bei Verwendung der 3D-ORM-Methode durch eine signifikante Änderung der gemessenen Längen (D10, D50, D90 (längengewichtet)) (zum Zeitpunkt 04:29:44 in Abb. 6-10, zum Zeitpunkt 01:52:55 in Abb. 6-11 sowie zum Zeitpunkt 00:16:51 in Abb. 6-12) identifiziert werden. Auf die in der Fallstudie mit Sulfathiazol gemessenen Signale (Ultraschallgeschwindigkeit und -dämpfung) beruhend, zeigt die Ultraschall-Methode keinerlei Empfindlichkeit bezüglich des polymorphen Phasenübergangs. Mit der 3D-ORM-Methode kann der polymorphe Phasenübergang von Sulfathiazol der polymorphen Form I in die Formen II und III jedoch über die Veränderung der gemessenen Längen D10, D50 und D90 (längengewichtet) kontrolliert werden. Die durch die Inline-PAT-Werkzeuge erzielten Ergebnisse werden ebenso durch die optische Mikroskopie bestätigt.

## 11. Abbreviation

<b>APAS</b>	Advanced particle analyzing system	<b>PSD</b>	Particle size distribution
<b>API</b>	Active pharmaceutical ingredient	<b>PVM</b>	Particle vision and measurement
<b>ATR</b>	Attenuated total reflectance	<b>SD</b>	Suspension density
<b>ATR-FTIR</b>	Attenuated total reflectance-fourier transform infrared	<b>SEM</b>	Scanning electron microscopy
<b>c</b>	concentration	<b>SsNMR</b>	Solid state nuclear magnetic resonance
<b>COP</b>	Coincidence probability	<b>T</b>	Temperature [°C]
<b>3D ORM</b>	3D optical reflectance measurement	<b>TG</b>	Thermogravimetry
<b>CLD</b>	Chord length distribution	<b>UV-Vis</b>	Ultraviolet visible (200-900 nm)
<b>CSD</b>	Crystal size distribution	<b>v</b>	Ultrasound velocity [m/s]
<b>DSC</b>	Differential scanning calorimetry	<b>XRD</b>	X-ray diffractometry
<b>Far-IR</b>	Far infrared (200-10 cm <sup>-1</sup> )		
<b>FBRM</b>	Focused beam reflectance measurement		
<b>FTIR</b>	Fourier transform infrared		
<b>MCST</b>	Multi capture signal technology		
<b>MIR</b>	Mid infrared (4000-200 cm <sup>-1</sup> )		
<b>MZW</b>	Metastable zone width		
<b>NIR</b>	Near-infrared (12800-4000 cm <sup>-1</sup> )		
<b>PAT</b>	Process analytical technology		

## 12. Reference

**[Abu08a]** Abu Bakar, M. R., Rielly, C. D., Investigation of the polymorphism of sulfathiazole by a combined DSC-HSM approach, in: proceeding 17<sup>th</sup> International Symposium on Industrial Crystallization (ISIC), Ulrich, J., Jansens, P. (Eds.), Maastricht, Netherlands, Vol. 3, 2008, 1483-1489.

**[Abu08b]** Abu Bakar, M. R., Nagy, Z. K., Rielly, C. D., Towards the development of a polymorphic control approach in sulfathiazole crystallization, in: Proceeding 15<sup>th</sup> International workshop on Industrial Crystallization (BIWIC), Lorenz, H., Kaemmerer, H. (Eds.), Shaker publishing, Aachen, Germany, 2008, 235-242.

**[Abu09a]** Abu Bakar, M. R., Nagy, Z. K., Rielly, C. D., Seeded batch cooling crystallization with temperature cycling for the control of size uniformity and polymorphic purity of sulfathiazole crystals, *Organic Process Research & Development*, 13 (2009) 1343-1356.

**[Abu09b]** Abu Bakar, M. R., Nagy, Z. K., Saleemi, A. N., Rielly, C. D., The impact of direct nucleation control of crystal size distribution in pharmaceutical crystallization processes, *Crystal Growth & Design*, 9 (2009) 1378-1384.

**[Abu10]** Abu Bakar, M. R., Process analytical technology based approaches for the monitoring and control of size and polymorphic form in pharmaceutical crystallization processes, Ph. D. Thesis, Loughborough university, United Kingdom, 2010, <http://creativecommons.org/licenses/by-nc-nd/2.5/>.

**[Abu11]** Abu Bakar, M. R., Nagy, Z. K., Rielly, C. D., Dann, S. E., Investigation of the riddle of sulfathiazole polymorphism, *International Journal of Pharmaceutics*, 414 (2011) 86-103.

**[Ahl90]** Ahlneck, C., Zografi, G., The molecular basis of moisture effects on the physical and chemical stability of drugs in the solid state, *International Journal of pharmaceutics*, 62 (1990) 87-95.

**[Ahu78]** Ahuja, A. S., Hendee, W. R., Effects of particle shape and orientation on propagation of sound in suspensions, *Journal of Acoustical Society of America*, 63 (1978) 1074-1080.

**[All88]** Allen, T., Davies, R., Lloyd, P. J. (Eds.), An evaluation of the Lab-Tec 100 particle size analyzer, *Particle Size Analysis, Proceedings, 6<sup>th</sup> Particle Size Analysis Conference*, Guildford/UK, Wiley, Chichester, 1988, 33-44.

**[Alz02]** Al-Zoubi, N., Koundourellis, J. E., Malamataris, S., FT-IR and Raman spectroscopic methods for identification and quantitation of orthorhombic and monoclinic paracetamol in powder mixes, *Journal of Pharmaceutical and Biomedical Analysis*, 29 (2002) 459-467.

**[Bab98]** Babick, F., Hinze, F., Stintz, M., Ripperger; Ultrasonic spectrometry for particle size analysis in dense submicron suspensions, *Particle and Particle System Characterization*, 15 (1998) 230-236.

**[Bar02]** Barrett, P., Glennon, B., Characterizing the metastable zone width and solubility curve using Lasentec FBRM and PVM, *Chemical Engineering Research & Design*, 80 (2002) 799-805.

**[Bar05]** Barrett, P., Smith, B., Worlitschek, J., Bracken, V., O'Sullivan, B., O Grady, D., A review of the use of process analytical technology for understanding and optimization of production batch crystallization processes, *Organic Process Research & Development*, 9 (2005) 348-355.

**[Ber02]** Berglund, K. A., Analysis and measurement of crystallization utilizing the population balance, in: *Hand book of industrial crystallization*, Myerson, A. S. (Ed.), 2nd Ed., Butterworth-Heinemann, Boston, 2002, 101-103.

**[Bee11]** De Beer, T., Burggraeve, A., Fonteyne, M., Saerens, L., Remon, J. P., Vervaet, C., Near infrared and Raman spectroscopy for the in-process monitoring of pharmaceutical production process, *International Journal of Pharmaceutics*, 417 (2011) 32-47.

**[Bil10]** Billot, P., Couty, M., Hosek, P., Application of ATR-UV spectroscopy for monitoring the crystallization of UV absorbing and non-absorbing molecules. *Organic Process Research and Development*, 14 (2010) 511-523.

**[Bon11]** Bondi, R. W., Drennen, J. K., Quality by design and importance of PAT QbD, in: *Handbook of modern pharmaceutical analysis*, Ahuja, S., Scypinski, S. (Eds.), Vol 10, Elsevier Inc., Burlington, 2011, 195-244.

**[Bor08]** Borissova, A., Khan, S., Mahmud, T., Roberts, K.J., Andrews, J., Dallin, P., Chen, Z., Morris, J., In situ measurement of solution concentration during the batch cooling crystallization of L- Glutamic acid using ATR-FTIR spectroscopy coupled with chemometrics, *Crystal Growth & Design*, 9 (2008) 692-706.

**[Bri99]** Brittain, H. G., Byrn, S. R., Structural aspects of polymorphism, in: *Polymorphism in pharmaceutical solids*, Brittain, H. G. (Ed.), Marcel Dekker Inc., New York, USA, 1999; 73-124.

**[Bri02]** Brittain, H. G., Effects of mechanical processing on phase composition, *Journal of Pharmaceutical Science*, 91 (2002) 1573-1580.

**[Bri06]** Brittain, H. G., Methods for the characterization of polymorphs and solvates, in: *Polymorphism: in the pharmaceutical industry*, Hilfiker, R. (Ed.), Wiley-VCH Verlag GmbH&Co., 2006, 226-271.

**[Bub95a]** Bubnik, Z., Kadlec, P., Sucrose properties and applications, Mathlouthi, M. (Eds.), Blackie academic and professional, London, UK, 1995, 105.

- [Bub95b]** Bubnik, Z., Kadlec, P., Sucrose properties and applications, Mathlouthi, M. (Eds.), Blackie academic and professional, London, UK, 1995, 34.
- [Bub03]** Bubnik, Z., Kadlec, P., Hinkova, A., Recent progress at crystallization of sugar, *Engineering in Life Sciences*, 3 (2003) 141-145.
- [Bug01]** Bugay, D. E., Characterization of the solid-state: spectroscopic techniques, *Advanced Drug Delivery Reviews*, 48 (2001) 43-65.
- [Bur51]** Burton, W. K., Cabera, N., Frank, F. C., The growth of crystals and the equilibrium structure of their surfaces, *Philosophical Transaction A* 243, 299-358.
- [Byr82]** Byrn, S. R., *Solid-state chemistry of drugs*, New York: Academic Press, 1982.
- [Cai06]** Caillet, A., Puel, F., Fevotte, G., In-line monitoring of partial and overall solid concentration during solvent-mediated phase transition using Raman spectroscopy, *International Journal of Pharmaceutics*, 307 (2006) 201-208.
- [Cai07]** Caillet, A., Rivoire, A., Galvan, J. M., Puel, F., Fevotte, G., Crystallization of Monohydrate Citric Acid. 1. In situ monitoring through the joint use of Raman spectroscopy and image analysis, *Crystal Growth & Design*, 7 (2007) 2080-2087.
- [Cai08]** Caillet, A., Puel, F., Fevotte, G., Quantitative in situ monitoring of citric acid phase transition in water using Raman spectroscopy, *Chemical Engineering and Process Intensification*, 47 (2008) 377-382.
- [Cal05]** Calderon De Anda, J., Wang, X. Z., Roberts, K. J., Multi-scale segmentation image analysis for the in-process monitoring of particle shape with batch crystallizatioers, *Chemical Engineering Science*, 60 (2005) 1053-1065.
- [Car85]** Cardew, P. T., Davey, R. J., The kinetics of solvent mediated phase transformation, *Proceedings of the Royal Society of London, A*, 398 (1985) 415-428.
- [Che07]** Chew, J., Yu, Z., Chow, P., Tan, R., Recent advances in crystallization control: An industrial perspective, *Chemical Engineering Research & Design*, 85 (2007) 893-905.
- [Che13]** <http://chemister.ru/Database/properties-en.php?dbid=1&id=371> [accessed: 16.09.2013]
- [Chi75]** Chivate, M. R., Tavare, N. S., Growth rate measurement in DTB crystallizer, *Chemical Engineering Science*, 30 (1975) 354-355.
- [Con96]** Connolly, M., Debenedetti, P. G., Tung, H. H., Freeze crystallization of imipenem, *Journal of Pharmaceutical Sciences*, 85 (1996) 174-177.

**[Cor08]** Cornel, J., Lindenberg, C., Mazzoti, M., Quantitative application of in-situ ATR-FTIR and Raman spectroscopy in crystallization processes, *Industrial & Engineering Chemistry Research*, 47 (2008) 4870-4882.

**[Cor12]** Cornel, J., Lindenberg, C., Schöll J., Mazzotti, M., Raman Spectroscopy, in: *Industrial crystallization process monitoring and control*, Chianese, A. (Eds.), Kramer, H. J. M., Wiley-VCH, Weinheim, Germany, 2012, 93-103.

**[Cro11]** Cronin, L., Kitson, P. J., Wilson, C. C., Process understanding-crystallization, in: *Process Understanding-For scale-up and manufacture of Active Ingredients*, Houson, I. (Ed.), Wiley-VCH Verlag, Weinheim, 2011, 199-225.

**[Dav02]** Davey, R. J., Blagden, N., Righini, S., Alison, H., Ferrari, E. S., Nucleation control in solution mediated polymorphic phase transformation: The case of 2,6-Dihydroxybenzoic acid, *Journal of Physical Chemistry B*, 106 (2002) 1954-1959.

**[Daw59]** Dawson, R. M. C., *Data for biochemical research*, Oxford, Clarendon Press, 1959, <http://en.wikipedia.org/wiki/Threonine>, [accessed: 16/09/2013].

**[Der03]** Derdour, L., Fevotte, G., Puel, F., Carvin, P., Real-time evaluation of the concentration of impurities during organic solution crystallization, *Powder Technology*, 129 (2003) 1-7.

**[Ela04]** Elahi, M., Untersuchungen zur Optimierung der Kühlrate der Kühlkristallisation von Nachprodukt-Kristallsuspensionen bei der Saccharosegewinnung, Dissertation: Technische Universität Berlin, 2004.

**[Eli98]** Elliot, S., *The physics and chemistry of solids*, Wiley, Chichester, 1998.

**[Eps53]** Epstein, P. S. Carhart, R. R., The absorption of sound in suspensions and emulsions. I. Water fog in air, *Journal of the Acoustic Society of America*, 25 (1953) 553-565.

**[Fda04]** U. S. Department of Health and Human Services, Food and Drug Administration, Guidance for Industry: PAT- a framework for innovative pharmaceutical development, Manufacturing and quality assurance, 2004; Online available:<http://www.fda.gov/downloads/Drugs/GuidanceComplianceRegulatoryInformation/Guidances/UCM070305.pdf>, 21/01/2015.

**[Fev07]** Fevotte, G., In situ Raman spectroscopy for in-line control of pharmaceutical crystallization and solids elaboration processes: a review, *Chemical Engineering Research and Design*, 85 (2007) 906-920.

**[Fro14]** Froberg, P., Ulrich, J., Single-frequency ultrasonic crystallization monitoring (UCM): Innovative technique for in-line analyzing of industrial crystallization processes, *Organic Process Research & Development*, 19 (2015) 84-88.



- [Fuj02]** Fujiwara, M., Chow, P. S., Ma, D. L., Braatz, R. D., Paracetamol crystallization using laser backscattering and ATR-FTIR spectroscopy: metastability, agglomeration and control, *Crystal Growth & Design*, 2 (2002) 363-370.
- [Gag09]** Gagniere, E., Mangin, D., Puel, F., Bebon, C., Klein, J.P., Monnier, O., Garcia co-crystal formation in the solution: in situ solute concentration monitoring of the two compounds, *Crystal Growth and Design*, 9 (2009) 3376-3383.
- [Gar82]** Garside, J., Gibilaroand, L. G., Tavare, N.S., Evaluation of crystal growth kinetics from a desupersaturation curve using initial derivations, *Chemical Engineering Science*, 37 (1982) 1625-1628.
- [Gav95]** Gavezzotti, A., Filippini, G., Polymorphic forms of organic crystals at room conditions: Thermodynamic and structural implications, *Journal of the American Chemical Society*, 117 (1995) 12299-12305.
- [Gee03]** Geers, H., Witt, W., Ultrasonic extinction for in-line measurement of particle size and concentration of suspensions and emulsions, In: *Proceeding Particulate System Analysis*, Harrogate, United Kingdom, 2003.
- [Gil06]** Gillon, A. L., Steele, G., Nagy, Z. K., Makwana, N., Rielly, C. D., PAT investigations in to the crystallization of caffeine, in: *Proceeding 13<sup>th</sup> International Workshop on Industrial Crystallization (BIWIC 2006)*, Jansens, P. J., ter Horst, J. H., Jiang, S. (Eds.), Delft, Netherlands, 2006, 35-42.
- [Giu03]** Giuletta, M., Guardani, R., Nascimento, A. O., Arntz, B., In-line monitoring of crystallization processes using Laser Reflection Sensor and a Neural Network Model, *Chemical Engineering & Technology*, 26 (2003) 267-272.
- [Gla04]** Glade, H., Ilyaskarov, M, Ulrich, J., Determination of crystal growth kinetics using ultrasound technique, *Chemical Engineering and Technology*, 27 (2004) 736-740.
- [Gme73]** Gmelin, L., Natrium, in: *Handbuch der Anorganischen Chemie*, 8th ed., R. J. Meyer, E. H. E. Pietsch (Eds.) , Verlag Chemie, Berlin, 1973.
- [Gov06]** Govindarajan, R., Suryanarayanan, R., Processing-induced phase transformations and their implications on pharmaceutical product quality, in: *Polymorphism in the pharmaceutical industry*, Hilfiker, R. (Ed.), Wiley VCH Verlag GmbH&Co. KGaA, Weinheim, 2006, 333-364.
- [Hei12]** Heinrich, J., Determination of crystallization kinetics using in-situ measurement techniques and model-based experimental design and analysis, Ph. D. Thesis, Martin-Luther university Halle-Wittenberg, Germany, 2008. <http://sundoc.bibliothek.uni-halle.de/diss-online/08/09H002/index.htm>.

**[Hel12a]** Helmdach, L., Pertig, D., Rüdiger, S., Lee, K. S., Stelzer, T., Ulrich, J., Bubbles-trouble-makers in crystallizers: Classical problems during inline measurement, *Chemical Engineering and Technology*, 35 (2012) 1017-1023.

**[Hel12b]** Helmdach, L., Feth, M. P., Ulrich, J., Online analytical investigations on solvent-, temperature- and water vapour-induced phase transformations of citric acid, *Crystal Research and Technology*, 47 (2012) 967- 984.

**[Hel13a]** Helmdach, L., Schwartz, F., Ulrich, J., Process control using advanced particle analyzing systems-application from crystallization to fermentation process, *Chemical Engineering and Technology*, 36 (2013) 1-8.

**[Hel13b]** Helmdach, L., Feth, M. P., Ulrich, J., Integration of Process Analytical Technology (PAT) tools in pilot plant setups for the real-time monitoring of crystallizations and phase transitions, *Organic Process Research & Development*, 17 (2013) 585-598.

**[Hel14]** Helmdach, L., Application of process analytical technology (PAT) tools to develop and monitor scalable crystallization processes of pharmaceuticals, Ph. D. Thesis, Martin-Luther university Halle-Wittenberg, 2014. [http://141.48.65.178/hs/content/titleinfo/1798244.](http://141.48.65.178/hs/content/titleinfo/1798244)

**[Hel15]** Helmdach, L., Feth, M. P., Ulrich, J., Application of ultrasound measurements as PAT tools for industrial crystallization process development of pharmaceutical compound, *Organic Process Research & Development*, 19 (2015) 110-121.

**[Hip00]** Hipp, A. K., Walker, B., Mazzotti, M., Morbidelli, M., In-situ monitoring of batch crystallization by ultrasound spectroscopy, *Industrial and Engineering Chemistry Research*, 39 (2000) 783-789.

**[Fal03]** Falcon, J., Berglund, K. A., Monitoring of antisolvent addition crystallization with Raman spectroscopy, *Crystal Growth & Design*, 3 (2003) 947-952.

**[Hea02]** Heath, A. R., Fawell, P. D., Bahri, P. A., Swift, J. D., Estimating average particle size by Focused Beam Reflectance Measurement (FBRM), *Particle and Particle Systems Characterization*, 19 (2002) 84-95.

**[How09]** Howard, K. S., Nagy, Z. K., Saha, B., Robertson, A. L., Steele, G., Martin, D., A process analytical technology based investigation of the polymorphic transformations during the anti-solvent crystallization of sodium benzoate from IPA/water mixture, *Crystal Growth and Design*, 9 (2009) 3964-3975.

**[Hu05]** Hu, Q., Rohani, S., Wang, D. X., Jutan, A., Optimal control of a batch cooling seeded crystallizer, *Journal of Powder Technology*, 156 (2005) 170-176.

**[Jon02]** Jones, A. G., *Crystallization Process Systems*, Butterworth-Heinemann, Boston, 2002.

- [Jou10]** Jouyban, A., Handbook of solubility data for pharmaceuticals, CRC Press, Boca Raton, 2010, 2.
- [Kai07]** Kail, N., Briesen, H., Marquardt, W., Advanced geometrical modeling of focused beam reflectance measurements (FBRM), Particle & Particle System Characterization, 24 (2007) 184-192.
- [Kai08]** Kail, N., Briesen, H., Marquardt, W., Analysis of FBRM measurements by means of a 3D optical model, Powder Technology, 185 (2008) 211-222.
- [Kar06]** Karpinski, P. H., Polymorphism of active pharmaceutical ingredients, Chemical Engineering & Technology, 29 (2006) 233-237.
- [Kem08]** Kempkes, M., Eggers, J., Mazzotti, M., Measurement of particle size and shape by FBRM and in situ microscopy, Chemical Engineering Science, 63 (2008) 4656-4675.
- [Kho93]** Khoshkhoo, S., Anwart, J., Crystallization of the polymorphs: the effect of solvent, Journal of Physics D: Applied Physics, 26 (1993) 890-893.
- [Kem08]** Kempkes, M., Eggers, J., Mazzotti, M., Measurement of particle size and shape by FBRM and in situ microscopy, Chemical Engineering Science, 63 (2008) 4656-4675.
- [Lag81]** Lagas, M., Lerk, C. F., The polymorphism of sulfathiazole, International Journal of Pharmaceutics, 8 (1981) 11-24.
- [Laf04]** Lafferre`re, L., Hoff, C., Veessler, S., in situ monitoring of the impact of liquid-liquid phase separation on drug crystallization by seeding, Crystal Growth & Design, 4 (2004) 1175-1180.
- [Lem13]** Le-Minh, T., Schwartz, M., Solubility and induction time of the L-Enantiomer of amino acid Arginine determination with in situ 3D-ORM, in: Proceeding of BIWIC 2013, 20th International Workshop on Industrial Crystallization, Qu, H., Rantaen, J., Malwade, C. (Eds.), Pub. University of Southern Denmark, Odense, Denmark, 2013, 373-379.
- [Lar07]** Larson, P. A., Rawlings, J. B., Ferrier, N. J., Model-based object recognition to measure crystal size and shape distributions from in-situ video images, Chemical Engineering Science, 62 (2007) 1430-1441.
- [Lek04]** Lekhal, A., Girard, Brown, M. A., Kiang, S., Khinast, J. G., Glasser, B. J., The effect of agitated drying on the morphology of L-threonine (needle like) crystals, International Journal of Pharmaceutics, 270 (2004) 263-277.
- [Lev78]** Levy, H. A., Lisensky, G. C., Crystal structures of sodium sulfate decahydrate (Glauber's salt) and sodium tetraborate decahydrate (borax), Acta Crystallographica, B34 (1978) 3502-3510.

**[Lew01]** Lewiner, F., Fevotte, G., Klein, J. P., Puel, F., Improving batch cooling seeded crystallization of an organic weed-killer using on-line ATR-FTIR measurement of supersaturation, *Journal of Crystal Growth*, 226 (2001) 348-362.

**[Lin12]** Lindenberg, C., Cornel, J., ATR-FTIR Spectroscopy, in: *Industrial crystallization process monitoring and control*, Chianese, A., Kramer, H. J. M. (Eds.), Wiley-VCH, Weinheim, Germany, 2012, 81-91.

**[Li05]** Li, M. Z., Wilkinson, D., Determination of non-spherical particle size distribution from chord length measurements, Part 2: experimental validation, *Chemical Engineering Science*, 60 (2005) 4992-5003.

**[Lun00]** Luner, P. E., Majuru, S., Seyer, J. J., Kemper, M. S., Quantifying crystalline form composition in binary powder mixtures using near-infrared reflectance spectroscopy, *Pharmaceutical Development & Technology*, 5 (2000) 231-246.

**[Man09]** Mangin, D., Puel, F., Veessler, S., Polymorphism in processes of crystallization in solution: A practical review, *Organic Process Research & Development*, 13 (2009) 1241-1253.

**[Mat 95]** Mathlouthi, M., Reiser, P., Sucrose properties and applications, Mathlouthi, M., Reiser, P. (Eds.), Blackie academic and professional, London, UK, 1995, 105.

**[Met14]** Mettler Toledo, [www.mt.com/FBRM](http://www.mt.com/FBRM), 10/2014.

**[Max98]** Maxwell, J. C., *A treatise on electricity and magnetism*, Vol 1, 3<sup>rd</sup> Ed., Clarendon Press, Oxford, New York, 1998.

**[Mer01]** Mersmann, A., Heyer, C., Eble, A., Activated nucleation, in: *Crystallization Technology Handbook*, Mersmann, A. (Ed.), Marcel-Dekker, New York, 2001, 45-76.

**[Mos14a]** Mostafavi, M., Petersen, S., Ulrich, J., The influence of air bubbles on the measurement of different crystal sizes and suspension densities by the 3D ORM measurement technique, in: *proceeding 19<sup>th</sup> international symposium of industrial crystallization (ISIC)*, Biscan, B., Mazzotti, M. (Eds.), Pub. Toulouse University, Toulouse, France, 2014, 375-377.

**[Mos14b]** Mostafavi, M., Petersen, S., Ulrich, J., Effect of particle shape on inline particle size measurement techniques, *Chemical Engineering & Technology*, 37 (2014)1721-1728.

**[Mos15]** Mostafavi, M., Ulrich, J., Monitoring phase transitions of crystals in-line, *Advanced Powder Technology*, 2015, in press.

**[Mou03]** Mougine, P., Wilkinson, D., Roberts, K. J., In-situ ultrasonic attenuation spectroscopic study of the dynamic evolution of particle size during solution-phase crystallization of urea, *Crystal Growth & Design*, 3 (2003) 67-72.

**[Mul01]** Mullin, J. W., *Crystallization*, 4th ed., Butterworth-Heinemann, Oxford, 2001.

**[Moh00]** Mohan, R., Boateng, K. A., Myerson, A. S., Estimation of crystal growth kinetics using differential scanning calorimetry, *Journal of Crystal Growth*, 212 (2000) 489-499.

**[Mou02]** Mouglin, P., Wilkinson, D., Robert, K. J., In situ measurement of particle size during the crystallization of L-glutamic acid under two polymorphic forms: influence of crystal habit on ultrasonic attenuation measurements, *Crystal Growth & Design*, 2 (2002) 227-234.

**[Nai98]** Naito, M., Hayakawa, O., Nakahira, K., Mori, H., Tsubaki, J., Effect of particle shape on the particle size distribution measured with commercial equipment, *Powder Technology*, 100 (1998) 52-60.

**[Nyv97]** Nyvlt, J., On the kinetics of solid-liquid-solid phase transformation, *Crystal Research & Technology*, 32 (1997) 695-699.

**[Oma99]** Omar, W., Zur Bestimmung von Kristallisationskinetiken auch unter der Einwirkung von Additiven mittels Ultraschallmeßtechnik, PhD thesis, University of Bremen, Germany, 1999.

**[O'Su03]** O'Sullivan, B., Barrett, P., Hsiao, G., Carr, A., Glennon, B., In situ monitoring of polymorphic transitions, *Organic Process Research Development*, 7 (2003) 977-982.

**[Osu05]** O'Sullivan, B., Glennon, B., Application of the in situ FBRM and ATR-FTIR to the monitoring of the polymorphic transformation of D-Mannitol, *Organic Process Research & Development*, 9 (2005) 884-889.

**[Ott02]** Otto, W., Magnesium Compounds, in: M. Bohnet (Eds.) *Ullmann's Encyclopedia of Industrial Chemistry*, 6<sup>th</sup> ed., Electronic Release, Wiley-VCH, Weinheim, 2002.

<http://cdnetz.bibliothek.uni-halle.de/NetManB...>

**[Per11]** Pertig, D., Buchfink, R., Petersen, S., Stelzer, T., Ulrich, J., Inline analyzing of industrial crystallization processes by an innovative ultrasonic probe technique, *Chemical Engineering and Technology*, 34 (2011) 639-646.

**[Per15]** Pertig, D., Fardmostafavi, M., Stelzer, T., Ulrich, J., Monitoring concept of single-frequency ultrasound and its application in dynamic crystallization processes, *Advanced Powder Technology*, 2015, accepted.

**[Pin95]** Pinfield, V. J., Povey, M. J. W., Dickinson, E., The application of modified forms of the Urick equation to the interpretation of ultrasound velocity in scattering systems, *Ultrasonics*, 33 (1995) 243-251.

**[Pov97]** Povey, M. J. W., *Ultrasonic technique for fluid characterization*, Edited by M. J. W. Povey, Pub. Academic Press, San Diego, CA, 1997.

- [Qu07]** Qu, H., Louhi-Kultanen, M., Kallas, J., Additive effects on the solvent-mediated anhydrate/hydrate phase transformation in a mixed solvent, *Crystal Growth & Design*, 7 (2007) 724-729.
- [Raw93]** Rawlings, J. B., Miller, A. G., Witkowaski, W. R., Model identification and control of solution crystallization processes: A review, *Industrial and Engineering Chemistry Research*, 32, 1275-1296.
- [Reu06]** Reutzel-Edens, S. M., Achieving polymorph selectivity in the crystallization of pharmaceutical solids: Basics considerations and recent advances, *Current Opinion in drug discovery and development*, 9 (2006) 806-815.
- [Rod99]** Rodriguez-Hornedo, N., Murphy, D., Significance of controlling crystallization mechanisms and kinetics in pharmaceutical systems, *Journal of Pharmaceutical Science*, 88 (1999) 651-660.
- [Rod03]** Rodrigues, J. J., Misoguti, L., Nunes, F. D., Mendonca, C. R., Zilio, S. C., Optical properties of L-Threonine crystals, *Optical Materials*, 22 (2003) 235-240.
- [Rod04]** Rodriguez-Spong, B., Price, C. P., Jayasankara, A., Matzgerb, A. J., Rodriguez-Hornedo, N., General principles of pharmaceutical solid in polymorphism: a supermolecular perspective, *Advanced Drug Delivery Reviews*, 56 (2004) 241-247.
- [Ruf00]** Ruf, A., Worlitschek, J., Mazzotti, M., Modeling and experimental analysis of PSD measurements through FBRM, *Particle & Particle System Characterization*, 17 (2000) 167-169.
- [Sac06]** Sachin, L., Grant, D. J. W., Thermodynamics of polymorphs, in: polymorphism: in the pharmaceutical industry, Hilfiker, R. (Ed.), WILEY-VCH Verlag GmbH & Co. KGaA, Weinheim; Germany, 2006, 21-41.
- [Sat10]** Sathe, D., Sawant, K., Mondkar, H., Naik, T., Deshpande, M., Monitoring temperature effect on the polymorphic transformation of Acitretin using FBRM-Lasentec, *Organic Process Research & Development*, 14 (2010) 1373-1378.
- [Say02]** Sayan, P., Ulrich, J., The effect of particle size and suspension density on the measurement of ultrasonic velocity in aqueous solutions, *Chemical Engineering and Processing*, 41 (2002) 281-287.
- [Sch95]** Schrader, B., Infrared and Raman spectroscopy: methods and applications, Schrader, B. (Ed.), Wiley-VCH Verlag GmbH, Weinheim, 1995.
- [Sch02a]** Schwartz, A. M., Myerson, A. S., Solutions and solution properties, in: Handbook of Industrial crystallization, Myerson, A. S. (Ed.), Butterworth-Heinemann, Boston, 2002, 1-32.
- [Sch06a]** Schoell, J., Bonalumi, D., Vicum, L., Mueller, M., Mazzotti, M., In situ monitoring and modeling of the solvent-mediated polymorphic transformation of L-glutamic acid, *Crystal Growth & Design*, 6 (2006a) 881-891.

- [Sch06b]** Schoell, J., Vicum, L., Mueller, M., Mazzotti, M., Precipitation of L-glutamic acid: determination of nucleation kinetics, *Chemical Engineering & Technology*, 29 (2006) 257-264.
- [Sch07]** Schöll, J., Lindenberg, C., Vicum, L., Brozio, J., Mazzoti, M., Precipitation of L-glutamic acid: determination of growth kinetics, *Faraday Discuss*, 136 (2007) 238-255.
- [Sch12a]** Schöll, J., Kempkes, M., Mazzotti, M., Focused Beam Reflectance Measurement, Chianese, A. Kramer, H. J. M., (Eds.), Wiely-VCH, Weinheim, Germany, 2012, 21-28.
- [Sch12b]** Schwartz, F., Schwartz, J., Crystal shadow surface area in situ analyzer, in: *Proceeding of BIWIC 2013, 20th International Workshop on Industrial Crystallization*, Sha, Z., Yin, Q., Chen, J., Xie, C., Pub. Authors, Tianjin, China, 2012, 165-170.
- [Sch13]** Schuster, A., Investigation on the formation of hollow acicular crystals and their usage as container systems, Ph. D. Thesis, Martin Luther University Halle-Wittenberg, Germany, 2013.
- [Sco05]** Scott, C., Black, S., In-line analysis of impurity effects in crystallization, *Organic Process Research & Development*, 9 (2005) 890-893.
- [Sei65]** Seidell, A., Linke, W. F., *Solubilities of Inorganic and Metal Organic Compounds*, 4<sup>th</sup> ed., W. F. Linke (Eds.), Washington: ACS, 1965.
- [Sen03]** Sensotech GmbH: <http://www.sensotech.com/>, 17.09.2003.
- [Seq13]** Sequip S&E GmbH: <http://www.sequip-particle-technology.16/09/2013>.
- [Ses20]** Sessiecq, P., Gruy, F., Cournil, M., Study of ammonium chloride crystallization in a mixed vessel, *Journal of Crystal Growth*, 208 (2000) 555-568.
- [Sim09]** Simon, L. L., Nagy, Z. K., Hungerbuehler, K., Comparison of external bulk video imaging with focused beam reflectance measurement and Ultra-Violet visible spectroscopy for metastable zone identification in food and pharmaceutical crystallization processes, *Chemical Engineering Science*, 64 (2009) 3344-3351
- [Sim14a]** Simone, E., Saleemi, A. N., Nagy, Z. K., Raman, UV, NIR, and Mid-IR spectroscopy with Focused Beam Reflectance Measurement in monitoring polymorphic transformations, *Chemical Engineering and Technology*, 37 (2014) 1305-1313.
- [Sim14b]** Simone, E., Saleemi, A. N., Nagy, Z. K., Application of quantitative Raman spectroscopy for the monitoring of polymorphic transformation in crystallization processes using a good calibration practice procedure, *Chemical Engineering Research and Design*, 92 (2014) 594-611.

**[Sim15a]** Simone, E., Saleemi, A. N., Nagy, Z. K., In situ monitoring of polymorphic transformations using a composite sensor array of Raman, NIR, and ATR-UV/vis spectroscopy, FBRM, and PVM for an intelligent decision support system, Organic Process Research & Development, 19 (2015) 167-177.

**[Smi02]** Smith, A. R., Boric oxide, boric acid and borates, in: M. Bohnet (Eds.) Ullmann's Encyclopedia of Industrial Chemistry, 6<sup>th</sup> ed., Electronic Release, Wiley-VCH, Weinheim, 2002.

<http://cdnetz.bibliothek.uni-halle.de/NetManB...>

**[Smi10]** Smith, A., Pankewitz, Berens, C., Ultrasonic extinction for full concentration, real time particle size analysis in the mining industry, In: Proceeding 2<sup>nd</sup> International Congress on Automation in the Mining Industry, Santiago, Chile, 2010.

**[Ste13]** Stelzer, T., Pertig, D., Ulrich, J., Ultrasound technique as tool to monitor in-line liquid and solid phase of industrial crystallization processes, Journal of Crystal Growth, 362 (2013) 71-76.

**[Str04]** Strege, C., On (pseudo) polymorphic phase transformations, Ph. D. Thesis, Martin Luther university Halle-Wittenberg, Germany, 2004.  
<http://141.48.65.178/hs/content/titleinfo/1148089>

**[Su10]** Su, W., Hao, H., Barrett, M., Glennon, The impact of operating parameters on the polymorphic transformation of D-Mannitol characterized in situ with raman spectroscopy, FBRM and PVM, Organic Process Research & Development, 14 (2010) 1432-1437.

**[Sym15]** Sympatec GmbH,  
<http://sympatec.com/EN/UltrasonicExtinction/UltrasonicExtinction.html/19.02.2015>.

**[Tit03]** Titiz-Sargut, S., Ulrich, J., Application of a protected ultrasound sensor for the determination of the width of the metastable zone, Chemical Engineering and Processing, 42 (2003) 841-846.

**[Ton07]** Tong, W.Q., Practical aspects of solubility determination in pharmaceutical preformulation; in: Solvent systems and their selection in pharmaceuticals and bio pharmaceuticals, Augustijns, P., Brewster, M. E (Eds.), Springer, New York, Volume VI, 2007, 137-149.

**[Tho05]** Thompson, D., Kougoulos, E., Jones, A., Wood-Kaczmar, M. J., Solute concentration measurement of an important organic compound using ATR-UV spectroscopy, Journal of Crystal Growth, 276 (2005) 230-236.

**[Ulr02]** Ulrich, J., Strege, C., Some aspects of the importance of metastable zone width and nucleation in industrial crystallizers, Journal of Crystal Growth, 237-239 (2002) 2130-2135.



**[Ulr06]** Ulrich, J., Jones, M. J., Heat and mass transfer operations-crystallization, in Encyclopedia of life support systems (EOLSS), Developed under the Auspices of the UNESCO, Eolss publishers, Oxford, UK, <http://www.eolss.net>.

**[Ulr12]** Ulrich, J., Jones, M. J., Speed of sound, in: Industrial crystallization process monitoring and control, Chianese, A., Kramer, H. J. M. (Eds.), Wiley-VCH, Weinheim, Germany, 2012, 59-69.

**[Van02]** Vankeirsbilck, T., Vercauteren, A., Baeyens, W., Van der Weken, G., Verpoort, F., Vergote, G., Remon, J. P., Applications of Raman spectroscopy in pharmaceutical analysis, Trends in Analytical Chemistry, 21 (2002) 869-877.

**[Var08]** Variankaval, N., Cote, A. S., Doherty, M. F., From form to function: crystallization of active pharmaceutical ingredients, American Institute of Chemical Engineers (AIChE) Journal, 54 (2008) 1682-1688.

**[Vit07]** Vitez, I. M., Newman, A. W., Thermal microscopy, in: Thermal Analysis of Pharmaceuticals, Craig, D. Q. M. & Reading, M. (Ed.), CRC Press, 2007, 221-264.

**[Wan08]** Wang, X. Z., Roberts, K. J., Ma, C., Crystal growth measurement using 2D and 3D imaging and perspectives for shape control, Chemical Engineering Science, 63 (2008) 1173-1184.

**[Wor03]** Worlitschek, J., Mazzotti, M., Choice of the focal point position using Lasentec FBRM, Particle & Particle System Characterization, 20 (2003) 12-17.

**[Wyn03]** Wynn, E. J. W., Relationship between particle size and chord-length distributions in focused beam reflectance measurement: stability of direct inversion and weighting, Journal of Powder Technology, 133 (2003) 125-133.

**[Wor05]** Worlitschek, J., Hocker, T., Mazzotti, M., Restoration of PSD from chord length distribution data using the method of projections onto convex sets, Particle & Particle System Characterization, 22 (2005) 81-98.

**[Yu98]** Yu, L., Reutzel, S. M., Stephenson, G. A., Physical characterization of polymorphic drugs: an integrated characterization strategy, Pharmaceutical Science Technology Today, 1 (1998) 118-127.

**[Yu04]** Yu, L. X., Lionberger, R. A., Raw, A. S., D'Costa, R., Wu, H., Hussain, A. S., Application of process analytical technology to crystallization processes, Advanced Drug Delivery Reviews, 56 (2004) 349-369.

**[Yu05]** Yu, Z. Q., Tan, R. B. H., Chow, P. S., Effects of operating conditions on agglomeration and habit of paracetamol crystals in anti-solvent crystallization, Journal of crystal growth, 279 (2005) 477-488.

**[Yu08]** Yu, Z. Q., Chow, P. S., Tan, R. B. H., Interpretation of focused beam reflectance measurement (FBRM) data via simulated crystallization, Organic Process Research & Development, 12 (2008) 646-654.

**[Zap02]** Zapp, K. H., Wostbrock, K. H., Schäfer, M., Sato, K., Seiter, H., Zwick, W., Creutziger, R., Leiter, H., Ammonium compounds, in: Bohnet, M. (Ed.), Ullmann's Encyclopedia of Industrial Chemistry, 6th Ed., Electronic Release, Wiley-VCH, Weinheim, 2002, <<http://cdnetz.bibliothek.uni-halle.de/NetManB>>.

**[Zha09]** Zhang, G. G., Zhou, D., Crystalline and Amorphous Solids, in: Developing Solid Oral Dosage Forms-Pharmaceutical Theory and Practice, Qiu. Y. (Ed.), Academic Press, New York, 2009, 25-60.

## 13. Appendix

### 13.1 Ultrasound device

**Table 13-1:** The features of the used ultrasound device (Liquisonic 50) [Sen03].

Supplier	SenseTech GmbH
Ultrasound velocity	Precision: 0.05 m/s
attenuation	Precision: 0.05 dB
Temperature of liquid	-20°C to 120°C (Optional up to 200°C)
Frequency	2MHz (0.1 W)
Pressure	Standard 16 bar
Diameter sensor head	40 mm
Diameter sensor bar	12 mm
Immersion length	Standard: 50 mm
Supply	6W, 24VDC
Data acquisition software	SonicWork 5.3



**Fig. 13-1:** Ultrasound device with ultrasound sensor and controller [Hei12].

## 13.2 Optical reflectance measurement

**Table 13-2:** The features of the used 3D ORM [Seq13].

Sensor name	APAS14
Supplier	Sequip S&E GmbH
Laser	785 nm, 10 mW, Laser class IIIb
Minimum laser cross point	120 nm
Maximum laser point distance in depth	2000 μm
Temperature	-120°C to 300°C
Particle size range	0.5-2000 μm
Fiber optic	One single-mode 4 μm fiber (fiber-optical coupler)
Immersion length	Standard: 50 mm
Supply	6W, 24VDC
Software	MCSA 1.0.3.48



**Fig. 13-2:** 3D ORM device with APAS sensor and controller [Seq13].

### 13.3 Focused beam reflectance measurement (FBRM)

**Table 13-3:** The features of the used FBRM [Hel13a, Hel14, Kai08, Met14].

Supplier	Mettler-Toledo GmbH, Giessen, Germany
Rotation of optical lens	Yes, with $2 \text{ ms}^{-1}$
Focal point	Fixed, (+20 $\mu\text{m}$ inside sapphire window)
Fiber optic	Two multimode 105/125 $\mu\text{m}$ fibers (beam splitter)
Fiber diameter	60 $\mu\text{m}$
Effective lens diameter	2.5 mm
Laser intensity	0.9 mW at the probe window
Laser wavelength	780 nm
Minimum laser diameter	1.2 $\mu\text{m}$
Extraction of raw reflection signals	yes
Measurement particle size range	0.5-2000 $\mu\text{m}$
Suspension density	SD: less than 80 wt%



**Fig. 13-3:** FBRM device with sensor and controller [Met14].

## **14. Statement of authorship**

I declare that I have written this document on my own. It is a compilation of the results of work carried out by my own. The used resources and tools or previously cited information have been distinguished by quotation marks.

Halle, 06.03.2015

Maryam Fardmostafavi

## 15. Curriculum Vitae (CV)

---

### **Personal Information**

**Name:** Maryam Mostafavi

**Place of Birth:** Tehran

**E-mail:** maryam.fardmostafavi@iw.uni-halle.de/mar\_mostafavi@yahoo.com

---

### **Educational Background**

- **PhD student**

04/2012-04/2015, PhD student at the chair of Thermal Process Technology, Martin- Luther University Halle-Wittenberg

**Dissertation: In-line/on-line Measuring Techniques in the Solution Crystallization Processes**

- **MSc ( Master of Science)**

09/2003-02/2006, Faculty of Engineering, Department of Chemical Engineering, Tarbiat Modares University, Tehran

**Dissertation: Modeling of Oxidative Dehydrogenation of Propane for Propylene Production in Membrane Reactor**

- **BSc (Bachelor of Science)**

09/1998 - 09/2002, Faculty of Engineering, Isfahan University of Technology, Isfahan

**Dissertation: Study of Air Pollution and the Methods for Prevention of it.**

---

### **Professional Training**

Worked as a trainee in Behran Oil Company (ESSO) in 2002.

---

## Employment / Professional Experience

- 04/2012-04/2015 Worked as research associate at the chair of Thermal Process Technology, Martin- Luther University Halle-Wittenberg
- 12/2006-09/2010 Worked in the Pars Khodro (GM), Engineering Section, Paint Shop

## Work Project

- Increase of paint shop capacity of Pars Khodro Company project from 35 units per hour to 40 units per hour. Investigation of total stations of the paint shop from 4 aspects (material, equipment, energy & man power) with cooperation of **Renault Company**
  - RFQ (Request for Quotation) preparation for new paint shop and new plastic paint shop
- 

## Conference paper

- Mostafavi, M., Petersen, S., Ulrich, J., **The influence of air bubbles on the measurement of different crystal sizes and suspension densities by the 3D ORM measurement technique**, in: proceeding 19<sup>th</sup> international symposium of industrial crystallization (ISIC), Biscan, B., Mazzotti, M. (Eds.), Pub. Toulouse University, Toulouse, France, 2014, 375-377.
  - Mostafavi, M., Omidkhah, M. R., **Modeling of oxidative dehydrogenation of propane for propylene production in membrane reactor**, Accepted to European Congress of Chemical Engineering (accepted date: 07/ 2007), Copenhagen, Denmark.
- 

## Publication

- Mostafavi, M., Petersen, S., Ulrich, J., **Effect of particle shape on inline particle size measurement techniques**, Chemical Engineering & Technology, 37 (2014) 1721-1728.
  - Mostafavi, M., Ulrich, J., **Monitoring phase transitions of crystals in-line**, Advanced Powder Technology, 2015, in press.
  - Pertig, D., Fardmostafavi, M., Stelzer, T., Ulrich, J., **Monitoring concept of single-frequency ultrasound and its application in dynamic crystallization processes**, Advance Powder Technology, 2015, in press.
-



## **Research activities**

### **Recent studies**

- Investigation of in-line/on-line measuring techniques in the solution crystallization process and polymorphic phase transition

### **Previous studies**

Studies on the technologies for wastewater treatment focused on the

- Reduction biological sludge production in wastewater treatment using membrane bioreactors (MBRs)
- Biosorption of heavy metals from sludge of wastewater treatment
- Modeling of oxidative dehydrogenation of propane for propylene production in a membrane reactor

---

### **Honors:**

- 10/2013-04/2015 achieving scholarship DAAD (Deutscher Akademischer Austausch Dienst)
- 161<sup>st</sup> rank in M.Sc. entrance exam among about 22,000 participants in 2003.
- 1610<sup>th</sup> rank in B.Sc. general entrance exam among about 500,000 participants in 1998.

---

### **Language skills:**

- Fluent in English
- French (B1)
- German (A2)

---

### **Software skills:**

*Software:* MATLAB, HYSYS, ASPEN, MS Office, Origin, CorelDraw